

1 **Gauging the impact of glacioeustasy on a mid-latitude early Silurian basin margin, mid**
2 **Wales, UK**

3 Jeremy R. Davies^{a,*}, Richard A. Waters^b, Stewart G. Molyneux^c, Mark Williams^d, Jan A.
4 Zalasiewicz^d, Thijs R.A. Vandenbroucke^e

5 ^a Department of Geography and Earth Sciences, Aberystwyth University, Aberystwyth SY23
6 3DB, UK

7 ^b Department of Geology, National Museum of Wales, Cathays Park, Cardiff CF10 3NP, UK

8 ^c British Geological Survey, Keyworth, Nottingham NG12 5GG, UK

9 ^d Department of Geology, University of Leicester, University Road, Leicester LE1 7RH, UK

10 ^e Department of Geology (WE13), Ghent University, Krijgslaan 281 S8, BE-9000 Ghent,
11 Belgium

12 *Corresponding author. E-mail address: jrdav@bgs.ac.uk (J.R. Davies).

13

14 **Abstract**

15 The early Silurian (Llandovery) Gondwanan South Polar ice sheet experienced episodes of
16 ice retreat and readvance. Marine base level curves constructed for the interval are widely
17 assumed to provide a record of the associated glacioeustasy. In revealing a series of
18 progradational sequences (progrades) bounded by flooding surfaces, recent work on the Type
19 Llandovery succession in mid Wales (UK) has provided an opportunity to test this
20 hypothesis. The grouping of these progrades into three composite sequences underpins the
21 construction of both low order (small amplitude, high frequency) and high order (large
22 amplitude, low frequency) base level movement curves. Revised biostratigraphical datasets
23 for the type succession permit the accurate dating of base level events. The composite
24 sequences record progradational acmes in the *acinaces*, lower *convolutus* and upper
25 *sedgwickii-halli* graptolite biozones. A series of transgressions that postdate the Hirnantian
26 glacial maximum culminated in an upper *persculptus* Biozone high-stand. Maximum
27 flooding events also occurred during the *revolutus* and lower *sedgwickii* biozones, and the
28 base of the early Telychian *guerichi* Biozone also marked the onset of a pronounced
29 deepening. A review of 62 published datasets, including global and other regional base level
30 curves, records of glacial activity, isotope data, patterns of facies and faunal flux and putative
31 climate models, permits an evaluation of the origins of these local base level events. The
32 concept of a Eustasy Index is introduced and shows that the impacts of global sea level
33 movements can only be demonstrated within narrow ‘eustatic windows’ coincident with
34 times of ice sheet collapse. At other times, the geometry of Llandovery area progrades
35 reflects their accumulation across a faulted basin margin where, during periods of slow ice
36 sheet advance, epeirogenic processes outstripped sea level movements as the dominant

37 forcing factors. Increased levels of Telychian subsidence at first enhanced and then
38 overwhelmed the influence of glacioeustasy as part of the region's response to the north
39 European Scandian deformation.

40 Keywords: Llandovery, Silurian, Glacioeustasy, Eustasy Index, Sequence stratigraphy,
41 Biostratigraphy, Epeirogenesis

42

43 **1. Introduction**

44 Recent studies have shown that, following its maximum in the Late Ordovician (Hirnantian),
45 the early Silurian retreat of the Gondwana-based South Polar ice sheet was punctuated by
46 separate episodes of ice re-advance (e.g. Grahn and Caputo, 1992; Caputo, 1998; Dias-
47 Martinez and Grahn, 2007). Glacioeustasy has been widely cited as significant in shaping
48 Llandovery age successions around the world, including the Type Llandovery succession in
49 mid Wales, UK (e.g. McKerrow, 1979; Johnson et al., 1991b), and in influencing the form of
50 Silurian sea level curves (e.g. Haq and Schutter, 2008; Johnson, 2010; Munnecke et al.,
51 2010). Remapping and extensive biostratigraphical resampling in the Llandovery area have
52 allowed a new sedimentary architecture to be erected and the positions of key biozonal
53 boundaries to be revised (Figs. 2–5) (Davies et al., 2013). Graptolite discoveries coupled to
54 new microfossil analyses underpin major changes to the biozonal cross-correlations put
55 forward by Cocks et al. (1984) that have informed global Llandovery analysis for over a
56 generation. In allowing more precise comparisons with other regional datasets, these
57 revisions have permitted a critical evaluation of the influence of glacioeustasy on the type
58 succession.

59 Deposition of the Type Llandovery succession took place in a ramp-like setting located along
60 the SE margin of the ensialic Lower Palaeozoic Welsh Basin, in mid-southern palaeolatitudes
61 (Cherns et al., 2006; Woodcock and Strachan, 2012). Though traditionally recognised as
62 forming part of the Eastern Avalonia microcraton, Waldron et al. (2011) suggested that the
63 Welsh Basin has more complex crustal foundations. However, the term ‘Avalonian’ remains
64 relevant in the biopalaeogeographical sense of Cocks and Fortey (1990) and as a label for a
65 group of loosely associated crustal terranes, the ‘Anglo-Acadian belt’ of Cocks and Fortey
66 (1982), that lay to the south of the contemporary Iapetus Ocean (Fig. 1). Docking of these
67 ‘Avalonian’ terranes with the more easterly craton of Baltica took place along the northern
68 European Tornquist Zone, and is recorded in Wales by the late Katian (mid Ashgill)
69 ‘Shelvian’ deformation (Toghill, 1992). By Llandovery times, these once separate crustal
70 elements formed part of a unified tectonic plate and faunal province (e.g. Cocks and Fortey,
71 1990). Early Llandovery closure of the northern sector of the Iapetus Ocean initiated the
72 Scandian Orogeny in Baltica (e.g. Ladenberger et al., 2012) at the same time as the late stages
73 of the Taconic and Salinic tectonic episodes were being felt in North America (e.g. Ettensohn
74 and Brett, 1998). Hence, tectonism was ongoing during the Llandovery throughout the
75 circum-Iapetus realm where, within migrating foreland basins and faulted-bounded

76 depocentres, evolving patterns of subsidence competed with eustasy in the shaping of
77 sedimentary successions (e.g. Baarli et al., 2003).

78 Nowhere is this more evident than in the Type Llandovery area, where active basin-bounding
79 faults accommodated the subsidence of the basin to the west and uplift of source areas to the
80 east (Davies et al., 2013). Notwithstanding this tectonic backdrop, early Hirnantian facies at
81 Llandovery and throughout the Welsh Basin, as elsewhere, record the impact of Late
82 Ordovician glacioeustasy (e.g. Brenchley and Cullen, 1984; Davies et al., 2009). Preserved in
83 distal settings are strata that were deposited during the maximum drawdown in sea level,
84 whereas an unconformity records the coincident emergence and deep erosion of proximal
85 regions. Late Hirnantian units record the pulsed transgression that post-dated the glacial
86 maximum, and the resulting re-ventilation and faunal re-stocking of the Welsh Basin and its
87 marginal shelf. The current study seeks to evaluate the role that eustasy, specifically
88 glacioeustasy, went on to play in the shaping of the succeeding Type Llandovery succession.

89 Telychian and lower Wenlock rocks at Llandovery provide a record of deep and distal shelfal
90 sedimentation and of increased subsidence and disruption by synsedimentary slides.
91 Coincidental increases in the volume and grade of sediment supplied to the Welsh Basin,
92 sourced from new quadrants and accommodated by active faulting, confirm that the late
93 Llandovery to early Wenlock was a time when regional tectonism was resurgent throughout
94 Wales (e.g. Woodcock et al., 1996; Davies et al., 1997). However, preceding Rhuddanian and
95 Aeronian rocks comprise a cyclical succession of variably bioturbated and fossiliferous
96 sandstones, sandy mudstones and mudstones that has proved better suited for eustatic
97 analysis. It is these strata, viewed in the context of a clinofacies model (see Davies et
98 al., 2013), on which this study principally focuses (Figs. 3, 6).

99 The parameters used to establish the base level history of the Llandovery area (Sections 3 and
100 4) allow comparison with global syntheses of Silurian sea level change and other regional
101 base level datasets (Fig. 1) that sample tectonic settings ranging from cratonic interiors and
102 passive margins to deep oceans and orogenic belts (Sections 5 and 6). They also enable
103 comparison with datasets that, by charting the distribution of glacial facies, changing isotope
104 ratios and faunal flux, purport to chronicle sea level-linked climatic events (Section 7). A
105 novel method of assessing the levels of correspondence between these varied datasets and the
106 record of base level movements in the Type Llandovery area is developed (Section 8).

107

108 **2. Implications of revised biostratigraphical correlations**

109 The revised cross-correlation of the various macro- and microfossil biozonal schemes
110 applicable to the Type Llandovery area is presented in Fig. 5. This forms the basis for the
111 nomenclature and calibration applied throughout the paper. The graptolite biozonal scheme is
112 that developed by Zalasiewicz et al. (2009) for the UK Silurian, with wider comparisons
113 based on Loydell's (2011) review of other regional schemes. Further information on relevant

114 aspects of Welsh and global Llandovery biostratigraphy, and on the sources used to compile
115 Fig. 5, are provided as Supplementary data.

116 Davies et al.'s (2013) re-examination of the type succession, and of the Aeronian and
117 Telychian stage GSSPs that it hosts, has important implications for international correlation.
118 Rhuddanian rocks in the type succession range into the *triangulatus* graptolite Biozone, and
119 earliest Telychian rocks pre-date the local FAD of *guerichi* Biozone graptolites. However, to
120 avoid confusion and facilitate global comparisons, the bases of the Aeronian and Telychian
121 stages herein follow the graptolitic definitions of current international usage (i.e. base
122 *triangulatus* Biozone = base Aeronian; base *guerichi* Biozone = base Telychian). The
123 consequences of applying this to the type succession are shown in Fig. 5. Moreover, where
124 stage recognition is based on the appearances of key brachiopod taxa, which is true of many
125 non-graptolitic successions in Europe and North America, it is now likely that the regional
126 stage boundaries correlate with neither the Type Llandovery GSSPs nor the graptolite zonal
127 boundaries on which they are based (see Davies et al., 2013).

128 Similarly, correlations based on the A1-4, B1-3 and C1-6 quasi-chronozonal scheme erected
129 in the Llandovery area by Jones (1925), which have been widely adopted as the standard
130 means for subdividing Llandovery strata both in the UK (e.g. Williams, 1951; Ziegler, 1966;
131 Ziegler et al., 1968b; Cocks et al., 1970; Cocks et al., 1984) and internationally (e.g. Berry
132 and Boucot, 1970; Johnson et al., 1985; Brett et al., 1998), should no longer be relied upon
133 without reference to the primary dating criteria.

134

135 **3. A sequence stratigraphy for the Type Llandovery area**

136 The event stratigraphy of uppermost Hirnantian strata in the Llandovery area has been
137 assessed by Davies et al. (2009). The overlying Rhuddanian to Aeronian facies comprise a
138 series of progradational sequences (progrades) bounded by flooding surfaces and correlative
139 unconformities. Such sequences represent transgressive–regressive (T–R) cycles in the sense
140 of Embry and Johannessen (1992; also Catuneanu et al., 2011) and ‘depositional sequences’
141 as defined by Embry et al. (2007; Embry, 2009). Lateral and vertical changes in lithology and
142 biota, including trace fossil assemblages, record the repeated basinward migration of
143 shallower, intensely bioturbated, sandy foreset facies across their deeper, more distal and
144 muddy bottomset counterparts (Davies et al., 2013) (Fig. 3). The reduced levels of
145 bioturbation displayed by bottomset facies and a trace fossil assemblage dominated by
146 *Chondrites* are consistent with deposition at depths that lay beyond the colonising reach of
147 contemporary shelly benthos. In contrast, foreset facies belts were home to a diverse and
148 abundant assemblage of soft-bodied, burrowing organisms that lived alongside *Stricklandia*
149 and deeper *Clorinda* community shelly benthic assemblages (e.g. Ziegler et al., 1968a).
150 Topset facies were anchored to an active and erosion-prone fault footwall region, but their
151 characteristic *Pentamerus* Community assemblages (Plate 1) extended into upper foreset
152 settings where they serve to identify periods of maximum shallowing (Fig. 6). It is of note
153 that, whereas appearances of *Stricklandia* and *Pentamerus* community assemblages in

154 cratonic interior successions are normally viewed as evidence of off-shore deposition and
155 deepening (e.g. Witzke, 1992), in the basin margin setting at Llandovery they are associated
156 with peak shoaling episodes. Truncation surfaces are present locally at the top of each
157 prograde. Shoreline ravinement (e.g. Embry, 2009) may have contributed to the development
158 of these surfaces, but where they merge to form the compound unconformities that
159 characterise condensed proximal successions (Figs. 3, 4) subaerial denudation was likely to
160 have been the dominant erosive process.

161 Ten flooding surfaces define nine (low order) prograde sequences that span the late
162 Hirnantian to Aeronian interval, the tenth and youngest of these flooding surfaces marking
163 the redefined local base of the *guerichi* Biozone and Telychian Stage (Figs. 4, 6). Davies et
164 al. (2013) labelled these progrades according to their dominant sandstone unit (e.g. Ceg⁰,
165 Ceg¹, Ceg¹¹, etc.) (Fig. 4). Differences in the scale, duration (as measured by graptolite
166 biozones) and basinward reach of the progrades, as well as the lateral extent and vertical
167 impact of erosion, allow these to be grouped into three compound (or high order) sequences
168 according to the criteria established by Embry (1995) and Schlager (2004) (also Catuneanu et
169 al., 2011; Embry, 2009) (Figs. 4, 6). In addition, many of the progrades comprise a
170 succession of smaller scale parasequences. Local FADs and/or LADs of key taxa permit these
171 newly recognised sequences to be dated using a range of biozonal criteria, with many FADs
172 linked to flooding events (Davies et al., 2013). Radiometric dates available for the
173 Llandovery Series suggest that the study interval spanned c. 6 myr (Cooper and Sadler, 2012;
174 Melchin et al., 2012) and, hence, that the average duration of the prograde sequences
175 recognised in the Llandovery area was well under 1 myr.

176

177 **4. Relative marine base level movements**

178 Facies and faunal variations within each sequence and compound sequence allow the
179 construction of both low and high order relative marine base level movement curves (e.g.
180 Embry, 2009; see also Section 6b) for the upper Hirnantian to lower Telychian succession
181 (Fig. 6). These differ significantly from those compiled by McKerrow (1979) and Cocks et al.
182 (2003). In the first instance, such curves plot the relative changes in depositional depth that
183 occurred at any given location through time. However, each Llandovery area prograde
184 appears to have been accompanied by the progressive erosion of its proximal portions, with
185 the depth of erosion increasing in a landward direction. This suggests that these progrades do
186 not simply record the cyclical infilling of accommodation space created by subsidence
187 beneath a static or slowly rising base level, but periods when base level fell. It implies they
188 were the product, at least in part, of forced regressions (e.g. Posamentier et al., 1992; Hunt
189 and Gawthorpe, 2000). The deeper, more distal facies that closely overlie flooding surfaces
190 provide a record of deposition during periods of rising and elevated relative base level within
191 transgressive and high-stand system tracts. In contrast, each transition into shallower, more
192 proximal facies signalled the onset of deposition within regressive/falling stage followed by
193 low-stand system tracts (e.g. Catuneanu et al., 2011).

194 Compiled from data beyond the limits of erosion, Fig. 6 identifies the main Llandovery area
195 base level events. The numbers used on this figure to identify sequence-defining flooding
196 surfaces and the letters for periods of maximum flooding and shallowing are those cited
197 throughout the remainder of the text. The first post-glacial maximum flooding surface (1),
198 present in rocks barren of graptolites, underlies the first appearance in Wales of *taugourdeaui*
199 Biozone chitinozoans (see Fig. 5 [12, 20]). A second flooding level (2) coincides with the
200 FAD of *persculptus* Biozone graptolites in Wales, but which is now thought to be later than
201 elsewhere (see Vandenbroucke et al., 2008; Davies et al., 2013; Challands et al., 2014; and
202 Supplementary data). A third intra- Hirnantian event (3) is succeeded by Llandovery flooding
203 surfaces that coincide with the local FADs of *revolutus* (4), *magnus* (6), middle and upper
204 *convolutus* (7, 8) and lower *sedgwickii* (9) graptolite biozone assemblages. A further intra-
205 *revolutus* Biozone event (5) is also recognised. The higher order base level curve points to
206 maximum deepening events during the deposition of the upper *persculptus*, *revolutus* and
207 lower *sedgwickii* Biozones (A–C). A marked flooding event that coincides with the local
208 FAD of *guerichi* Biozone graptolites (10) is seen on both the high and low order datasets.

209 To facilitate the wider correlation of these events, it is important also to place them in the
210 context of the revised ranges for the key brachiopod lineages and microfossil assemblages
211 used in Llandovery correlation (Fig. 5). Thus, flooding events 1 and 2 lie within the range of
212 the Hirnantia Fauna (Davies et al., 2009) and event 3 is closely related to the first appearance
213 of primitive forms of *Stricklandia lens*. Event 4 coincides with the FAD of the more evolved
214 *S. lens intermedia* alongside *eoplanktonica* Biozone acritarchs. Flooding events 5 and 6 also
215 fall within the range of *S. lens intermedia*, event 5 marking the appearance of *maennili*
216 Biozone chitinozoans, and event 6 of a precursor of the chitinozoan *Eisenackitina*
217 *dolioliformis* within the range of *tenuis* Biozone conodonts. The intra-*convolutus* Biozone
218 transition between *S. lens intermedia* and *S. lens progressa*, well documented in the Welsh
219 Borderland (Cocks and Rickards, 1969; Ziegler et al., 1968b), appears related to event 7,
220 which also marks the entry of *microcladum* Biozone acritarchs. Fully evolved forms of *S.*
221 *lens progressa* are first recorded above flooding level 8, coincident with the local FADs of
222 *estillis* Biozone acritarchs and *dolioliformis* Biozone chitinozoans. The earliest records of
223 *Eocoelia hemispherica* at Llandovery are also from above this flooding surface, though the
224 species is believed to first appear in the *leptotheca* graptolite Biozone (e.g. Cocks et al., 1984;
225 Bassett, 1989). Event 9 marks the entry of the more highly evolved *E. intermedia* alongside
226 *S. laevis*, yet specimens from above this level identified as *E. hemispherica* and *S. lens*
227 *progressa* (Williams, 1951; Cocks et al., 1984) confirm an interval of overlapping ranges
228 within the lower parts of the *sedgwickii* graptolite Biozone and the *staurognathoides*
229 conodont Biozone. The records of *E. curtisi* at Llandovery are from a slump deposit (Davies
230 et al., 2010, 2011), but this more evolved taxon has elsewhere also been shown to have its
231 FAD in rocks of *sedgwickii* Biozone age (Doyle et al., 1991). No in situ shelly assemblages
232 have been recognised closely overlying event 10 at Llandovery. However, data from
233 elsewhere appear to confirm that only *S. laevis* and *E. curtisi* survive into and above the
234 *guerichi* Biozone (Bassett, 1989), within which *encantador* Biozone acritarchs first appear
235 (Davies et al., 2013).

236 The fault-generated uplift and deep erosion of proximal parts of the succession preclude the
237 construction of an onlap curve (e.g. Haq and Schutter, 2008). However, the lateral extent of
238 each of the main progrades provides an arbitrary measure of the basinward shift of facies
239 belts associated with each relative lowering of base level (Fig. 6). The three composite
240 sequences reached their progradational acmes (D, E and F) during the *acinaces*, lower
241 *convolutus* and upper *sedgwickii-halli* graptolite biozones. Significant lower order
242 progradations occurred during the *revolutus*, *triangulatus* and in the middle and upper
243 *convolutus* biozones.

244 Was the forcing mechanism for these Llandovery area progrades regional isostasy, tectonism,
245 or global eustasy and, if the latter, was this glacioeustasy, and did these factors operate in
246 concert or separately at different times? Regional base level movement curves differ
247 conceptually from true sea level movement curves (e.g. Grabau, 1940; Artyushkov and
248 Chekhovich, 2001; Miall, 2004). The latter seek to provide a record of changes in sea level
249 elevation through geological time relative to a fixed global datum, nominally taken to be
250 modern sea level (e.g. Vail et al., 1977; Haq and Schutter, 2008). Such changes, if properly
251 identified, must be eustatic (i.e. of global reach), even though their impacts might be rendered
252 unrecognisable by local isostatic and/ or tectonic effects. In reality, local and regional
253 variations in rates of subsidence, source area uplift and sediment supply, all of which are
254 linked to ambient epeirogenesis, must play a role in fashioning the detailed shape of such
255 curves (e.g. Artyushkov and Chekhovich, 2001, 2003; Zhang et al., 2006) and can be the
256 dominant factors, as during the Telychian in Wales (e.g. Schofield et al., 2009). These same
257 factors make it unlikely that the base level history and hierarchy recognised in one area will
258 be fully replicated in another.

259 When seeking to discern whether regional base level movements record a global (eustatic)
260 signal, it is therefore gross trends, major flooding surfaces and peak events that offer the best
261 potential for testing. For this reason, the Llandovery area base level history depicted on Figs.
262 7 to 14 is divided into broad intervals of deepening and elevated base level (coloured blue)
263 and of shallowing and lowered base level (coloured red) rather than simply into transgressive
264 and regressive components. Parasequence-scale movements (Fig. 6) have been ignored.
265 Where the boundaries between these sectors coincide with flooding surfaces, their location is
266 precise, but where they are located on the regressive portions of the curves their placement is
267 more arbitrary. Nevertheless, in providing a single template for comparison, this approach
268 emerges as a practical means of gauging the broad similarities and differences displayed by a
269 range of datasets (see Section 8).

270

271 **5. Regional and UK comparisons (Fig. 7)**

272 Comparisons with other successions appear to confirm that many of the late Hirnantian–early
273 Telychian base level events recognised in the type area occur widely throughout the UK (Fig.
274 7). To the east of Llandovery, in a palaeo-landward direction, the coeval rocks of the Welsh
275 Borderland, notably in the Church Stretton area, testify to the pulsed transgression of a

276 dissected topography (Johnson et al., 1998). Rhuddanian rocks were either largely excluded
277 or subsequently eroded from much of this region. The work of Ziegler et al. (1968b; also
278 Cocks and Rickards, 1969), reinterpreted in the light of the Type Llandovery findings, point
279 to an initial inundation of more deeply incised settings around the Rhuddanian–Aeronian
280 boundary (B), with evidence for subsequent pre- and intra-*convolutus* Biozone flooding
281 episodes (6 and 7). Transgressive *Pentamerus*-bearing sandstones of *sedgwickii* Biozone age
282 bear testimony to a more extensive inundation (9 and C), and the subsequent deepening that
283 widely introduced *Clorinda* Community benthic assemblages can be matched to the *guerichi*
284 Biozone flooding event at Llandovery (10).

285 Further west, in the contiguous, graptolitic, deep water Welsh Basin succession, many of the
286 events documented in the type area are mirrored by the alternation of oxic and anoxic
287 mudstones facies and by evolving patterns of coarse clastic deposition (e.g. Woodcock et al.,
288 1996; Davies et al., 1997; Schofield et al., 2009) (Fig. 7). Periods of falling base level are
289 argued to have promoted the better mixing of surface and deep water layers. The introduction
290 of oxygenated waters then allowed a burrowing fauna to colonise the basin floor (e.g. Page et
291 al., 2007; Challands et al., 2008). The resulting mudstone facies are, accordingly, strongly
292 burrow-mottled. The coincident rejuvenation of sediment source areas and increased clastic
293 input is recorded by the expansion and migration of sand-dominated turbidite lobes locally
294 present on the basin floor (e.g. Cave and Hains, 1986; Davies and Waters, 1995; Davies et al.,
295 2006 a, b; Wilson et al., 2016). In contrast, episodes of rising base level have been linked to
296 the establishment of a strongly stratified basin water column, the imposition of anoxic
297 (anaerobic) bottom waters and, due to the exclusion of burrowing organisms, the
298 accumulation of laminated, organic-rich mudstones (e.g. Leggett, 1978). The coeval
299 drowning of source areas and the decline in sediment supply is reflected in the synchronous
300 contraction of the basin's deepwater sandy systems (e.g. Schofield et al., 2009).

301 This level of linkage between the successions of the Welsh Basin and its contiguous margin
302 is to be expected. Closely comparable oxic/anoxic alternations are recognised in Llandovery
303 successions that also formed along the southern seaboard of Iapetus at Llanystumdwy and
304 Conway (North Wales) and in the English Lake District (e.g. Baker, 1981; Rickards, 1970;
305 Rickards and Woodcock, 2005) (Fig. 2). Their presence in the Llandovery succession at
306 Dob's Linn in the Scottish Southern Uplands is more telling. There, in Aeronian strata, units
307 that are barren of graptolites, with quasi-oxic mudstone beds, alternate with richly graptolitic,
308 anoxic intervals (Toghill, 1968) in a pattern that can be matched to that in the Welsh Basin
309 (Baker, 1981; Loydell, 1998; Page et al., 2007) and, by extrapolation, to many Type
310 Llandovery events. This is significant since the succession in Scotland has been interpreted as
311 an accretionary prism of Iapetus ocean floor sediments accreted during subduction along the
312 southern edge of Laurentia (e.g. Leggett et al., 1979; Woodcock and Strachan, 2012; but see
313 Stone et al., 1987). Hence, it offers evidence that many of the base level events recognised in
314 the Llandovery area can be linked to changes in seawater chemistry that affected both intra-
315 cratonic and oceanic settings alike. Only in the mid Rhuddanian do these successions fail to
316 provide clear evidence of correlatable changes in facies and base level.

317

318 **6. Llandovery eustasy**

319 Whether it is feasible to discern a eustatic signal in ancient sedimentary successions is widely
320 questioned by those who argue that the ‘noise’ of regional factors is always likely to ‘drown
321 out’ the impacts of all but the largest and most rapid global sea level movements (e.g. Miall,
322 2010) (see Section 8). Those who have published on Silurian eustasy take care to
323 acknowledge and to counter such concerns (e.g. Witzke, 1992; Johnson, 2010). They point to
324 facies, faunal and, increasingly, isotopic shifts that can be linked to changes in bathymetry,
325 and appear to be widely correlatable, as evidence of global movements in marine base level.
326 Johnson et al. (1991b) labelled this empirical approach the pursuit of ‘practical eustasy’ and,
327 utilising regional datasets, many have since attempted to construct curves that purport to chart
328 changing Silurian sea levels (Fig. 8).

329 The varied methods used in the construction of Silurian sea level curves and the concepts that
330 underpin them have been reviewed by Johnson (2006, 2010). In shallow shelfal settings,
331 systematic changes in benthic brachiopod (e.g. Johnson, 1987, 1996; Johnson et al., 1991a)
332 and conodont (e.g. Zhang and Barnes, 2002b) assemblages have proved effective in
333 identifying gross trends and peak events, despite the misgivings of some (e.g. Aldridge et al.,
334 1993; Loydell, 1998). Johnson et al. (1985) (also Rong et al., 1984) suggest that variations in
335 graptolite diversity may similarly reveal the impact of sea level changes in otherwise uniform
336 deep water mudstones. Linked changes in lithofacies and biofacies have been used in both
337 shallow water carbonate (e.g. Witzke, 1992; Copper and Long, 1998) and siliciclastic
338 successions (e.g. Brett et al., 1998; Melchin and Holmden, 2006), and, in a variant of this
339 approach, Baarli (1988, 1998; also Baarli et al., 1992) and Long (2007) chart changes in the
340 frequency and thickness of storm beds (tempestites). Johnson et al. (1998) gauged the onlap
341 of palaeotopography. Many of these studies deliberately target the successions of cratonic
342 interiors on the assumption that tectonically stable regions are those most likely to preserve
343 the imprint of eustatic events (e.g. Johnson et al., 1991b). Evidence of regional epeirogenesis
344 within and along the margins of intra-cratonic basins in which many of the most extensively
345 studied Llandovery successions accumulated tells a different story (e.g. Artyushkov and
346 Chekhovich, 2001, 2003; Baarli et al., 2003; Davies et al., 1997).

347 The ‘graptolitic approach’ of Loydell (1998) benefits from the precise dating achievable for
348 graptolite-bearing intervals, which, when shown to be widely correlatable, are argued to
349 record global flooding events and, as a consequence, widespread anoxia (e.g. Leggett, 1980;
350 Davies et al., 1997; see Section 5). Other explanations for anoxic events, however, such as
351 basin restriction and/or locally elevated levels of organic productivity, suggest that the link
352 between widespread anoxia and eustasy may be more complex (e.g. Challands et al., 2008).
353 This is illustrated in recent studies documenting redox control on faunal (Vandenbroucke et
354 al., 2015) and facies variations (McLaughlin et al., 2012) that have previously been used to
355 infer changes in Silurian sea level. Regional sequence analysis, used in tandem with these
356 other methods, is widely seen as a prerequisite to curve construction (e.g. Harris et al., 1998;
357 Brett et al., 1998, 2009; Haq and Schutter, 2008) and is the approach adopted here.

359 **6.1. Methodology**

360 This study replicates the approach applied to North American datasets by Johnson (1987) and
361 first attempted on a global scale by McKerrow (1979), prior to the influential studies of
362 Johnson et al. (1991b), Johnson and McKerrow (1991) and Johnson (1996). Figs. 8 to 12
363 present a range of published curves that purport to chart either regional or global movements
364 in late Hirnantian to early Telychian marine base level. Many of their authors label them ‘sea
365 level curves’. These are compared with the base level trends and events recognised at
366 Llandovery in an effort to gauge the levels of similarity. The implicit assumption is that
367 trends and events that can be shown to be widely correlatable are those most likely to be
368 eustatic (see Section 8). For many regions, more than one curve is included. This reflects the
369 availability of datasets compiled using different methods to gauge bathymetry. Some of these
370 reveal a coincidence of trends and events, as for example on Anticosti Island (e.g. Zhang and
371 Barnes, 2002b; Long, 2007). However, intra-regional curves that display marked differences
372 and may reveal the impacts of local tectonism and/or isostasy, notably in Siberia and on the
373 Yangtze Platform of China (e.g. Johnson et al., 1985; Yolkin et al., 2003), are also utilised for
374 purposes of objectivity. Other Llandovery datasets (Figs. 13, 14) argued to provide a proxy
375 record of sea level change, based on physical evidence of glacial advance and retreat and the
376 flux of stable isotope ratios, faunas and ocean states are assessed in Section 8.

377 **6.2. Curve construction and alignment**

378 Given the current paucity of radiometric dates and stable isotope profiles, the correlation of
379 many Llandovery successions necessarily remains reliant on biostratigraphical methods. To
380 facilitate this, all the curves presented in Figs. 8 to 13 have been recalibrated to align with the
381 UK Llandovery graptolite biozonation (Fig. 5), and this has required the vertical warping of
382 many. In recalibrating each curve, the dating criteria provided by their authors have largely
383 been relied upon. The justification for any amendments is provided via the numbered
384 references [in square brackets] to Supplementary data. The use of FADs and LADs has been
385 a common theme in such re-evaluations and brings the virtue of consistency to the datasets.
386 Nevertheless, the roles of facies control, provincialism, diachronous and divergent patterns of
387 dispersal and cryptic omission, as well as collecting bias, all introduce uncertainty (e.g.
388 Zalasiewicz et al., 2009; Miall, 2004). Sadler (2004; also Sadler et al., 2009) shows that FAD
389 and LAD-based biozonal boundaries when correlated on a global scale can rarely be viewed
390 as truly isochronous and Cramer et al. (2015) suggest that, by using multiple high resolution
391 datasets, it may soon be possible evaluate these levels of uncertainty. As it is, Silurian
392 chronostratigraphy remains predicated on the assumption that such uncertainties fall within
393 geologically acceptable limits (e.g. Cramer et al., 2011a; Melchin et al., 2012) and, as Witzke
394 (1992) argues, that in the pursuit of ‘practical eustasy’, “parallel changes in relative sea level
395 coincident with biozonal boundaries are most reasonably interpreted as synchronous.”

396 The horizontal axes of the curves are as used by their authors and reflect the different criteria
397 they employed for calibration. Very few claim to chart changes in absolute bathymetric

398 value, those of Ross and Ross (1996), Johnson et al. (1998), Artyushkov and Chekhovich
399 (2001) and Haq and Schutter (2008) being notable exceptions. This use of varied criteria
400 emphasises the need, when seeking to identify correlatable events, to focus on abrupt changes
401 and gross trends rather than to compare precise profiles.

402 Before drawing conclusions from curve comparisons it is also important to consider the
403 relative orders of movement and the relationships between the events that such curves
404 portray. That different orders of sea level movement, superimposed upon one another, can be
405 discerned in the stratigraphical record and that these record not just differences in vertical
406 scale and duration, but ultimately in causative mechanism is a concept that has evolved (e.g.
407 Vail et al., 1977; Duval et al., 1992; Embry, 1995; Schlager, 2004; Miller et al., 2005).
408 Catuneanu et al. (2011) point to inconsistencies in this approach and highlight the misuse of
409 numerical (1st, 2nd, 3rd, etc.) and comparative (high, low) hierarchies. In this account, high
410 order refers to sea level curves that purport to record vertical movements of many 10s or 100s
411 of metres that took place over time periods that can range up to several millions of years.
412 Lower order curves depict more frequent, lower amplitude events. The concept is valuable in
413 enabling different levels of comparison between published datasets and offering a potentially
414 broader insight into the origins of the base level movements recorded, but the distinction is
415 not always straightforward (e.g. Embry, 1995; Schlager, 2004) and can result in the arbitrary
416 inclusion of lower order events on high order curves.

417 Periods of high order global deepening may be interrupted at the local level by prograde
418 events that record the impact of either low order eustatic regressions and/or local influences
419 on sediment supply and accommodation space. In the same way, low order flooding events
420 can be expected to punctuate episodes of high order global shallowing. The offset between
421 high order, global maxima and regional, lower order oscillations accounts, arguably, for
422 many of the marked discrepancies in the shapes of published curves and the problems
423 encountered when attempting to match events. It follows that modest perturbations on high
424 order curves may reflect the impact of lower order events that, at the local level and in the
425 field, can appear every bit as significant as those associated with high order peaks.
426 Conversely, detailed dating can show that what appears to be a minor event in the field – a
427 mudstone on mudstone contact for example – conceals a more significant base level history,
428 as with the contact between the Lower and Upper Sodus Shale in New York State (Brett et
429 al., 1998) (see Supplementary data). It is against these difficulties that the correlations
430 presented on Figs. 8 to 12 should be viewed.

431 **6.3. Analysis: global sea level curves (Fig. 8)**

432 In Fig. 8, a selection of some of the most widely cited global sea level curves for the late
433 Hirnantian to early Telychian interval are compared with the inferred base level movements
434 recognised in the Llandovery area. Informed by the plots of McKerrow (1979), the curve of
435 Johnson et al. (1991b) established what many came to view as the ‘standard’ for Silurian sea
436 level movements, and the ages it established for key high-stand events remain essentially
437 unmodified in all Johnson's subsequent reviews (1996, 2006, 2010). Yet, from a comparison
438 of some of the most recent and authoritative examples of global sea level curves by Haq and

439 Schutter (2008) and Johnson (2010), it is clear that a consensus is some way off. The
440 suspicion also emerges (see below) that some of the most commonly used curves are over-
441 reliant on the data from a single region (e.g. Ross and Ross, 1996) and/or are a conflation of
442 higher and lower order base level events, but are fully representative of neither.

443 In the first instance it is worth comparing the late Rhuddanian to early Telychian portion of
444 the high order Type Llandovery curve with the same part of many of the other curves. The
445 broad alignment of independently constructed peaks appears to offer support for a global
446 signal within the Type Llandovery data. Several recognise a high order Rhuddanian
447 transgression that peaked in the *revolutus* Biozone (B) (e.g. Ross and Ross, 1996; Page et al.,
448 2007) or close to the *revolutus*–*triangulatus* biozonal boundary (e.g. Johnson, 1996, 2010).
449 Loydell (1998) and Haq and Schutter (2008) delay the culmination of this event until the
450 *magnus* Biozone and it is not inconsistent to suggest that flooding levels 4, 5 and 6 seen at
451 Llandovery were lower order increments that contributed to this global high-stand.

452 The lower *sedgwickii* Biozone is also widely seen as a period of elevated sea levels (C).
453 Some see this as the peak of a prolonged deepening episode that spanned much of the
454 preceding *convolutus* Biozone (e.g. Johnson, 2010), and to which lower order events (7, 8,
455 and 9) may again have contributed. Others, by showing it as a pronounced, but short-lived
456 deepening event (e.g. Ross and Ross, 1996), imply a wider significance for the basal
457 *sedgwickii* Biozone flooding surface (9). The late *sedgwickii*-*halli* biozonal interval is widely
458 recognised as a period of falling sea levels, shown by Johnson (1996), Ross and Ross (1996)
459 and Page et al. (2007) to have reached its acme close to the base of the *guerichi* Biozone (F).
460 Loydell's (1998) curve is notably at odds with the majority in its depiction of late Aeronian
461 sea level movements.

462 Many curves acknowledge the presence of a pre-*sedgwickii* Biozone Aeronian low-stand, but
463 opinions differ as to its scale and timing. Ross and Ross (1996; also Page et al., 2007) restrict
464 it to the *convolutus* Biozone. Others, by recognising its peak in the mid Aeronian *leptotheca*
465 Biozone (e.g. Loydell, 1998, 2007; Johnson, 1996, 2010), imply a link with at least part of
466 shoaling episode E. The depiction of a discrete early Aeronian lowering of sea level by Ross
467 and Ross (1996) is replicated in the subsequent curves of Page et al. (2007) and Haq and
468 Schutter (2008). It compares with a lower order progradation (Ceg⁰) seen at Llandovery, but
469 the biostratigraphical dating of this global event is suspect (see Fig. 9 and Supplementary
470 data). Evidence of other lower order events, including both mid (7) and upper (8) *convolutus*
471 Biozone flooding levels is provided by the curves of Loydell (1998, 2007). In marked
472 contrast to the Type Llandovery data, most global curves show the early-mid Rhuddanian as
473 a period of steadily rising sea levels. There is no indication of a discrete *persculptus* Biozone
474 deepening maximum (A), or of a subsequent shallowing event on the scale seen at
475 Llandovery (D). Ross and Ross (1996) and Page et al. (2007) depict what appears to be a low
476 order pre-*revolutus* Biozone regression, but the dating and global credentials of this event are
477 again questionable (see below and Supplementary data). The marked *guerichi* Biozone
478 deepening at Llandovery (10) appears to show the abrupt termination of the preceding
479 progradation (F) and the rapid onset of deep and distal sedimentation. This is consistent with

480 the onset of regional subsidence (Davies et al., 2013) and of a period when contemporary
481 orogenesis became the dominant influence on sedimentation within the Welsh Basin (e.g.
482 Woodcock et al., 1996; Davies et al., 1997). A broadly coeval event widely recognised in the
483 global datasets suggests that there was a coincidence of local and global forcing mechanisms,
484 although the curves of Haq and Schutter (2008) and Johnson (2010) are inconsistent with
485 this.

486 **6.4. Analysis: regional curves from circum-Iapetus provinces (Figs. 9, 10)**

487 Following the studies of Johnson (e.g. 1979, 1987; Johnson et al., 1985; Johnson et al.,
488 1991b) and Witzke (1992; Witzke and Bunker, 1996), Johnson (1996) recognised Laurentian-
489 based eastern Iowa as the ‘type district’ for his four Llandovery high-stand events. The
490 adjacent, closely comparable succession in Illinois appears to have influenced Ross and Ross
491 (1996, Fig. 2) in the construction of their sea level curve published in the same volume. Thus,
492 the dating and interpretation of these mid USA successions has been critical in the evolution
493 and application of the eustatic concept to the early Silurian in North America and globally.
494 This is significant as the dating of many of the key events recognised in Iowa and Illinois is
495 open to question (see Supplementary data) and has implications for their wider correlation.
496 Despite this, recalibrated regional curves mainly from Laurentian North America and from
497 Baltica (e.g. Baarli et al., 2003) offer insights into the number and scale of lower order base
498 level events in these areas (Figs. 9, 10).

499 The *revolutus* Biozone deepening maximum (B) and the *sedgwickii* Biozone transgression
500 (9), deepening maximum (C) and subsequent progradation (F) appear to be widely recorded
501 in many of the recalibrated Laurentian datasets (e.g. Harris and Sheehan, 1997, 1998). A
502 deepening during the *guerichi* Biozone (10) is also acknowledged where rocks of this age
503 have escaped intra-Telychian erosion (Kluessendorf and Mikulic, 1996), as on Anticosti
504 Island and in Arctic Canada (e.g. Zhang and Barnes, 2002b; Melchin and Holmden, 2006). In
505 contrast to the global datasets, several North American curves (Figs. 9, 10) suggest the
506 presence of both early and mid Aeronian shallowing events, though, with the exception of the
507 curve for Iowa (Fig. 9, curve 1), few endorse the scale and duration of prograde E seen at
508 Llandovery. In addition to the base *magnus* Biozone transgression (6), multiple flooding
509 events in strata believed to span the *leptotheca* and *convolutus* biozones (e.g. Harris et al.,
510 1998; Long, 2007) raise the possibility that flooding surfaces matching those that define
511 parasequences at Llandovery may be present, as well as those that define Llandovery area
512 sequences (7 and 8). On the other hand, it is clear that significant non-sequences interrupt
513 many of these successions and, whilst offering evidence of shallowing and subaerial erosion,
514 these may also account for the non-preservation of key flooding levels (see Section 8). Zhang
515 and Barnes (2002b) recorded a marked lowstand on Anticosti Island that matches closely the
516 upper *convolutus* Biozone prograde at Llandovery. It succeeds a pre-*sedgwickii* Biozone
517 deepening episode (8) and underlies a flooding surface that marks the local FAD of
518 *sedgwickii* Biozone graptolites (9). The recalibrated curves for Iowa and Illinois offer
519 evidence for a comparable shoaling between the regional FADs of *S. lens progressa* and *S.*
520 *laevis* (Johnson, 1975; Witzke, 1992). The data from Baltica (Norway, Sweden, Estonia and

521 Russia) are more varied (Fig. 10), consistent with deposition in tectonically active basins (e.g.
522 Baarli et al., 2003; Dahlqvist and Bergström, 2005). In northern Estonia, Nestor and Einasto
523 (1997) recognised flooding levels consistent with events 4, 5 and 6 at Llandovery. This level
524 of detail is not replicated by other Baltic datasets, although most show a *revolutus* Biozone
525 deepening episode (B) (e.g. Johnson et al., 1991a; Baarli et al., 2003). Many of the
526 recalibrated Baltic curves also indicate a period of sustained Aeronian shallowing. In the
527 Russian Timan–Petchora Basin, this peaked during the *leptotheca* Biozone, but it is shown
528 elsewhere to have extended into the *convolutus* Biozone (E). The impact of a deepening that
529 spanned the late *convolutus* to early *sedgwickii* biozonal interval, consistent with the
530 conflation of flooding events 7, 8 and 9 and high-stand C, is seen throughout the Baltic
531 region. Also widely acknowledged are a late Aeronian shallowing (F) and a subsequent
532 *guerichi* Biozone deepening (10), the latter marked in Estonia by the transgressive base of the
533 Rumba Formation (e.g. Nestor and Nestor, 2002; but see Supplementary data).

534 Strata of *persculptus* Biozone age are absent from many circum-Iapetus sections (see Section
535 7a), but where preserved in Iowa and Illinois, on Anticosti Island and in Arctic Canada, there
536 is evidence of a deepening maximum (A) (e.g. Witzke and Bunker, 1996; Dewing, 1999;
537 Zhang and Barnes, 2002b; Melchin and Holmden, 2006; Long, 2007). Other curves show a
538 deepening episode extending from the Hirnantian that peaked at different times during the
539 early Rhuddanian (e.g. Johnson et al., 1991a; Nestor and Einasto, 1997; Copper and Long,
540 1998). Nonetheless, several regional base level curves, notably from North America, record a
541 subsequent high-order regression that, in common with the Llandovery area (D), peaked prior
542 to the *revolutus* Biozone and was followed by a deepening episode (4).

543 The Cornwallis Island (Arctic Canada) curve of Melchin and Holmden (2006) differs
544 significantly from other Laurentian, ‘Avalonian’ and Baltic datasets (Fig. 10). It shows the
545 early–mid Aeronian as a period of slowly rising base level that culminated in an early
546 *convolutus* Biozone high-stand, and the early *sedgwickii* Biozone as a time of falling base
547 level that peaked well below the base of the *guerichi* Biozone. From a comparison of depth-
548 controlled conodont assemblages, Zhang et al. (2006) concluded that Anticosti Island and
549 Cornwallis Island experienced very different tectonic and base level movement histories.

550 **6.5. Analysis: curves from other palaeoplates (Figs. 11, 12)**

551 Interpreting base level curves compiled for Llandovery successions that accumulated on other
552 early Silurian palaeoplates is more challenging. Many of these curves appear to focus on high
553 order events and very few extend down into the Hirnantian. An exception is the well-dated,
554 high southern palaeolatitude Gondwanan succession examined by Underwood et al. (1998).
555 This (Fig. 12, curve 21) provides evidence of a late Hirnantian flooding episode (2) that, in
556 common with the Llandovery area, culminated in an upper *persculptus* Biozone highstand
557 (A). A subsequent shoaling into the *atavus* to *acinaces* biozonal interval (commonly also
558 referred to as the *vesiculosus* graptolite Biozone) is also recognised in the Murzuq Basin of
559 Saharan North Africa (Legrand, 2003) (Fig. 12, curve 22), where Loydell et al. (2009; 2013)
560 view it as evidence for a glacioeustatic sea-level fall. However, the likely impact of
561 glacioisostasy in this region persuaded Johnson (2010) that the local record of base level

562 movements may not accurately reflect global events (see also Berry and Boucot, 1973).
563 Certainly, curves for more northerly Gondwanan successions, which typically show the
564 Rhuddanian as a time of generally rising and elevated base levels, more closely resemble
565 many global datasets (Fig. 8). The Gondwanan curves for Australia (Jell and Talent, 1989;
566 Talent et al., 2003) and the Himalayas (Talent and Bhargava, 2003) (Fig. 12, curves 23, 24),
567 and for parts of Cathaysia (South China) (Johnson et al., 1985; also Rong et al., 2003) and
568 Siberia (Artyushkov and Chekhovich, 2001; Yolkin et al., 2003) (Fig. 11) offer some support
569 for a high order, *revolutus* Biozone flooding maximum (B).

570 Many curves, including that for the Peri-Gondwanan Prague Basin (Fig. 12, curve 18), mirror
571 the Llandovery data in their depiction of the early-mid Aeronian as a time of falling or
572 lowered base levels. There is evidence locally of a shoaling peak close to the base of the
573 *convolutus* Biozone (E) followed by a high-stand event that could be viewed as a conflation
574 of flooding episodes 7, 8 and 9. However, a majority of the curves presented by Koren et al.
575 (2003) for Kazakhstan (Fig. 11) show only a base *sedgwickii* Biozone transgression (9).
576 Siberian datasets, including Tesakov et al. (1998), though they record Aeronian base level
577 movements on a range of scales, are significant for the lateral variability in base level
578 histories that they imply. Artyushkov and Chekhovich (2001) viewed this as evidence that
579 regional isostasy was more influential than eustasy. Many curves associate the *sedgwickii*-
580 *halli* biozonal interval with a period of shoal deposition (F) and, though the form of the
581 subsequent deepening episode differs markedly on curves for Cathaysia, Siberia, Peri-
582 Gondwana and Gondwanan North Africa and Australia, the *guerichi* Biozone is shown
583 overlapping a period of elevated base levels in all these areas (e.g. Kříž et al., 2003; Jell and
584 Talent, 1989; Talent et al., 2003). In contrast, the records of base level change during this
585 latter interval in other parts of Gondwana, in India and in Kazakhstan for example, show this
586 as a period of base level lowering.

587 7. Glacioeustatic credentials

588 Davies et al. (2009) assessed the latest Hirnantian facies present in the Type Llandovery area
589 that encompass events 1–3 of Fig. 6. These record the pulsed early progress in Wales of the
590 global transgression that immediately followed the period of maximum Gondwanan ice sheet
591 expansion (e.g. Hambrey, 1985; Ghienne, 2003; Ghienne et al., 2014). They suggested that,
592 following the deep erosion associated with the Hirnantian glacial maximum, it was only in
593 basin margin settings, or where there was deeply incised palaeotopography, that the earliest
594 phases of the late Hirnantian transgression were likely to be felt and its deposits preserved.
595 Such palaeotopography was locally effective in excluding much of the late Hirnantian
596 (*persculptus* Biozone) to Rhuddanian succession from the Laurentian interior (e.g. Witzke,
597 1992; Ross and Ross, 1996; Johnson and Baarli, 2007), Baltica (e.g. Nestor, 1997) and Africa
598 (e.g. Underwood et al., 1998). Such exclusion may account for the poor and inconsistent
599 record of events within this interval (see Section 8). However, it is now acknowledged that
600 this global transgressive event marked only the partial collapse of the ice sheet (e.g. Le Heron
601 and Craig, 2008). The discovery of Llandovery glacigenic deposits in South America (e.g.
602 Caputo, 1998) suggested to Dias-Martinez and Grahn (2007) that the locus of the

603 Gondwanan-based glaciation shifted over time, although facies of comparable age recently
604 reported from Libya (e.g. Le Heron et al., 2013) confirm that a diminished ice mass
605 continued to occupy parts of Africa. These findings support the widely held assumption that
606 many Llandovery base level events, both high and low order, provide a record of sea level
607 change linked to dynamic changes in the shape and extent of an extant South Polar Ice Sheet
608 (e.g. Ross and Ross, 1996; Loydell, 1998, 2007; Nestor et al., 2003; Zhang and Barnes,
609 2002b; Page et al., 2007; Haq and Schutter, 2008; Johnson, 2010; Munnecke et al., 2010). It
610 is argued that the changes in global climate and ocean state associated with these glacial
611 events are reflected in plots of stable isotope ratios and faunal flux, fostering the belief that
612 these too provide a proxy record of Llandovery glacioeustasy (e.g. Melchin and Holmden,
613 2006; Cramer et al., 2011a). The scale and duration of many Silurian base level events are
614 also seen as consistent with glacioeustatic forcing (e.g. Johnson and McKerrow, 1991),
615 vertical movements of 10s of metres over time periods of less than a million years generally
616 being seen as too great for epeirogenic effects to achieve on their own (e.g. Miller et al.,
617 2005; Csato and Catuneanu, 2012). However, this is not to say that glacioeustasy alone was
618 instrumental, or was always dominant, particularly in tectonic settings such as the faulted
619 margin of the Welsh Basin, where high rates of subsidence were likely to have been a
620 significant factor (cf. Gawthorpe et al., 1994).

621 **7.1. Analysis: known glacial events (Fig. 13)**

622 The limited dating available for the South American glaciogenic successions, reviewed by
623 Kaljo et al. (2003), is based principally on chitinozoans recovered from interbedded marine
624 deposits. These data suggest that an extensive South Polar ice mass continued to occupy that
625 part of Gondwana during the early Rhuddanian. The late Rhuddanian deepening seen in most
626 global and some regional curves appears to reflect the first major period of melting of the
627 South American ice mass (e.g. Dias-Martinez and Grahn, 2007). Subsequently, according to
628 Caputo's (1998) log of glaciogenic deposits (Fig. 13), a re-advance during the *triangulatus*
629 Biozone established an extensive, slowly down-wasting ice mass that was sustained
630 throughout much of the Aeronian, prior to an abrupt and marked retreat at or close to the base
631 of the *sedgwickii* Biozone. This preceded a late Aeronian to early Telychian re-advance and
632 there is evidence also for a discrete late Telychian glaciation. Periods of ice retreat
633 (interglacials), it can be assumed, were also periods of sea level rise.

634 Given the paucity and nature of the fossil evidence, the suspicion persists that the dating of
635 these glacial events is based partly on their 'best fit' to the 'standard' Llandovery sea level
636 curve and lacks both independent corroboration and precision. At face value, the findings
637 from South America can be seen broadly to endorse glacioeustatic credentials of the late
638 Rhuddanian (*revolutus* Biozone) base level events seen at Llandovery (4, 5, B). Waxing and
639 waning of the Aeronian ice sheet may account for the base level movements noted at the base
640 of the *magnus* Biozone (6) and within the *leptotheca-convolutus* biozonal interval (7, 8),
641 though the limited data from South America offer nothing to confirm this and these are the
642 events that many other datasets fail to depict (see Section 8). Evidence of a discrete mid
643 Aeronian ice advance on the scale and duration implied by the prograde seen at Llandovery

644 (E) is also lacking. However, episodes of interglacial deepening are seen to offer a ready
645 explanation for the *sedgwickii* Biozone (9, C) and *guerichi* Biozone (10) deepening events.

646 **7.2. Analysis: proxy records of climate change (Figs. 13, 14)**

647 Key datasets include those compiled for a range of stable isotopes and for faunal events.
648 Here, any alignment of trends and peaks with those shown by base level curves does not offer
649 direct proof of glacially linked sea level movements, but does imply that there may have been
650 a causative link (e.g. Munnecke et al., 2010).

651 **7.2.1. Isotopic trends and excursions**

652 Curves showing temporal variations in $\delta^{18}\text{O}$ and $\delta^{13}\text{C}$ are thought to reflect changes in global
653 temperature and ice volume, and organic productivity and carbon burial respectively (e.g.
654 Azmy et al., 1998, 1999; Cooper and Sadler, 2004; Page et al., 2007; Munnecke et al., 2010;
655 Cramer et al., 2011a; McLaughlin et al., 2012; Melchin et al., 2013; Vandenbroucke et al.,
656 2013). A review of the causal relationships between environmental and isotopic flux is
657 outside the scope of this paper (see Griffiths, 1998; Gradstein et al., 2012 and references
658 therein). The mechanisms by which isotopic fractionation is achieved are hotly debated (e.g.
659 Attendorn and Bowen, 1997; Melchin and Holmden, 2006; Stanley, 2010; Gouldley et al.,
660 2010) and the patterns of flux in oxygen and carbon isotope values do not always match one
661 another (e.g. Long, 1993). Nevertheless, as many of the positive excursions seen in these
662 isotope datasets appear to be widely correlatable, such curves have been seen to offer a proxy
663 record of Late Ordovician and Silurian climatic events and, by extension, associated
664 glacioeustasy.

665 The abundant $\delta^{13}\text{C}$ isotope data now available for the Hirnantian Series generally support
666 linked climatic and sea level changes that facies and faunal variations appear to record,
667 including a *persculptus* Biozone deepening maximum (A) (e.g. Underwood et al., 1997;
668 Kaljo et al., 2008; Desrochers et al., 2010; Finnegan et al., 2011). Published curves for the
669 Rhuddanian to early Telychian interval, including Cramer et al.'s (2011a) synthesis of
670 published $\delta^{13}\text{C}$ carb data, depict negative excursions consistent with the late Rhuddanian
671 high-stand and its component events (4, 5 and B) (e.g. Melchin and Holmden, 2006;
672 Gouldley et al., 2010). Support for the pronounced flooding surface (7) that terminated the
673 *convolutus* Biozone Ceg¹ prograde, for an early *sedgwickii* Biozone deepening episode (9),
674 and for a deepening event that spanned the Aeronian–Telychian boundary (10), is also
675 provided. Positive $\delta^{13}\text{C}$ excursions in the early and late Aeronian have been linked to periods
676 of global cooling, glacial advance and sea level fall (Fig. 13). Cramer et al. (2011a)
677 recognised their early Aeronian positive excursion as peaking during the *triangulatus*
678 Biozone. This would endorse the glacioeustatic credentials of the Ceg⁰ progradation and its
679 defining flooding event (6), but it is unclear whether this level of precision is justified (e.g.
680 Melchin and Holmden, 2006). The isotopic evidence for a *sedgwickii-halli* biozone shoaling
681 event (F) is also ambiguous, both in terms of its timing and impact. The regional curves of
682 Melchin and Holmden (2006) and Gouldley et al. (2010; based on Kaljo and Martma, 2000)
683 differ from global sea level curves (Fig. 8) in providing support for a mid Rhuddanian

684 shallowing as seen at Llandovery (D). Isotope excursions on the brachiopod-derived $\delta^{18}\text{O}$
685 curve of Azmy et al. (1998) broadly align with the main $\delta^{13}\text{C}$ excursions and offer support for
686 Llandovery highstands during the late Rhuddanian (B) and mid Aeronian and for early and
687 late Aeronian glacially induced regressions (Fig. 13). In common with other datasets, support
688 for a *leptotheca*-lower *convolutus* Biozone low-stand event (E) is lacking and the impacts of a
689 base *sedgwickii* Biozone deepening are not seen. However, the processes that led to these
690 excursions, particularly the role played by biodiagenesis, are debated, and many authors
691 question the unambiguous relationship between sea levels and $\delta^{18}\text{O}$ values (see Munnecke et
692 al., 2010).

693 **7.2.2. Graptolite faunal flux**

694 Many of the flooding surfaces that define the Llandovery area prograde sequences are
695 associated with the local FADs of biozonal graptolite assemblages. This implies an empirical
696 relationship between base level events and changes in contemporary graptolite assemblages.
697 Melchin et al. (1998) (also Storch, 1995) discussed the complex interplay of climatic, oceanic
698 and ecological factors that likely contributed to the flux in Silurian graptolite populations.
699 Cooper et al. (2014) pointed to an empirical relationship between Llandovery population
700 dynamics and the global $\delta^{13}\text{C}$ curve, from which they too inferred climatic influence. It
701 follows that the plots produced by these studies provide a further proxy means of assessing
702 the impacts of glacioeustasy at Llandovery (Fig. 14).

703 In general, these plots fail to endorse biozonal scale, low order base level events, but trends
704 that match the high order, Type Llandovery curve are clearly apparent. Cooper et al. (2014)
705 recorded patterns of reduced extinction and elevated origination for highstands that span the
706 *persculptus*–*ascensus*–*acuminatus* (A) interval and the *revolutus*–*magnus* biozones (B). The
707 flux in populations also mirror the mid Rhuddanian (D) and mid Aeronian (E) shoaling
708 episodes and the rising base levels associated with the *convolutus*–*sedgwickii* biozonal
709 boundary (C), though in these cases the relationships between diversity, extinction and
710 putative sea level movements appear contrary to that proposed by Melchin et al. (1998). The
711 impacts of a late *sedgwickii*–*halli* Biozone shoaling event (F) and subsequent *guerichi*
712 Biozone transgression (10) are also evident in the graptolite plots.

713 **7.2.3. Oceanic and climate models**

714 It is pertinent briefly to discuss the influential, if controversial oceanic model of Jeppsson
715 (1990, 1998). Based on empirical associations of sedimentary facies and faunas, particularly
716 patterns of conodont extinction, Jeppsson (1990, 1998) contended that the Silurian global
717 ocean passed repeatedly between two distinct states: ‘primo episodes’ linked to periods of
718 glacial advance; and ‘secundo episodes’ associated with times of ice retreat (see Johnson,
719 2006). It follows that glacially driven movements in sea level should closely mirror the
720 pattern of primo and secundo states. Page et al. (2007), in their extension to this model,
721 argued for a cyclical, self-regulating mechanism. They contended that the sequestration of
722 carbon in deep water black shales and shallow water carbonates during periods of elevated
723 global temperature led to cooling, glacial re-advance, and sea level fall. This, in turn,

724 triggered the shutdown of mass sequestration, rising atmospheric CO₂ levels then promoting
725 the next warming phase. Whether glacioeustasy was the cause or the effect is a moot point,
726 but it is clear that there should be a close alignment of chemostratigraphical and sea level
727 events.

728 Many dispute the universal applicability of the Jeppsson model and point to inconsistencies
729 between its key events and those based on other sedimentary and fossil criteria (e.g. Johnson,
730 2006). Nevertheless, Jeppsson's (1998) schematic model of changing sea level elevations
731 offers support for curves that show the Rhuddanian and early Aeronian as a period of
732 elevated sea levels (e.g. Loydell, 1998) (Fig. 14). There is no evidence for a putative early
733 Aeronian glacial advance, but there is evidence for mid-Aeronian shallowing linked to the
734 *convolutus* Biozone (E). Jeppsson's (1998) Sandvika Event records a primo-secundo
735 transition that is consistent with an early *sedgwickii* Biozone deepening (9 and C), but his
736 model is at odds with many other datasets in suggesting that the resulting high-stand persisted
737 throughout the remainder of the biozone and much of the early Telychian.

738 **8. An index of Llandovery eustasy**

739 In the pursuit of 'practical eustasy', there is always a temptation to invoke the periodic
740 prevalence of local forces to explain discrepancies between regional and global trends, both
741 in timing and scale. Subsidence is always on hand to account for regional deepening events
742 that fall outside eustatic templates, just as tectonic uplift can be used to account for
743 unexpected shoaling episodes. The assumption by critics of deep-time eustatic research is that
744 it is for the exponents of eustasy to demonstrate the widespread correlatability of events
745 (Miall, 2004). Yet, the absence of objective proof for one forcing factor does not of itself
746 confirm the importance of others. For the relative roles played by tectonism and isostasy in
747 fashioning local stratigraphies to be properly quantified, the relative impact of contemporary
748 eustasy in creating and destroying accommodation space must also be evaluated (e.g.
749 Ettensohn and Brett, 1998; Artyushkov and Chekhovich, 2001, 2003; Dahlqvist and
750 Bergström, 2005). The need to calibrate the ambient eustatic signal is essential to both camps,
751 particularly during 'icehouse' periods when ongoing glacioeustasy can be anticipated (e.g.
752 Zecchin 2007; Csato and Catuneanu, 2012). The Eustasy Index methodology presented
753 herein is intended as a possible first step towards untangling these conflicting factors at the
754 regional level.

755 **8.1. Eustasy index methodology**

756 The range of techniques used to compile the 62 datasets examined as part of this study, allied
757 to their wide palaeogeographical distribution (Fig. 1; Table 1), supports their use in an
758 attempt to quantify the role played by eustasy in shaping the Type Llandovery succession.
759 Each of the twelve UK graptolite biozones that have been the focus for this study (upper
760 *persculptus* to *guerichi* biozones) have been arbitrarily subdivided into three to create a
761 matrix with 36 rows for scoring the levels of similarity (see Supplementary data). For each of
762 the studied datasets (Figs. 7–14), every subdivision that displays a trend comparable to (or,
763 for proxy datasets, inferred to be consistent with) the low order curve at Llandovery – and is

764 coloured blue or red for 50% or more of its duration – has been given a score of 1.0 (see
765 Eustasy Index scores in Supplementary data). Segments displaying trends that compare more
766 closely with the high order base level curve at Llandovery rather than the low order curve,
767 indicated by the diagonal ornament on Figs. 7 to 14, are given a score of 0.5.

768 Account is also taken of the incomplete nature of many datasets. Where this reflects
769 limitations of outcrop or exposure, or, as for some proxy curves, the restricted range of the
770 sampled interval (e.g. Underwood et al., 1997), the ‘missing’ subdivisions are omitted from
771 the scoring process. More difficult to account for are gaps that record the local impacts of
772 emergence and erosion. Those of short duration – a subdivision or less – are included since it
773 is reasonable to infer that they record the impacts of a single, short-lived episode of local base
774 level lowering. However, where non-sequences span several subdivisions and record
775 prolonged and/or multiple phases of emergence, it is likely that evidence of local base level
776 movements has been lost. Therefore, with the exception of the final subdivision prior to the
777 resumption of deposition, these too are omitted from the scoring mechanism. Analysis of the
778 levels of representation (Fig. 15) confirms that late Hirnantian and early Rhuddanian
779 deposits, which might otherwise record the early progress of the post-glacial maximum
780 transgression, have been widely excluded from many of the areas for which Llandovery base
781 level and proxy curves have been compiled. The score for each subdivision across the
782 complete range of datasets, expressed as a percentage of its level of representation, provides
783 the Eustasy Index (EI) for that section of the Type Llandovery base level curve (Fig. 15 and
784 Supplementary data):

$$785 \qquad \qquad \qquad EI = (EI_r/tR)\% \qquad \qquad \qquad (1)$$

786 where EI_r is the sum of the Eustasy Index raw scores for a subdivision and tR is the total
787 number of datasets in which that subdivision is represented.

788 The scores obtained for each subdivision of the Llandovery curve should be viewed as
789 providing an indication only of the likelihood that eustasy was a significant factor rather than
790 a measure of the relative importance of sea level movements in any absolute sense. Since
791 Llandovery area events that obtain the highest EI scores are those recognised on a majority of
792 the other datasets, it follows that eustasy was likely a factor in shaping these events wherever
793 they have been identified. Conversely, intervals with low EI values, for which matching
794 events in other successions are least apparent, are more likely to have been periods when
795 regional influences on the Llandovery succession were dominant. Importantly, this need not
796 imply that eustasy was insignificant during low scoring events (see below), or was not the
797 dominant factor in shaping other datasets.

798 **8.2. Eustasy Index results (Fig. 15)**

799 At first sight, the results of this analysis appear paradoxical. Their high eustasy indices show
800 that the Type Llandovery highstands that peaked during the *persculptus* (A), *revolutus* (B)
801 and early *sedgwickii* biozone (C) align with episodes of global deepening, as does the basal
802 *guerichi* Biozone flooding event (10). Many of the lower order flooding events that

803 contributed to these deepening episodes, in the early *revolutus* Biozone and linked to the
804 appearance of *magnus* and mid and late *convolutus* biozonal assemblages, are also inferred to
805 have had a strong eustatic component. However, the intervening lowstands are characterised
806 by low Eustasy Index values, notably in the early–mid Rhuddanian and mid Aeronian
807 intervals.

808 The low eustasy indices for the principal Llandovery area progrades perhaps testifies to their
809 accumulation along the margins of a tectonically active basin, a setting where regional
810 epeirogenesis operated alongside eustasy to rejuvenate source areas and create
811 accommodation space. Widespread source area uplift coincident with the early stages of the
812 Scandian Orogeny and reactivation of the Tornquist Zone in Europe (e.g. Johnson et al.,
813 1991a; Baarli et al., 2003), and with late stages of the Taconic Orogeny in North America
814 (e.g. Ettensohn and Brett, 1998; also Brett et al., 1998), can be invoked as an alternative or
815 enhancing mechanism for the marked early–mid Rhuddanian shallowing not widely seen
816 outside the circum-Iapetus realm (but see below). It is principally the datasets from this same
817 region that offer evidence of a *leptotheca* to lower *convolutus* Biozone shoaling episode on
818 the scale observed at Llandovery. However, such analysis illustrates the difficulties of
819 ‘practical eustasy’ as a thesis that requires us to focus on the similarities in the datasets. An
820 alternative interpretation, consistent with its tectonic setting, is to see the influence of
821 regional epeirogenesis on Type Llandovery base levels as normally dominant (cf. Gawthorpe
822 et al., 1994). Periods with a high Eustasy Index can then be seen as episodes either of tectonic
823 quiescence, during which global sea level movements were able preferentially to influence
824 sedimentation, or when such movements were of sufficient magnitude and rate to overwhelm
825 the regional signal. It may not be a coincidence that it is base level movements linked to
826 interglacial high-stand events that are most clearly identified as eustatic at Llandovery (Fig.
827 13). The rapid and substantial rises in sea level associated with the disintegration and collapse
828 of maritime ice sheets are those most likely to overwhelm regional epeirogenic processes,
829 whereas the slowly falling sea levels that accompany periods of gradual ice sheet expansion
830 are less able to outstrip regional effects as the most active forcing factors (e.g. Berry and
831 Boucot, 1973; Morton and Suter, 1996). Yet, it remains curious that at least two of the major
832 lowstand episodes seen at Llandovery overlap with known periods of ice sheet expansion
833 seen in South America (Fig. 13) when glacioeustatic drawdown would be anticipated to have
834 had an impact.

835 **8.3. Significance of glacioeustatic, epeirogenic and orogenic interactions (Fig. 16)**

836 EI scores, as obtained for the Type Llandovery succession, are a function of global and
837 regional forcing factors, the detailed form of any regional base level curve reflecting the
838 interplay between eustasy and near-field orogenesis, epeirogenesis and sediment supply. High
839 levels of subsidence can serve locally to exaggerate the impacts of marine transgressions, in
840 terms of both rate and reach, and to offset and mask the effects of falling sea levels (cf.
841 Artyushkov and Chekhovich, 2003). Changes in sea level on at first drained and then flooded
842 shelves are also accompanied by the removal and then the imposition of hydrostatic and
843 sediment load (e.g. Long, 2007). Such changes in load will be accommodated either by

844 isostasy or, in tectonically active settings, by the differential movement of faulted blocks (e.g.
845 McGuire, 2012; Stammer et al., 2013; Steffen et al., 2014). Similar adjustments must have
846 affected early Silurian source areas and depocentres, notably during periods of falling sea
847 level when, it can be inferred, the deep erosion of a landscape supporting little vegetation
848 (e.g. Wellman et al., 2013) resulted in the rapid transfer of sediment to marine shelves and
849 basins (e.g. Davies and Gibling, 2010). Hence, glacioeustatic regressions and transgressions
850 would themselves have been forcing factors in regional Silurian epeirogenesis.

851 Accordingly, low Eustasy Index scores should not be taken as evidence that changes in sea
852 level were insignificant during the development of Llandovery area lowstands (Fig. 16).
853 Coeval glacioeustasy likely contributed to these base level events, but, as sediment source
854 areas were exposed, the rapid transfer of sediment to the subsidence prone basin margin
855 triggered a self-sustaining epeirogenic response that quickly outstripped eustasy as the
856 dominant forcing factor. Local base level movements then diverged from global trends.
857 Viewed in this way, Eustasy Index results can be seen not simply as offering a measure of
858 when eustatic forcing was dominant, but also of changing rates of eustasy (or eustatic flux).
859 Intervals with high eustasy indices appear to equate with periods of rapid and/or frequent sea
860 level movement. Periods with lower scores may record times when sea levels changed more
861 slowly and epeirogenic forcing was able to dominate. These may have been periods of slowly
862 rising or static sea level, but can also be seen as consistent with the slow, but possibly
863 substantial falls in sea level that accompanied episodes of sustained glacial advance. Such
864 analysis negates the need to invoke episodic tectonic events. It implies a self-regulating
865 mechanism to account for why global and regional influences alternated in their impacts on
866 local sedimentation, and it explains why the eustasy indices for parts of the Type Llandovery
867 succession fail to track precisely the pronounced falls in sea level that must have
868 accompanied known periods of ice sheet growth in South America (Caputo, 1998; Dias-
869 Martinez and Grahn, 2007; Fig. 13). This model can be applied more widely. It is likely to
870 have been interglacial flooding events that were most successful in drowning cratonic
871 interiors and therefore these that are recorded preferentially by base level curves for cratonic
872 successions. It is clear too that ‘practical eustasy’ as a methodology has tended to focus on
873 the timing of flooding events rather than lowstands (e.g. Johnson et al., 1991b) and therefore
874 unsurprising that Johnson's (1996, 2006, 2010) ‘standard’ sea level curve for the early
875 Silurian, based on a ‘type district’ in Laurentian Iowa, is also biased towards such events.

876 Subsequently, in Wales, the Telychian onset of a more dynamic phase of regional tectonism,
877 though it seems initially coincident with glacioeustatic deepening, signalled a long-term
878 departure from the far field influence of glacial activity on sedimentation. The erosion of
879 upper Aeronian and lower Telychian strata across much of Laurentia and eastern Baltica
880 suggests that broadly coeval effects were again widely felt throughout circum-Iapetus regions
881 where, in Europe, they record an encroaching Scandian orogenic front (e.g. Kirkland et al.,
882 2006).

883 **8.4. Wider implications**

884 The Eustasy Index calculations for the Llandovery succession have implications for global
885 sea level models. Contrary to Haq and Schutter (2008), these calculations strongly endorse
886 the separate early and late Aeronian highstand events that the majority of global curves depict
887 (Fig. 8). Johnson (2010) departed from previous models (e.g. Johnson, 1996) in showing the
888 early Telychian as a lowstand, but the Llandovery area data offer support for curves that
889 recognise this as a time of rising or elevated sea levels (e.g. Johnson et al., 1991b; Loydell,
890 2007; Page et al., 2007). Of particular interest is the high Eustasy Index obtained for a
891 discrete late *persculptus* Biozone highstand seen at Llandovery (Fig. 15).

892 The Type Llandovery base level curves fail to offer support for the precise timing, duration
893 and scale of glacial lowstands. Nevertheless, glaciogenic deposits in South America show
894 that separate episodes of Gondwanan ice re-advance during the Aeronian (Fig. 13; see
895 Section 7) overlap two of the main Llandovery area lowstands characterised by reduced rates
896 of eustatic flux (see above). The Llandovery area findings challenge researchers to look for
897 evidence of such activity during the comparable Rhuddanian interval also. The findings of
898 Dias-Martinez and Grahn (2007) imply that an extensive ice mass was in place in South
899 America at this time. The work in Africa of Underwood et al. (1998), Legrand (2003) and
900 Loydell et al. (2009; 2013) suggests this may, in part, have been the product of a discrete
901 intra-Rhuddanian re-advance (Fig. 12) for which some proxy datasets offer support (Figs. 13,
902 14). Confirmation of such an event has implications for the interpretation of shallow and deep
903 water Rhuddanian facies in Wales previously seen as unrelated to eustatic events (e.g. Davies
904 and Waters, 1995; Schofield et al., 2009; Davies et al., 2013). It would also imply that all the
905 most widely cited global curves (Fig. 8) may be in error in depicting the late Hirnantian to
906 late Rhuddanian as a period of almost uninterrupted rising sea levels.

907 It follows that the Eustasy Index methodology should now be applied more widely and that
908 many of the datasets examined herein could be the focus of similar analysis. The results of
909 such studies will serve to distinguish the impacts of local epeirogenesis and, when viewed
910 collectively, allow the ‘standard sea level curve’ for the Llandovery to be refined. Moreover,
911 this methodology has the potential to be used in assessing the base level credentials of
912 correlatable marine successions of any age.

913 **9. Conclusions**

914 For the first time, a detailed and biostratigraphically well-constrained sequence stratigraphy is
915 available for the Type Llandovery Series succession in mid Wales. The recognition of a
916 series of prograde sequences with bounding flooding surfaces has enabled the construction of
917 both high and low order relative base level movement curves for those parts of the succession
918 that preceded the onset of Telychian tectonism in Wales. Qualified comparisons with widely
919 cited sea level curves, isotope data, examples of facies and faunal flux and nascent climatic
920 models allow the relative importance of global (eustatic) and regional (tectonic/isostatic)
921 forcing to be evaluated, and the far field impacts of glacioeustasy to be tested.

922 The concept of a Eustasy Index emerges as a useful tool to evaluate the potentially complex
923 interplay of local, regional and global forcing factors that shaped base level curves. Its

924 application to the Llandovery succession suggests the presence of ‘eustatic windows’ linked
925 to interglacial global highstands. In contrast, the glacioeustasy that accompanied the slow re-
926 growth of contemporary ice sheets is suggested to have triggered regional epeirogenic
927 responses that saw base level patterns during the main Llandovery area lowstands diverge
928 from global trends, negating the need to invoke episodic tectonic events. Such an analysis
929 invites speculation that a significant ice advance unrecognised by current global Silurian sea
930 level models occurred during the mid Rhuddanian. Subsequently, the Telychian response to
931 the Scandian Orogeny, though initially coincident with glacioeustatic deepening, signalled a
932 long-term departure from the far field influence of glacial activity on sedimentation in Wales.

933 It is anticipated that future application of the Eustasy Index methodology to other marine
934 successions will similarly highlight the impacts of local epeirogenesis and, in so doing, allow
935 a more precise history of global sea level activity to be elucidated, both during the
936 Llandovery and for other time intervals.

937 **Acknowledgments**

938 This widely ranging review has only been possible with the help and advice of numerous co-
939 workers. Work on the Llandovery area succession has benefited enormously from the input of
940 staff from the British Geological Survey, most notably David Schofield and David Wilson.
941 Specific queries relating to ongoing biostratigraphical recalibration for the Llandovery Series
942 were addressed by Brad Cramer (Iowa University), Jacques Verniers (Ghent University) and
943 the late Dick Aldridge (University of Leicester). The figures are testimony to the skill and
944 professionalism of Antony Smith and Ian Gully, the latter sadly also now deceased, both of
945 Aberystwyth University. We wish to dedicate this paper to both Dick and Ian. Annalisa
946 Ferretti and an unnamed reviewer are thanked for their constructive comments. Jeremy
947 Davies and Stewart Molyneux publish with the permission of the Executive Director, British
948 Geological Survey. This study is a contribution to IGCP 591 ‘The Early to Middle Paleozoic
949 revolution’.

950

951 **References**

952 Aldridge, R.J., Schonlaub, H.P., 1989. Conodonts. In: Holland, C.H., Bassett, M.G. (Eds.), A
953 Global Standard for the Silurian System, Geological Series 9. National Museum of Wales,
954 pp. 274–279.

955 Aldridge, R.J., Jeppsson, L., Dorning, K.J., 1993. Early Silurian oceanic episodes and events.
956 *J. Geol. Soc. Lond.* 150, 501–513.

957 Artyushkov, E.V., Chekhovich, P.A., 2001. The East Siberian basin in the Silurian: evidence
958 for no large-scale sea-level changes. *Earth Planet. Sci. Lett.* 193, 183–196.

959 Artyushkov, E.V., Chekhovich, P.A., 2003. Silurian sedimentation in East Siberia. Evidence
960 for variations in the rate of tectonic subsidence occurring without any significant sea-level

- 961 changes. In: McCann, T., Saintot, A. (Eds.), Tracing Tectonic Deformation Using the
962 Sedimentary Record. Geol. Soc. Lond., Spec. Publ. 208, pp. 321–350.
- 963 Attendorn, H.G., Bowen, R., 1997. Radioactive and Stable Isotope Geology. Springer.
- 964 Azmy, K., Veizer, J., Bassett, M.G., Copper, P., 1998. Oxygen and carbon isotopic
965 composition of Silurian brachiopods: implications for coeval seawater and glaciations. Geol.
966 Soc. Am. Bull. 110, 1499–1512.
- 967 Azmy, K., Veizer, J., Wenzel, B., Bassett, M.G., Copper, P., 1999. Silurian strontium isotope
968 stratigraphy. Geol. Soc. Am. Bull. 111, 475–483.
- 969 Baarli, B.G., 1986. A biometric re-evaluation of the Silurian brachiopod lineage *Stricklandia*
970 *lens/S. laevis*. Palaeontology 29, 187–205.
- 971 Baarli, B.G., 1988. Bathymetric co-ordination of proximality trends and level bottom
972 communities: a case study from the Lower Silurian of Norway. PALAIOS 3, 577–587.
- 973 Baarli, B.G., 1998. Silurian cycles and proximality-trend analysis of tempestite deposits. In:
974 Landing, E., Johnson, M.E. (Eds.), Silurian Cycles: Linkages of Dynamic Stratigraphy With
975 Atmospheric, Oceanic and Tectonic Changes. New York State Museum Bulletin 491, pp. 75–
976 88.
- 977 Baarli, B.G., Johnson, M.E., 1988. Biostratigraphy of selected brachiopods from the
978 Llandovery Series (Lower Silurian) of the Oslo region. Nor. Geol. Tidsskr. 68, 259–274.
- 979 Baarli, B.G., Brande, S., Johnson, M.E., 1992. Proximality-trends in the Red Mountain
980 Formation (Lower Silurian) of Birmingham, Alabama. Okla. Geol. Surv. Bull. 145, 1–17.
- 981 Baarli, B.G., Johnson, M.E., Antoshkina, A.I., 2003. Silurian stratigraphy and
982 palaeogeography of Baltica. In: Landing, E., Johnson, M.E. (Eds.), Silurian Lands and Seas:
983 Palaeogeography Outside of Laurentia. New York State Museum Bulletin 492, pp. 3–34.
- 984 Baker, S.J., 1981. The graptolite biostratigraphy of a Llandovery outlier near Llanystumdwy,
985 Gwynedd, North Wales. Geol. Mag. 118, 355–365.
- 986 Bassett, M.G., 1989. Brachiopods. In: Holland, C.H., Bassett, M.G. (Eds.), A Global Standard
987 for the Silurian System, Geological Series 9. National Museum of Wales, pp. 232–242.
- 988 Bergström, S.M., Chen, X., Gutiérrez-Marco, J.C., Dronov, A., 2009. The new
989 chronostratigraphic classification of the Ordovician System and its relations to major regional
990 series and stages and to $\delta^{13}\text{C}$ chemostratigraphy. Lethaia 42, 97–107.
- 991 Berry, W.B.N., Boucot, A.J., 1970. Correlation of the North American Silurian rocks. Geol.
992 Soc. Am. Spec. Publ. 102, 1–289.

- 993 Berry, W.B.N., Boucot, A.J., 1973. Glacio-eustatic control of late Ordovician–Early Silurian
994 platform sedimentation and faunal changes. *Geol. Soc. Am. Bull.* 84, 275–284.
- 995 Blackett, E., Page, A., Zalasiewicz, J.A., Williams, M., Rickards, R.B., Davies, J.R., 2009. A
996 refined graptolite biostratigraphy for the late Ordovician–early Silurian of central Wales.
997 *Lethaia* 43, 83–96.
- 998 Boucot, A.J., 1975. *Evolution and Extinction Rate Control*. Elsevier, New York.
- 999 Brenchley, P.J., Cullen, B., 1984. The environmental distribution of associations belonging to
1000 the Hirnantia fauna—evidence from North Wales and Norway. In: Bruton, D.L. (Ed.),
1001 *Aspects of the Ordovician System. Palaeontological Contributions from the University of*
1002 *Oslo* 295, pp. 113–125.
- 1003 Brett, C.E., Baarli, B.G., Chowns, T., Cotter, E., Driese, S., Goodman, W., Johnson, M.E.,
1004 1998. Early Silurian condensed intervals, ironstones, and sequence stratigraphy in the
1005 Appalachian Foreland Basin. In: Landing, E., Johnson, M.E. (Eds.), *Silurian Cycles:*
1006 *Linkages of Dynamic Stratigraphy with Atmospheric, Oceanic, and Tectonic Changes*. New
1007 *York State Museum Bulletin* 491, pp. 89–143.
- 1008 Brett, C.E., Ferretti, A., Histon, K., Schönlaub, H.P., 2009. Silurian sequence stratigraphy of
1009 the Carnic Alps, Austria. *Palaeogeogr. Palaeoclimatol. Palaeoecol.* 279, 1–28.
- 1010 Burgess, N.D., 1991. Silurian cryptospores and miospores from the type Llandovery area,
1011 south-west Wales. *Palaeontology* 34, 575–599.
- 1012 Caputo, M.V., 1998. Ordovician–Silurian glaciations and global sea-level changes. In:
1013 Landing, E., Johnson, M.E. (Eds.), *Silurian Cycles: Linkages of Dynamic Stratigraphy With*
1014 *Atmospheric, Oceanic and Tectonic Changes*. *New York State Museum Bulletin* 491, pp. 15–
1015 25.
- 1016 Catuneanu, O., Galloway, W.E., Kendall, C.G.St.C., Miall, A.D., Posamentier, H.W.,
1017 Strasser, A., Tucker, M.E., 2011. Sequence stratigraphy: methodology and nomenclature.
1018 *Newsl. Stratigr.* 44, 73–245.
- 1019 Cave, R., Hains, B.A., 1986. *Geology of the country between Aberystwyth and Machynlleth.*
1020 *Memoir of the British Geological Survey. The Stationary Office, London (Sheet 163*
1021 *(England and Wales))*.
- 1022 Challands, T.J., Armstrong, H.A., Maloney, D.P., Davies, J.R., Wilson, D., Owen, A.W.,
1023 2008. Organic-carbon deposition and coastal upwelling at mid-latitudes during the Upper
1024 Ordovician (Late Katian): a case study from the Welsh Basin, UK. *Palaeogeogr.*
1025 *Palaeoclimatol. Palaeoecol.* 273, 395–410.

- 1026 Challands, T.J., Vandenbroucke, T.R.A., Armstrong, H.A., Davies, J.R., 2014. Chitinozoan
1027 biozonation in the upper Katian (Ashgill) and Hirnantian of the Welsh Basin, UK. *Rev.*
1028 *Palaeobot. Palynol.* 210, 1–21.
- 1029 Cherns, L., Cocks, L.R.M., Davies, J.R., Hillier, R.D., Waters, R.A., Williams, M., 2006.
1030 Silurian: the influence of extensional tectonics and sea-level changes on sedimentation in the
1031 Welsh Borderland and on the Midland Platform. In: Brenchley, P.J., Rawson, P.F. (Eds.), *The*
1032 *Geology of England and Wales*, second edition. The Geological Society, London, pp. 75–
1033 102.
- 1034 Cocks, L.R.M., 1989. The Llandovery Series in the Llandovery area. In: Holland, C.H.,
1035 Bassett, M.G. (Eds.), *A Global Standard for the Silurian System*, Geological Series 9.
1036 National Museum of Wales, Cardiff, pp. 36–50.
- 1037 Cocks, L.R.M., Fortey, R.A., 1982. Faunal evidence for oceanic separations in the Palaeozoic
1038 of Britain. *J. Geol. Soc. Lond.* 139, 467–480.
- 1039 Cocks, L.R.M., Rickards, R.B., 1969. Five boreholes in Shropshire and the relationships of
1040 shelly and graptolitic facies in the Lower Silurian. *Q. J. Geol. Soc. Lond.* 124, 213–238.
- 1041 Cocks, L.R.M., Fortey, R.A., 1990. Biogeography of Ordovician and Silurian faunas. In:
1042 McKerrow, W.S., Scotese, C.R. (Eds.), *Palaeozoic Palaeogeography and Biogeography*.
1043 *Geol. Soc. Lond. Mem.* 12, pp. 97–104.
- 1044 Cocks, L.R.M., Toghil, P., Ziegler, A.M., 1970. Stage names within the Llandovery Series.
1045 *Geol. Mag.* 107, 79–87.
- 1046 Cocks, L.R.M., Woodcock, N.H., Rickards, R.B., Temple, J.T., Lane, P.D., 1984. The
1047 Llandovery Series of the type area. *Bull. Br. Mus. Nat. Hist. Geol. Ser.* 38, 131–182.
- 1048 Cocks, L.R.M., McKerrow, W.S., Verniers, J., 2003. The Silurian of Avalonia. In: Landing,
1049 E., Johnson, M.E. (Eds.), *Silurian Lands and Seas: Paleogeography Outside of Laurentia*.
1050 *New York State Museum Bulletin* 493, pp. 35–53.
- 1051 Cooper, R.A., Sadler, P.M., 2012. The Ordovician Period. In: Gradstein, F.M., Ogg, J.G.,
1052 Schmitz, M.D., Ogg, G.M. (Eds.), *The Geologic Time Scale 2012*. Elsevier, pp. 489–523.
- 1053 Cooper, R.A., Sadler, P.M., Munnecke, A., Crampton, J.S., 2014. Graptoloid evolutionary
1054 rates track Ordovician–Silurian climate change. *Geol. Mag.* 151, 349–364.
- 1055 Cooper, R.A., Sadler, P.M., 2004. The Ordovician system. In: Gradstein, F., Ogg, J., Smith,
1056 A. (Eds.), *A Geologic Time Scale*. Cambridge University Press, pp. 165–187.
- 1057 Copper, P., Long, D.G.F., 1998. Sedimentology and paleontology of the Late Ordovician
1058 through Early Silurian shallow water carbonates and reefs of the Anticosti Island, Quebec. In:
1059 Desrochers, A., Copper, P., Long, D.G.F. (Eds.), *Field Trip B8 Guidebook: Sedimentology*
1060 *and Paleontology of Early Ordovician Through Early Silurian Shallow-water Carbonates of*

- 1061 the Mingan Islands and Anticosti Island, pp. 55–94 (Geological Association of
1062 Canada/Mineralogical Association of Canada, Joint Annual Meeting, Quebec City, Quebec,
1063 20–26 May, 1998).
- 1064 Cramer, B.D., Brett, C.E., Melchin, M.A., Männik, P., Kleffner, M.A., McLaughlin, P.I.,
1065 Loydell, D.K., Munnecke, A., Jeppsson, L., Corradini, C., Brunton, F.R., Saltzman, M.R.,
1066 2011a. Revised chronostratigraphic correlation of the Silurian System of North America with
1067 global and regional chronostratigraphic units and $\delta^{13}\text{C}_{\text{carb}}$ chemostratigraphy. *Lethaia* 44,
1068 185–202.
- 1069 Cramer, B.D., Davies, J.R., Ray, D.C., Thomas, A.T., Chernes, L., 2011b. Siluria revisited: an
1070 introduction. In: Ray, D.C. (Ed.), *Siluria Revisited: A Field Guide*. International
1071 Subcommission on Silurian Stratigraphy, Field Meeting 2011, pp. 7–28.
- 1072 Cramer, B.D., Vandenbroucke, T.R.A., Ludvigson, G.A., 2015. High-Resolution Event
1073 Stratigraphy (HiRES) and the quantification of stratigraphic uncertainty: Silurian examples of
1074 the quest for precision in stratigraphy. *Earth-Sci. Rev.* 141, 136–153.
- 1075 Csato, I., Catuneanu, O., 2012. Systems tract architecture under variable climatic and tectonic
1076 regimes: a quantitative approach. *Stratigraphy* 9, 109–130.
- 1077 Dahlqvist, P., Bergström, S.M., 2005. The lowermost Silurian of Jämtland, central Sweden:
1078 conodont biostratigraphy, correlation and biofacies. *Trans. R. Soc. Edinb. Earth Sci.* 96, 1–
1079 19.
- 1080 Davies, J.R., Waters, R.A., 1995. The Caban Conglomerate and Ystrad Meurig Grits
1081 Formation — nested channels and lobe switching on a mud-dominated latest Ashgill to
1082 Llandovery slope apron, Welsh Basin, UK. In: Pickering, K.T., Hiscott, R.N., Kenyon, N.H.,
1083 Lucci, F. Ricci, Smith, R.D.A. (Eds.), *Atlas of Deep Water Environments: Architectural Style*
1084 *in Turbidite Systems*. Chapman & Hall, pp. 184–193.
- 1085 Davies, J.R., Fletcher, C.J.N., Waters, R.A., Wilson, D., Woodhall, D.G., Zalasiewicz, J.A.,
1086 1997. *Geology of the country around Llanilar and Rhayader*. Memoir of the British
1087 Geological Survey. British Geological Survey, Keyworth, Nottingham (Sheets 178 and 179
1088 (England and Wales)).
- 1089 Davies, J.R., Schofield, D.I., Sheppard, T.H., Waters, R.A., Williams, M., Wilson, D., 2006a.
1090 *Geology of the Lampeter district – a brief explanation of the geological map*. Sheet
1091 explanation of the British Geological Survey. British Geological Survey, Keyworth,
1092 Nottingham 1:50 000 Sheet 195 Lampeter (England and Wales).
- 1093 Davies, J.R., Sheppard, T.H., Waters, R.A., Wilson, D., 2006b. *Geology of the Llanranog*
1094 *district – a brief explanation of the geological map*. Sheet explanation of the British
1095 Geological Survey. British Geological Survey, Keyworth, Nottingham 1:50 000 Sheet 194
1096 Llanranog (England and Wales).

- 1097 Davies, J.R., Waters, R.A., Williams, M., Wilson, D., Schofield, D.I., Zalasiewicz, J.A.,
1098 2009. Sedimentary and faunal events revealed by a revised correlation of postglacial
1099 Hirnantian (late Ordovician) strata in the Welsh basin, U.K. *Geol. J.* 44, 322–340.
- 1100 Davies, J.R., Waters, R.A., Zalasiewicz, J.A., Molyneux, S.G., Vandenbroucke, T.R.A.,
1101 Williams, M., 2010. A revised sedimentary and biostratigraphical architecture for the type
1102 Llandovery and Garth areas, central Wales: a field guide. British Geological Survey Open
1103 Report (OR/10/037).
- 1104 Davies, J.R., Molyneux, S.G., Vandenbroucke, T.R.A., Verniers, J., Waters, R.A., Williams,
1105 M., Zalasiewicz, J.A., 2011. Pre-conference field trip to the Type Llandovery area. In: Ray,
1106 D.C. (Ed.), *Siluria Revisited: A Field Guide*, pp. 29–72 (International Subcommittee on
1107 Silurian Stratigraphy, Field Meeting, 2011).
- 1108 Davies, J.R., Waters, R.A., Molyneux, S.G., Williams, M., Zalasiewicz, J.A.,
1109 Vandenbroucke, T.R.A., Verniers, J., 2013. A revised sedimentary and biostratigraphical
1110 architecture for the Type Llandovery area, central Wales, UK. *Geol. Mag.* 150, 300–332.
- 1111 Davies, N.S., Gibling, M.R., 2010. Cambrian to Devonian evolution of alluvial systems: the
1112 sedimentological impact of the earliest land plants. *Earth Sci. Rev.* 98, 171–200.
- 1113 Desrochers, A., Farley, C., Achab, A., Asselin, E., Riva, J.F., 2010. A far-field record of the
1114 end Ordovician glaciation: the Ellis Bay Formation, Anticosti Island, Eastern Canada.
1115 *Palaeogeogr. Palaeoclimatol. Palaeoecol.* 296, 248–263.
- 1116 Dewing, K., 1999. Late Ordovician and Early Silurian strophomenid brachiopods of Anticosti
1117 Island, Quebec, Canada. *Palaeontogr. Can.* 17, 1–143.
- 1118 Dias-Martinez, E., Grahn, Y., 2007. Early Silurian glaciation along the western margin of
1119 Gondwana (Peru, Bolivia and northern Argentina): palaeogeography and geodynamic setting.
1120 *Palaeogeogr. Palaeoclimatol. Palaeoecol.* 252, 62–81.
- 1121 Doyle, E.N., Hoey, A.N., Harper, D.A.T., 1991. The rhynchonellide brachiopod *Eocoelia*
1122 from the upper Llandovery of Ireland and Scotland. *Palaeontology* 34, 439–454.
- 1123 Duval, B., Cramez, C., Vail, P.R., 1992. Types and hierarchy of stratigraphic cycles.
1124 *Sequence Stratigraphy of European Basins, Abstracts volume*. Centre National de la
1125 Recherche Scientifique & Institut Francais du Pétrole, Dijon, pp. 44–45.
- 1126 Embry, A.F., 1995. Sequence boundaries and sequence hierarchies: problems and proposals.
1127 *Nor. Pet. Soc. Spec. Publ.* 5, 1–11.
- 1128 Embry, A.F., 2009. Practical sequence stratigraphy. Canadian Society of Petroleum
1129 Geologists (Online at www.cspg.org, 79 pp.).
- 1130 Embry, A.F., Johannessen, E.P., 1992. T–R sequence stratigraphy, facies analysis and
1131 reservoir distribution in the uppermost Triassic–Lower Jurassic succession, western Sverdrup

- 1132 Basin, Arctic Canada. In: Vorren, T.O., Bergsager, E., Dahl-Stamnes, O.A., Holter, E.,
1133 Johansen, B., Lie, E., Lund, T.B. (Eds.), *Arctic Geology and Petroleum Potential*. Norwegian
1134 Petroleum Society, Special Publication 2, pp. 121–146.
- 1135 Embry, A., Johannessen, E., Owen, D., Beauchamp, B., Gianolla, P., 2007. Sequence
1136 stratigraphy as a “concrete” stratigraphic discipline. Report of the ISSC Task Group on
1137 Sequence Stratigraphy.
- 1138 Ettensohn, F.R., Brett, C.E., 1998. Tectonic components in third-order Silurian cycles:
1139 examples from the Appalachian basin and global implications. In: Landing, E., Johnson, M.E.
1140 (Eds.), *Silurian Cycles: Linkages of Dynamic Stratigraphy With Atmospheric, Oceanic, and*
1141 *Tectonic Changes*. New York State Museum, Bulletin 491, pp. 143–162.
- 1142 Finnegan, S., Bergmann, K., Eiler, J.M., Jones, D.S., Fike, D.A., Eisenman, I., Fischer,
1143 W.W., 2011. The magnitude and duration of Late Ordovician–Early Silurian glaciation.
1144 *Science* 331, 903–906.
- 1145 Gawthorpe, R.L., Fraser, A.J., Collier, R.E., 1994. Sequence stratigraphy in active
1146 extensional basins: implications for the interpretation of ancient basin-fills. *Mar. Pet. Geol.*
1147 11, 642–658.
- 1148 Ghienne, J.F., 2003. Late Ordovician sedimentary environments, glacial cycles, and
1149 postglacial transgression in the Taoudeni Basin, West Africa. *Palaeogeogr. Palaeoclimatol.*
1150 *Palaeoecol.* 189, 117–145.
- 1151 Ghienne, J.F., Desrochers, A., Vandenbrouke, T.R.A., Achab, A., Asselin, E., Dabard, M.-P.,
1152 Farley, C., Loi, A., Paris, F., Wickson, S., Veizier, J., 2014. A Cenozoic-style scenario for the
1153 end-Ordovician glaciation. *Nat. Commun.* 5, 4485.
- 1154 Gouldley, J.C., Saltzman, M.R., Young, S.A., Kaljo, D., 2010. Strontium and carbon isotope
1155 stratigraphy of the Llandovery (Early Silurian): implications for tectonics and weathering.
1156 *Palaeogeogr. Palaeoclimatol. Palaeoecol.* 296, 264–275.
- 1157 Grabau, A.W., 1940. *The Rhythm of the Ages*. Henri Vetch, Peking (561 pp.).
- 1158 Gradstein, F.M., Ogg, J.G., Schmitz, M., Ogg, G. (Eds.), 2012. *The Geologic Time Scale*
1159 2012 vol. 1. Elsevier.
- 1160 Grahn, Y., Caputo, M.V., 1992. Early Silurian glaciations in Brazil. *Palaeogeogr.*
1161 *Palaeoclimatol. Palaeoecol.* 99, 9–15.
- 1162 Griffiths, H., 1998. *Stable Isotopes: Integration of Biological, Ecological and Geochemical*
1163 *Processes*. Bios Scientific Publishers, Oxford.
- 1164 Hambrey, M.J., 1985. The Late Ordovician–Early Silurian glacial period. *Palaeogeogr.*
1165 *Palaeoclimatol. Palaeoecol.* 51, 273–289.

- 1166 Haq, B.U., Schutter, S.R., 2008. A chronology of Paleozoic sea-level change. *Science* 322,
1167 64–68.
- 1168 Harris, M.T., Sheehan, P.M., 1997. Carbonate sequences and fossil communities from the
1169 Upper Ordovician–Lower Silurian of the Eastern Great Basin. *Brigham Young Univ. Geol.*
1170 *Stud.* 42, 105–128.
- 1171 Harris, M.T., Sheehan, P.M., 1998. Early Silurian stratigraphic sequences of the eastern Great
1172 Basin (Utah and Nevada). In: Landing, E., Johnson, M.E. (Eds.), *Silurian Cycles: Linkages of*
1173 *Dynamic Stratigraphy with Atmospheric, Oceanic, and Tectonic Changes*. New York State
1174 *Museum, Bulletin* 491, pp. 51–61.
- 1175 Harris, M.T., Kuglitsch, J.J., Watkins, R., Hegrenes, D.P., Waldhuetter, K.R., 1998. Early
1176 Silurian stratigraphic sequences of eastern Wisconsin. In: Landing, E., Johnson, M.E. (Eds.),
1177 *Silurian Cycles: Linkages of Dynamic Stratigraphy with Atmospheric, Oceanic and Tectonic*
1178 *Changes*. New York State Museum Bulletin 491, pp. 15–25.
- 1179 Hunt, D., Gawthorpe, R.L., 2000. Sedimentary responses to forced regressions. *Geol. Soc.*
1180 *Lond. Spec. Publ.* 172.
- 1181 Jell, J.S., Talent, J.A., 1989. Australia: the most instructive sections. In: Holland, C.H.,
1182 Bassett, M.G. (Eds.), *A Global Standard for the Silurian System*, Geological Series 9.
1183 *National Museum of Wales*, pp. 232–242.
- 1184 Jeppsson, L., 1990. An oceanic model for lithological and faunal changes tested on the
1185 Silurian record. *J. Geol. Soc. Lond.* 147, 663–674.
- 1186 Jeppsson, L., 1998. Silurian oceanic events: Summary of general characteristics. In: Landing,
1187 E., Johnson, M.E. (Eds.), *Silurian Cycles: Linkages of Dynamic Stratigraphy with*
1188 *Atmospheric, Oceanic, and Tectonic Changes*. New York State Museum, Bulletin 491, pp.
1189 239–257.
- 1190 Johnson, M.E., 1975. Recurrent community patterns in epeiric seas: the Lower Silurian of
1191 eastern Iowa. *Proc. Iowa Acad. Sci.* 82, 130–149.
- 1192 Johnson, M.E., 1979. Evolution of brachiopod lineages from the Llandovery Series of
1193 Eastern Iowa. *Palaeontology* 22, 549–567.
- 1194 Johnson, M.E., 1987. Extent and bathymetry of North American platform seas in the Early
1195 Silurian. *Paleoceanography* 2, 185–211.
- 1196 Johnson, M.E., 1996. Stable cratonic sequences and a standard for Silurian eustasy. In:
1197 Witzke, B.J., Ludvigson, G.A. (Eds.), *Palaeozoic Sequence Stratigraphy: Views From the*
1198 *North American Craton*. *Geol. Soc. Am., Special Paper* 306, pp. 203–211.
- 1199 Johnson, M.E., 2006. Relationship of Silurian sea-level fluctuations to oceanic episodes and
1200 events. *GFF* 128, 115–121.

- 1201 Johnson, M.E., 2010. Tracking Silurian eustasy: alignment of empirical evidence or pursuit
1202 of deductive reasoning? *Palaeogeogr. Palaeoclimatol. Palaeoecol.* 296, 276–284.
- 1203 Johnson, M.E., McKerrow, W.S., 1991. Sea level and faunal changes during the latest
1204 Llandovery and earliest Ludlow (Silurian). *Hist. Biol.* 5, 153–169.
- 1205 Johnson, M.E., Baarli, B.G., 2007. Topography and depositional environments at the
1206 Ordovician–Silurian boundary in the Iowa–Illinois–Wisconsin region, USA. In: Li, J., Fan, J.,
1207 Percival, I. (Eds.), *The Global Ordovician and Silurian*. *Acta Palaeontologica Sinica* 46, pp.
1208 208–217 (Proceedings of the 10th International Symposium on the Ordovician System).
- 1209 Johnson, M.E., Rong, J.U., Yang, X.C., 1985. Intercontinental correlation by sea-level events
1210 in the early Silurian of North America and China (Yangtze platform). *Bull. Geol. Soc. Am.*
1211 96, 1384–1397.
- 1212 Johnson, M.E., Baarli, B.G., Nestor, H., Rubel, M., Worsley, D., 1991a. Eustatic sea-level
1213 patterns from the Lower Silurian (Llandovery Series) of southern Norway and Estonia. *Geol.*
1214 *Soc. Am. Bull.* 103, 315–335.
- 1215 Johnson, M.E., Kaljo, D.K., Rong, J.-Y., 1991b. Silurian eustasy. In: Bassett, M.G., Lane,
1216 P.D., Edwards, D. (Eds.), *The Murchison Symposium: Proceedings of an International*
1217 *Conference on the Silurian System, Special Papers in Palaeontology* 44. The Palaeontological
1218 Association, pp. 145–163.
- 1219 Johnson, M.E., Rong, J., Kershaw, S., 1998. Calibrating Silurian eustasy against the erosion
1220 and burial of coastal paleotopography. In: Landing, E., Johnson, M.E. (Eds.), *Silurian Cycles:*
1221 *Linkages of Dynamic Stratigraphy With Atmospheric, Oceanic, and Tectonic Changes*. New
1222 York State Museum Bulletin 491, pp. 3–13.
- 1223 Jones, O.T., 1925. The geology of the Llandovery district. Part I: the southern area. *Q. J.*
1224 *Geol. Soc. Lond.* 81, 344–388.
- 1225 Kaljo, D., Martma, T., 2000. Carbon isotopic composition of Llandovery rocks (East Baltic
1226 Silurian) with environmental interpretation. *Proc. Estonian Acad. Sci. Geol.* 49, 267–283.
- 1227 Kaljo, D., Hints, L., Mannik, P., Nõlvak, J., 2008. The succession of Hirnantian events based
1228 on data from Baltica: brachiopods, chitinozoans, conodonts, and carbon isotopes. *Estonian J.*
1229 *Earth Sci.* 57, 197–218.
- 1230 Kaljo, D., Martma, T., Mannik, P., Viira, V., 2003. Implications of Gondwana glaciations in
1231 the Baltic Late Ordovician and Silurian and a carbon isotopic test of environmental cyclicality.
1232 *Bull. Soc. Géol. Fr.* 174, 59–66.
- 1233 Kirkland, C.L., Daly, J.S., Eide, E.A., Whitehouse, M.J., 2006. The structure and timing of
1234 lateral escape during the Scandian Orogeny: a combined strain and geochronological
1235 investigation in Finnmark, Arctic Norwegian Caledonides. *Tectonophysics* 425, 159–189.

- 1236 Kluessendorf, J., Mikulic, D.G., 1996. An early sequence boundary in Illinois and Wisconsin.
 1237 In: Witzke, B.J., Ludwigson, G.A., Day, J. (Eds.), *Palaeozoic Sequence Stratigraphy: Views*
 1238 *From the North American Craton*. Geol. Soc. Am., Special Paper 306, pp. 177–185.
- 1239 Koren, T.N., Popov, L.E., Degtjarev, K.E., Kovalevsky, O.P., Modzalevskaya, T.L., 2003.
 1240 Kazakhstan in the Silurian. In: Landing, E., Johnson, M.E. (Eds.), *Silurian Lands and Seas:*
 1241 *Palaeogeography Outside of Laurentia*. New York State Museum Bulletin 493, pp. 323–343.
- 1242 Křiž, J., Degardin, J.M., Ferretti, A., Hansch, W., Gutiérrez-Marco, J.C., Paris, P., D-
 1243 Almieda, J.M.P., Rodardet, M., Schonlaub, H.P., Serpagli, E., 2003. Silurian stratigraphy and
 1244 paleogeography of north Gondwanan and Perunian Europe. In: Landing, E., Johnson, M.E.
 1245 (Eds.), *Silurian Lands and Seas: Palaeogeography Outside of Laurentia*. New York State
 1246 Museum Bulletin 493, pp. 105–178.
- 1247 Ladenberger, A., Gee, D., Be'eri Shlevin, Y., Claesson, S., Majka, J., 2012. The Scandian
 1248 collision revisited — when did the orogeny start? *Geophys. Res. Abstr.* 14 (EGU2012-
 1249 12633).
- 1250 Le Heron, D.P., Craig, J., 2008. First-order reconstructions of a Late Ordovician Saharan ice
 1251 sheet. *J. Geol. Soc.* 165, 19–29.
- 1252 Le Heron, D.P., Meinhold, G., Page, A., Whitham, A., 2013. Did lingering ice sheets
 1253 moderate anoxia in the Early Palaeozoic of Libya? *J. Geol. Soc.* 170, 327–339.
- 1254 Leggett, J.K., 1978. Eustacy and pelagic regime in the Iapetus Ocean during the Ordovician
 1255 and Silurian. *Earth Planet. Sci. Lett.* 41, 163–169.
- 1256 Leggett, J.K., 1980. British Lower Palaeozoic black shales and their palaeo-oceanographic
 1257 significance. *J. Geol. Soc. Lond.* 137, 139–156.
- 1258 Leggett, J.K., McKerrow, W.T., Eales, M.H., 1979. The Southern Uplands of Scotland: a
 1259 lower Palaeozoic accretionary prism. *J. Geol. Soc. Lond.* 136, 755–770.
- 1260 Legrand, P., 2003. Silurian stratigraphy and palaeogeography of the northern African margin
 1261 of Gondwana. In: Landing, E., Johnson, M.E. (Eds.), *Silurian Lands and Seas:*
 1262 *Palaeogeography Outside of Laurentia*. New York State Museum Bulletin 493, pp. 59–104.
- 1263 Long, D.G.F., 1993. Oxygen and carbon isotopes and event stratigraphy near the Ordovician–
 1264 Silurian boundary, Anticosti Island, Quebec. *Palaeogeogr. Palaeoclimatol. Palaeoecol.* 104,
 1265 49–59.
- 1266 Long, D.G.F., 2007. Tempestite frequency curves: a key to Late Ordovician and Early
 1267 Silurian subsidence, sea-level change, and orbital forcing in the Anticosti foreland basin,
 1268 Quebec, Canada. *Can. J. Earth Sci.* 44, 413–431.
- 1269 Loydell, D.K., 1998. Early Silurian sea-level changes. *Geol. Mag.* 135, 447–471.

- 1270 Loydell, D.K., 2007. Early Silurian positive $\delta^{13}\text{C}$ excursions and their relationship to
1271 glaciations, sea level changes and extinction events. *Geol. J.* 42, 531–546.
- 1272 Loydell, D.K., 2011. Graptolite biozone correlation charts. *Geol. Mag.* 149, 124–132.
- 1273 Loydell, D.K., Butcher, A., Frýda, J., Lüning, S., Fowler, M., 2009. Lower Silurian “hot
1274 shales” in Jordan: a new depositional model. *J. Pet. Geol.* 32, 261–270.
- 1275 Loydell, D.K., Nestor, V., Mannik, P., 2010. Integrated biostratigraphy of the lower-Silurian
1276 of the Kolka-54 core, Latvia. *Geol. Mag.* 147, 253–280.
- 1277 Loydell, D.K., Butcher, A., Fryda, J., 2013. The middle Rhuddanian (lower Silurian) ‘hot
1278 shale’ of North Africa and Arabia: an atypical hydrocarbon source rock. *Palaeogeogr.*
1279 *Palaeoclimatol. Palaeoecol.* 386, 233–256.
- 1280 Mannik, P., 2007. An updated Telychian (Late Llandovery, Silurian) conodont zonation
1281 based on Baltic faunas. *Lethaia* 40, 45–60.
- 1282 McGuire, B., 2012. *Waking the Giant: How a Changing Climate Triggers Earthquakes,*
1283 *Tsunamis, and Volcanoes.* Oxford University Press.
- 1284 McKerrow, W.S., 1979. Ordovician and Silurian changes in sea level. *J. Geol. Soc. Lond.*
1285 136, 137–145.
- 1286 McLaughlin, P.I., Emsbo, P., Brett, C.E., 2012. Beyond black shales: the sedimentary and
1287 stable isotope records of oceanic anoxic events in a dominantly oxic basin (Silurian;
1288 Appalachian Basin, USA). *Palaeogeogr. Palaeoclimatol. Palaeoecol.* 367–368, 153–177.
- 1289 Melchin, M.J., Holmden, C., 2006. Carbon isotope chemostratigraphy of the Llandovery in
1290 Arctic Canada: implications for global correlation and sea-level change. *GFF* 128, 173–180.
- 1291 Melchin, M.J., Koren, T.N., Storch, P., 1998. Global diversity and survivorship patterns of
1292 Silurian graptoloids. In: Landing, E., Johnson, M.E. (Eds.), *Silurian Cycles: Linkages of*
1293 *Dynamic Stratigraphy With Atmospheric, Oceanic, and Tectonic Changes.* New York State
1294 *Museum Bulletin* 491, pp. 165–182.
- 1295 Melchin, M.J., Sadler, P.M., Cramer, B.D., 2012. The Silurian Period. In: Gradstein, F.M.,
1296 Ogg, J.G., Smith, A.G. (Eds.), *A Geologic Time Scale 2012.* Elsevier, pp. 525–558.
- 1297 Melchin, M.J., Mitchell, C.E., Holmden, C., Storch, P., 2013. Environmental changes in the
1298 Late Ordovician-early Silurian: review and new insights from black shales and nitrogen
1299 isotopes. *Geol. Soc. Am. Bull.* 125, 1635–1670.
- 1300 Miall, A.D., 2004. Empiricism and model building in stratigraphy: the historical roots of
1301 present-day practices. *Stratigraphy* 1, 3–25.

- 1302 Miall, A.D., 2010. *Geology of Stratigraphic Sequences*. Second ed. Springer Verlag, Berlin
1303 (522 pp.).
- 1304 Miller, K.G., Kominz, M.A., Browning, J.V., Wright, J.D., Mountain, G.S., Katz, M.E.,
1305 Sugarman, P.J., Cramer, B.S., Christie-Blick, N., Pekar, S.F., 2005. The Phanerozoic record
1306 of global sea-level change. *Science* 310, 1293–1298.
- 1307 Morton, R.A., Suter, J.R., 1996. Sequence stratigraphy and composition of late Quaternary
1308 shelf margin deltas, northern Gulf of Mexico. *Am. Assoc. Pet. Geol. Bull.* 80, 505–530.
- 1309 Munnecke, A., Calner, M., Harper, D.A.T., Servais, T., 2010. Ordovician and Silurian
1310 seawater chemistry, sea level and climate: a synopsis. *Palaeogeogr. Palaeoclimatol.*
1311 *Palaeoecol.* 296, 389–413.
- 1312 Nestor, H., 1997. Silurian. In: Raukas, A., Teedumaes, A. (Eds.), *Geology and Mineral*
1313 *Resources of Estonia*. Estonian Academy Publishers, Tallinn, pp. 89–106.
- 1314 Nestor, H., Einasto, R., 1997. Ordovician and Silurian carbonate sedimentation basin. In:
1315 Raukas, A., A. Teedumäes (Eds.), *Geology and Mineral Resources of Estonia*. Estonian
1316 Academy Publishers, Tallinn, pp. 192–204.
- 1317 Nestor, H., Nestor, V., 2002. Upper Llandovery to middle Wenlock (Silurian)
1318 lithostratigraphy and chitinozoan biostratigraphy in southwestern Estonia and northernmost
1319 Latvia. *Proc. Estonian Acad. Sci. Geol.* 51, 67–87.
- 1320 Nestor, H., Einasto, R., Männik, P., Nestor, V., 2003. Correlation of lower–middle
1321 Llandovery sections in central and southern Estonia and sedimentation cycles of lime muds.
1322 *Proc. Estonian Acad. Sci. Geol.* 52, 3–27.
- 1323 Nestor, V., 2012. A summary and revision of the East Baltic Silurian chitinozoan
1324 biozonation. *Estonian J. Earth Sci.* 61, 242–260.
- 1325 Page, A.A., Zalasiewicz, J.A., Williams, M., Popov, L.E., 2007. Were transgressive black
1326 shales a negative feedback modulating glacioeustasy during the Early Palaeozoic Icehouse?
1327 In: Williams, M., Haywood, A.M., Gregory, F.J., Schmidt, D.N. (Eds.), *Deep Time*
1328 *Perspectives on Climate Change: Marrying the Signal From Computer Models and Biological*
1329 *Proxies*, The Micropalaeontological Society Special Publications. The Geological Society,
1330 London, pp. 123–156.
- 1331 Posamentier, H.W., Allen, G.P., James, D.P., Tesson, M., 1992. Forced regressions in a
1332 sequence stratigraphic framework: concepts, examples, and exploration significance (1). *Am.*
1333 *Assoc. Pet. Geol. Bull.* 76, 1687–1709.
- 1334 Rickards, R.B., 1970. The Llandovery (Silurian) graptolites of the Howgill Fells. Northern
1335 England. *Palaeontogr. Soc. [Monogr]* 1–108.

- 1336 Rickards, R.B., Woodcock, N.H., 2005. Stratigraphical revision of the Windermere
1337 Supergroup (Late Ordovician–Silurian) in the southern Howgill Fells, NW England. *Proc.*
1338 *Yorks. Geol. Soc.* 55, 263–285.
- 1339 Rong, J.-Y., Chen, X., 2003. Silurian biostratigraphy of China. In: Zhang, W.-T., Chen, P.-J.,
1340 Palmer, A.R. (Eds.), *Biostratigraphy of China*. Science Press, Beijing, pp. 173–237.
- 1341 Rong, J.-Y., Johnson, M.E., Yang, X.-C., 1984. Early Silurian (Llandoveryan) sea level
1342 changes in the upper Yangtze Region central and southwestern China. *Acta Palaeontol. Sin.*
1343 23, 672–693.
- 1344 Ross, C.A., Ross, R.P., 1996. Silurian sea level fluctuations. In: Witzke, B.J., Ludvigson,
1345 G.A., Day, J. (Eds.), *Paleozoic Sequence Stratigraphy: Views From the North American*
1346 *craton*. Geological Society of America Special Paper 306, pp. 187–192.
- 1347 Sadler, P.M., 2004. Quantitative biostratigraphy — achieving finer resolution in global
1348 correlation. *Annu. Rev. Earth Planet. Sci.* 32, 187–213.
- 1349 Sadler, P.M., Cooper, R.A., Melchin, M.J., 2009. High-resolution, early Paleozoic
1350 (Ordovician–Silurian) time scales. *Geol. Soc. Am. Bull.* 121, 887–906.
- 1351 Schlager, W., 2004. Fractal nature of stratigraphic sequences. *Geology* 32, 185–188.
- 1352 Schofield, D.I., Davies, J.R., Waters, R.A., Williams, M., Wilson, D., 2009. A new Early
1353 Silurian turbidite system in Central Wales: insights into eustatic and tectonic controls on
1354 deposition in the southern Welsh basin. *Geol. Mag.* 146, 121–132.
- 1355 Stammer, D., Cazenave, A., Ponte, R.M., Tamisiea, M.E., 2013. Causes for contemporary
1356 regional sea level changes. *Annu. Rev. Mar. Sci.* 5, 21–46.
- 1357 Stanley, S.M., 2010. Relation of Phanerozoic stable isotope excursions to climate, bacterial
1358 metabolism and major extinctions. *Proc. Natl. Acad. Sci. U. S. A.* 107, 19185–19189.
- 1359 Steffen, R., Wu, P., Steffen, H., Eaton, D.W., 2014. On the implementation of faults in finite-
1360 element glacial isostatic adjustment models. *Comput. Geosci.* 62, 150–159.
- 1361 Stone, P., Floyd, J.D., Barnes, R.P., Lintern, B.C., 1987. A sequential back-arc and foreland
1362 basin thrust duplex model for the Southern Uplands of Scotland. *J. Geol. Soc.* 144, 753–764.
- 1363 Storch, P., 1995. Biotic crises and post-crisis recoveries recorded by Silurian planktonic
1364 graptolite faunas of the Barrandian area (Czech Republic). *Geolines* 3, 59–70.
- 1365 Talent, J.A., Bhargava, O.N., 2003. Silurian of the Indian subcontinent and adjacent regions.
1366 In: Landing, E., Johnson, M.E. (Eds.), *Silurian Lands and Seas: Palaeogeography Outside of*
1367 *Laurentia*. New York State Museum Bulletin 493, pp. 221–239.

- 1368 Talent, J.A., Mawson, R., Simpson, A., 2003. Silurian of Australia and New Guinea:
1369 biostratigraphic correlations and paleogeography. In: Landing, E., Johnson, M.E. (Eds.),
1370 Silurian Lands and Seas: Palaeogeography Outside of Laurentia. New York State Museum
1371 Bulletin 493, pp. 181–219.
- 1372 Taylor, A.M., Goldring, R., 1993. Description and analysis of bioturbation and ichnofabric. *J.*
1373 *Geol. Soc. Lond.* 159, 141–148.
- 1374 Temple, J.T., 1987. Early Llandovery brachiopods of Wales. Monograph of the
1375 Palaeontographical Society, London, Publication 572 (part of Vol. 139 for 1985).
- 1376 Tesakov, Y.I., Johnson, M.E., Predtetchensky, N.N., Khromych, V.G., Berger, A.Y.A., 1998.
1377 Eustatic fluctuations in the East Siberian Basin (Siberian Platform and Taymyr Peninsula).
1378 In: Landing, E., Johnson, M.E. (Eds.), *Silurian Cycles: Linkages of Dynamic Stratigraphy*
1379 *With Atmospheric, Oceanic, and Tectonic Changes*. New York State Museum Bulletin 491,
1380 pp. 63–73.
- 1381 Toghil, P., 1968. The graptolite assemblages and zones of the Birkhill Shales (lower
1382 Silurian) at Dobb's Linn. *Palaeontology* 11, 654–668.
- 1383 Toghil, P., 1992. The Shelvian event, a late Ordovician tectonic episode in Southern Britain
1384 (Eastern Avalonia). *Proc. Geol. Assoc.* 10, 31–35.
- 1385 Torsvik, T.H., 2012. BugPlates: Linking Biogeography and Palaeogeography.
1386 <http://www.geodynamics.no/Web/Content/Software/>.
- 1387 Underwood, C.J., Crowley, S., Marshall, J., Brenchley, P., 1997. Carbon isotope stratigraphy
1388 of the Ordovician–Silurian Stratotype (Dob's Linn, Scotland) and its global correlation. *J.*
1389 *Geol. Soc.* 154, 709–718.
- 1390 Underwood, C.J., Deynoux, M., Ghiene, J.-F., 1998. High palaeolatitude (Hodh,
1391 Mauritania) recovery of graptolite faunas after the Hirnantian (end Ordovician) extinction
1392 event. *Palaeogeogr. Palaeoclimatol. Palaeoecol.* 142, 91–103.
- 1393 Vail, P.R., Mitchum Jr., R.M., Thompson III, S., 1977. Seismic stratigraphy and global
1394 changes of sea level, part 4: global cycles of relative changes of sea level. In: Payton, C.E.
1395 (Ed.), *Seismic Stratigraphy — Applications to Hydrocarbon Exploration*. American
1396 Association of Petroleum Geologists Memoir 26, pp. 83–97.
- 1397 Vandenbroucke, T.R.A., Emsbo, P., Munnecke, A., Nuns, N., Duponchel, L., Lepot, K.,
1398 Quijada, M., Paris, F., Servais, T., Kiessling, W., 2015. Metal-induced malformations in early
1399 Palaeozoic plankton are harbingers of mass extinction. *Nat. Commun.* 6, 7966.
- 1400 Vandenbroucke, T.R.A., Hennissen, J., Zalasiewicz, J.A., Verniers, J., 2008. New
1401 chitinozoans from the historical type area of the Hirnantian and additional key sections in the
1402 Wye Valley, Wales, UK. *Geol. J.* 43, 397–414.

- 1403 Vandenbroucke, T.R.A., Munnecke, A., Leng, M.J., Bickert, T., Hints, O., Gelsthorpe, D.,
 1404 Maier, G., Servais, T., 2013. Reconstructing the environmental conditions around the Silurian
 1405 Ireviken Event using the carbon isotope composition of bulk and palynomorph organic
 1406 matter. *Geochem. Geophys. Geosyst.* 14 (1), 86–101.
- 1407 Verniers, J., Nestor, V., Paris, F., Dufka, P., Sutherland, S., Van Grootel, G., 1995. A global
 1408 Chitinozoa biozonation for the Silurian. *Geol. Mag.* 132, 651–666.
- 1409 Waldron, J.W.F., Schofield, D.I., White, C.E., Barr, S.M., 2011. Cambrian successions of the
 1410 Meguma Terrane, Nova Scotia, and Harlech Dome, North Wales: dispersed fragments of a
 1411 peri-Gondwanan basin? *J. Geol. Soc. Lond.* 168, 83–98.
- 1412 Wellman, C.H., Steemans, P., Vecoli, M., 2013. Palaeophytogeography of Ordovician–
 1413 Silurian land plants. In: Harper, D.A.T., Servais, T. (Eds.), *Early Palaeozoic Biogeography
 1414 and Palaeogeography*. Geological Society of London, Memoir 38, pp. 461–476.
- 1415 Williams, A., 1951. Llandovery brachiopods from Wales with special reference to the
 1416 Llandovery district. *Q. J. Geol. Soc. Lond.* 107, 85–136.
- 1417 Wilson, D., Burt, C.E., Davies, J.R., Hall, H., Jones, N.S., Leslie, P.A.J., Lusty, P.R., Wilby,
 1418 P.R., Aspden, J.A., 2016. Geology of the Llanidloes district - a brief explanation of the
 1419 geological map. Sheet explanation of the British Geological Survey. 1:50 000 Sheet 164
 1420 Llangranog (England and Wales).
- 1421 Witzke, B.J., 1992. Silurian stratigraphy and carbonate mound facies of eastern Iowa. Iowa
 1422 Department of Natural Resources, Geological Survey Bureau, Guidebook Series 11 111 pp.
- 1423 Witzke, B.J., Bunker, B.J., 1996. Relative sea-level changes during Middle Ordovician
 1424 through Mississippian deposition in the Iowa area, North American craton. In: Witzke, B.J.,
 1425 Ludwigson, G.A., Day, J. (Eds.), *Paleozoic Sequence Stratigraphy: Views From the North
 1426 American Craton*. Geological Society of America Special Paper 306, pp. 307–330.
- 1427 Woodcock, N.H., Strachan, R., 2012. *Geological History of Britain and Ireland*. second ed.
 1428 Blackwell Publishing.
- 1429 Woodcock, N.H., Butler, A.J., Davies, J.R., Waters, R.A., 1996. Sequence stratigraphical
 1430 analysis of late Ordovician and early Silurian depositional systems in the Welsh basin: a
 1431 critical assessment. In: Hesselbo, S.P., Parkinson, D.N. (Eds.), *Sequence Stratigraphy in
 1432 British Geology*. *Geol. Soc. Spec. Publ.* 103, pp. 197–208.
- 1433 Yolkin, E.A., Sennikov, N.V., Bakharav, N.K., Izokh, N.G., Klets, A.G., 2003. Silurian
 1434 palaeogeography along the southwest margin of the Siberian continent: Altai-Sayan folded
 1435 area. In: Landing, E., Johnson, M.E. (Eds.), *Silurian Lands and Seas: Palaeogeography
 1436 Outside of Laurentia*. *New York State Museum Bulletin* 493, pp. 299–322.

- 1437 Zalasiewicz, J.A., Taylor, L., Rushton, A.W.A., Loydell, D.K., Rickards, R.B., Williams, M.,
1438 2009. Graptolites in British stratigraphy. *Geol. Mag.* 146, 785–850.
- 1439 Zecchin, M., 2007. The architecturally variability of small scale cycles in shelf and ramp
1440 clastic systems: the controlling factors. *Earth Sci. Rev.* 84, 21–55.
- 1441 Zhang, S., Barnes, C.R., 2002b. Late Ordovician-Early Silurian (Ashgillian-Llandovery) sea
1442 level curve derived from conodont community analysis, Anticosti Island, Quebec.
1443 *Palaeogeogr. Palaeoclimatol. Palaeoecol.* 180, 5–32.
- 1444 Zhang, S., Barnes, C.R., Jowett, D.M.S., 2006. The paradox of the global standard Late
1445 Ordovician–Early Silurian sea level curve: evidence from conodont community analysis from
1446 both Canadian Arctic and Appalachian margins. *Palaeogeogr. Palaeoclimatol. Palaeoecol.*
1447 236, 246–271.
- 1448 Ziegler, A.M., 1966. The Silurian brachiopod *Eocelia hemisphaerica* (J. de C. Sowerby) and
1449 related species. *Palaeontology* 9, 523–543.
- 1450 Ziegler, A.M., Cocks, L.R.M., Bambach, R.K., 1968a. The composition and structure of
1451 Lower Silurian marine communities. *Lethaia* 1, 1–27.
- 1452 Ziegler, A.M., Cocks, L.R.M., McKerrow, W.S., 1968b. The Llandovery transgression of the
1453 Welsh Borderland. *Palaeontology* 11, 736–782.
- 1454

1455 **Figure Captions**

1456 **Fig. 1.** Global Llandovery palaeogeography (after Torsvik, 2012, 440Ma) showing the
1457 distribution of tectonic plates and the locations of sections used in this study (numbers are
1458 those used on Fig. 7, Fig. 8, Fig. 9, Fig. 10, Fig. 11 and Fig. 12). Abbreviation: Su, Southern
1459 Uplands. Note, according to Ladenberger et al. (2012), the collision between Laurentia and
1460 Baltica that initiated the northern Europe Scandian Orogeny was already in progress during
1461 earliest Llandovery times (but see Kirkland et al., 2006). Cathaysia is commonly referred to
1462 as South China.

1463 **Fig. 2.** a) Key areas of Llandovery aged rocks in the UK; b) Llandovery Series rocks in
1464 Wales; c) Type Llandovery area showing location of traverse lines used in the construction of
1465 Fig. 4 (after Davies et al., 2013). Abbreviations: BF, Bala Fault; CSFZ, Church Stretton Fault
1466 Zone; ELD, English Lake District; LL, Llandovery town; LPWB, Lower Palaeozoic Welsh
1467 Basin; PL, Pontesford Lineament; SSU, Scottish Southern Uplands; TL, Tywi Lineament;
1468 WBFS, Welsh Borderland Fault System.

1469 **Fig. 3.** Facies model for Rhuddanian and Aeronian strata at Llandovery showing the
1470 sedimentary and faunal characteristics of the principal facies (after Davies et al., 2013).
1471 Benthic Communities are those of Ziegler et al. (1968a); BA refers to the broadly equivalent
1472 Benthic Associations of Boucot (1975); BI refers to the Bioturbation Index of Taylor and
1473 Goldring (1993). For other abbreviations see Fig. 4.

1474 **Fig. 4.** Architectural models for the Type Llandovery succession (after Davies et al., 2013):
1475 a) lithostratigraphy and thickness; b) chronostratigraphy model calibrated using UK graptolite
1476 biozonation of Zalasiewicz et al. (2009); c) as b, but recast to show distribution of facies belts
1477 and progradational sequences (numbers refer to facies belts of Fig. 3). See Fig. 2 for location
1478 of lines of traverse. Abbreviations for stratigraphical nomenclature: BrF, Bronydd Formation;
1479 CcF, Crychan Formation; Ceg, Cefnigarreg Sandstone Formation; Cer, Cerig Formation; ChF,
1480 Chwefri Formation; db, slump-disturbed units; DD, Derwyddon Formation; GHF, Garth
1481 House Formation; Gol, Goleugoed Formation; Rdg, Rhydings Formation; Tff, Trefawr
1482 Formation; Wow, Wormwood Formation; Ydw, Ydw Member; Yst, Ystradwalter Member.
1483 Note in b use of symbols such as Ceg0, Ceg1, etc. to distinguish separate prograde units
1484 within individual formations; and in b and c alternative base positions for the Aeronian and
1485 Telychian stages based either on current GSSPs (*) or internationally applied biozonal
1486 criteria (see Fig. 5 and Davies et al., 2013).

1487 **Fig. 5.** Compilation of selected biostratigraphical ranges and biozonal schemes in use for the
1488 late Hirnantian and Llandovery series. Principal sources for columns: A, Zalasiewicz et al.
1489 (2009); B, Cocks et al. (1984), Baarli (1986; also Baarli and Johnson, 1988), Temple (1987)
1490 and Davies et al. (2013); C, Aldridge and Schonlaub (1989), Dahlqvist and Bergström
1491 (2005), Mannik (2007) and Cramer et al., 2011a and Cramer et al., 2011b; D, Verniers et al.
1492 (1995), Loydell et al. (2010), Nestor (2012) and Davies et al. (2013); E, Davies et al. (2013);
1493 F, Burgess (1991); G, Brett et al. (1998); H, Loydell (2011); I, Bergström et al. (2009) and
1494 Cramer et al. (2011a) with selected GTS 2012 (Spline) Ages of Melchin et al. (2012). Notes:

1495 1, historic base of the Silurian System in Wales (see Davies et al., 2009; note that recent
1496 syntheses suggest that the FADs of both *taugourdeaui* Biozone chitinozoans (t) and
1497 *persculptus* Biozone graptolites (p) are significantly younger in Wales than in other parts of
1498 the world; see Supplementary data); 2, base of former Idwian Stage; 3, base Aeronian
1499 according to internationally applied criteria (Melchin et al., 2012); 4, approximate base of
1500 former Fronian Stage; 5, former base Telychian of Cocks et al. (1970); 6, base Telychian
1501 based on internationally applied criteria (Cocks, 1989 and Melchin et al., 2012); 7, historic
1502 base Wenlock Series, but see discussion in Melchin et al. (2012); T = onset of post-glacial
1503 maximum transgression in Wales (see Supplementary data for discussion re revised age of
1504 this event); GSSP = positions of current stage stratotypes (see Davies et al., 2013). In Column
1505 B solid lines show known ranges of brachiopod taxa in the Type Llandovery area; dashed
1506 lines show known ranges in Wales and the Welsh Borderlands; and dotted lines show known
1507 ranges in other areas. In other columns horizontal dashed lines denote uncertainty. Note the
1508 *persculptus* and *convolutus* biozones are expanded to allow FADs and LADs to be better
1509 illustrated; post-*guerichi* biozones are foreshortened; subdivisions 1–4 of the upper
1510 *persculptus* Biozone refer to the successive morphotypes of *Normalograptus? parvulus*
1511 recognised in Wales by Blackett et al. (2009). For additional sources and discussion see the
1512 notes and numbered links [in square brackets] to information submitted as Supplementary
1513 data.

1514 **Fig. 6.** Generalised log of the late Hirnantian to early Telychian succession in the Type
1515 Llandovery area showing sequence stratigraphy and derived base level movement curves. UK
1516 graptolite biozone bases are taken at the first appearances (FADs) of diagnostic biozonal
1517 assemblages using the criteria of Zalasiewicz et al. (2009) (see also Fig. 5). GSSPI — relative
1518 position of Aeronian Stage GSSP; GSSPII — relative position of Telychian Stage GSSP (see
1519 text and Supplementary data). See Fig. 2 and Fig. 3 for lithostratigraphical abbreviations and
1520 explanation of facies belts. N.B. sequence stratigraphy has not been applied to Telychian
1521 strata and parasequence-scale base level movements within the *convolutus* Biozone have
1522 been omitted for clarity. *See Supplementary data for usage of upper *persculptus* Biozone;
1523 numbers 1, 2 and 3, 4 show inferred ranges of Blackett et al.'s (2009) divisions (see Fig. 5).

1524 **Fig. 7.** Comparison of the Type Llandovery relative base level curves with other UK
1525 Llandovery datasets (see Fig. 1 and Fig. 2 for locations). Coloured blocks identify trends in
1526 these datasets inferred to be consistent with the base level changes recognised at Llandovery
1527 (see text) without necessarily implying a causal relationship; diagonal ruling is used for
1528 segments of datasets consistent only with inferred high order base level movements at
1529 Llandovery. All datasets have been recalibrated to fit the standard UK graptolite biozonal
1530 scheme of Zalasiewicz et al. (2009); the biozones are not drawn to scale, and are divided into
1531 three or, in the case of the *atavus-acinaces* and *sedgwickii-halli* biozonal intervals, six
1532 arbitrary subdivisions to facilitate comparisons between the datasets (see Section 8). Numbers
1533 [in square brackets] refer to notes provided as Supplementary data; dashed vertical lines on
1534 subsequent figures indicate the presence of putative non-sequences (see Section 8a).

1535 **Fig. 8.** Comparison of the Type Llandovery relative base level curves with a selection of
1536 published late Hirnantian to early Telychian global sea level curves showing levels of
1537 correspondence (see Fig. 7 for explanation).

1538 **Fig. 9.** Comparison of the Type Llandovery relative base level curves with a selection of
1539 published late Hirnantian to early Telychian regional base level curves for Laurentia showing
1540 levels of correspondence (see Fig. 7 for explanation). The curve of Zhang and Barnes (2002b)
1541 is simplified; that of Dewing (1999) shows the late Hirnantian–Rhuddanian portion only.

1542 **Fig. 10.** Comparison of the Type Llandovery relative base level curves with a selection of
1543 published late Hirnantian to early Telychian regional base level curves for Laurentia and
1544 Baltica showing levels of correspondence (see Fig. 7 for explanation).

1545 **Fig. 11.** Comparison of the Type Llandovery relative base level curves with a selection of
1546 published late Hirnantian to early Telychian regional base level curves for Siberia,
1547 Kazakhstan and Cathaysia (South China) showing levels of correspondence (see Fig. 7 for
1548 explanation).

1549 **Fig. 12.** Comparison of the Type Llandovery relative base level curves with a selection of
1550 published late Hirnantian to early Telychian regional base level curves for Peri-Gondwana
1551 and Gondwana showing levels of correspondence (see Fig. 7 for explanation). Note, the curve
1552 for the Murzuq Basin is a conflation of two overlapping curves from different parts of the
1553 basin.

1554 **Fig. 13.** Comparison of the Type Llandovery relative base level curves with a selection of
1555 published proxy datasets (including distribution of South American glacial facies and isotope
1556 curves) for the late Hirnantian to early Telychian showing levels of correspondence (see Fig.
1557 7 for explanation).

1558 **Fig. 14.** Comparison of the Type Llandovery relative base level curves with a selection of
1559 published datasets of trends in late Hirnantian to early Telychian graptolite populations and
1560 the oceanic events of Jeppsson (1998), showing levels of correspondence (see Fig. 7 for
1561 explanation).

1562 **Fig. 15.** Eustasy Index for late Hirnantian to early Telychian base level movements in the
1563 Type Llandovery area based on a comparison of the Type Llandovery relative base level
1564 curve with the 62* regional and global datasets presented in Fig. 7, Fig. 8, Fig. 9, Fig. 10,
1565 Fig. 11, Fig. 12, Fig. 13 and Fig. 14 (see Supplementary data for detailed breakdown of
1566 scores). Shaded areas indicate base level events that score incrementally higher than the mean
1567 EI value (see Supplementary data) considered those most likely to include a dominant
1568 eustatic component. *The 62 datasets exclude the Type Llandovery relative base level curves,
1569 but include the part curve of Dewing (1999) used on Fig. 9; the Welsh Basin turbidite
1570 sandbodies shown on Fig. 7 are considered as a single dataset.

1571 **Fig. 16.** Matrix of global and regional forcing factors that interact to influence Eustasy Index
1572 scores (see text).

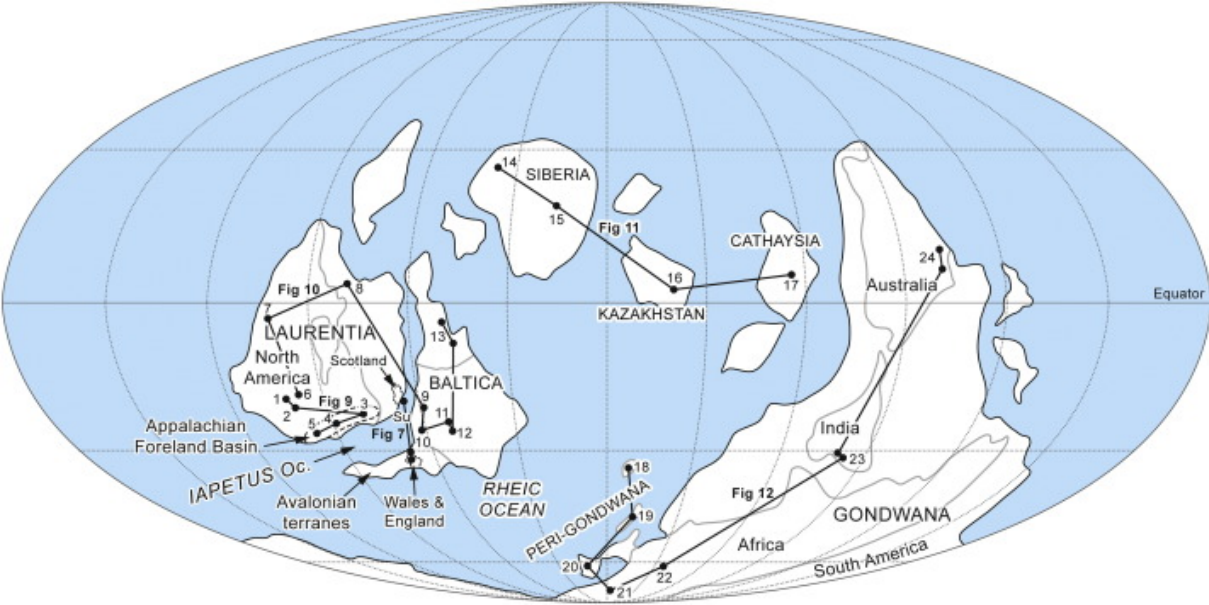
1573 **Plate caption**

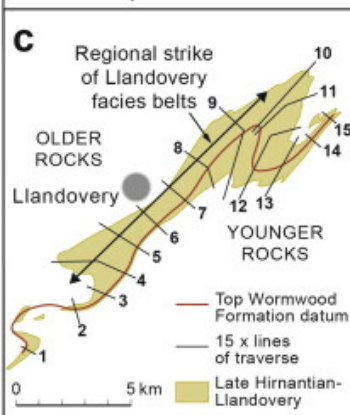
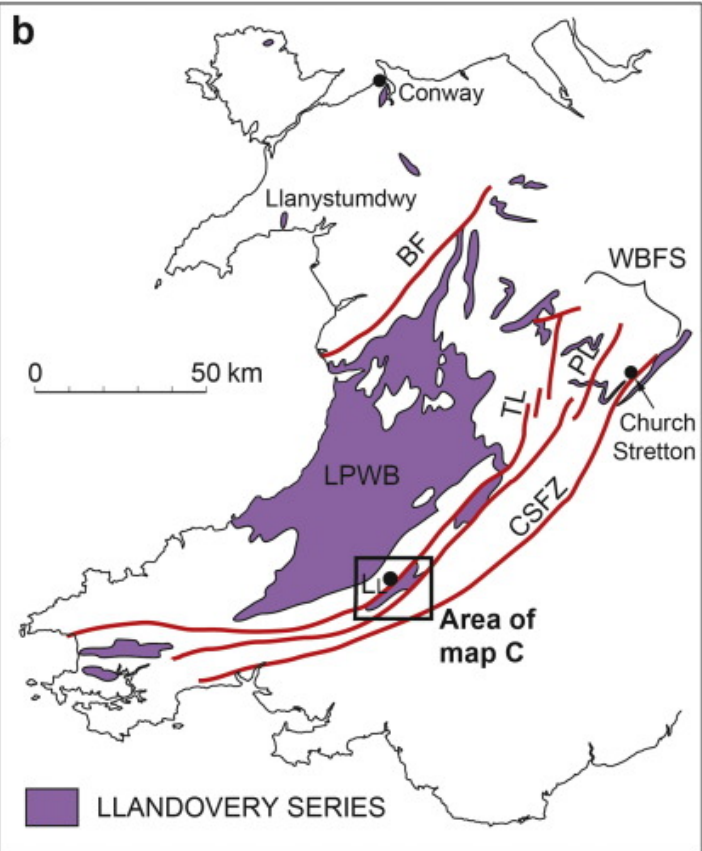
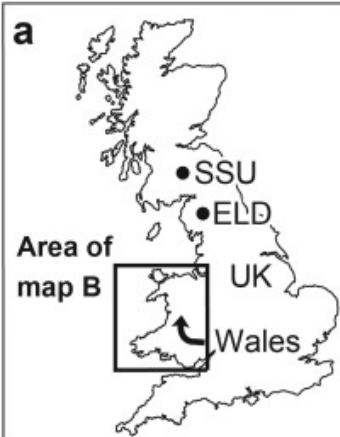
1574 **Plate 1.** Coquina of adult and juvenile *Pentamerus oblongus* valves, solitary rugose corals
1575 and bivalves in topset sandstone facies, Derwyddon Formation, Crychan Forest track section,
1576 UK National Grid Reference [SN 853 385] (Torsvik, 2012).

1577

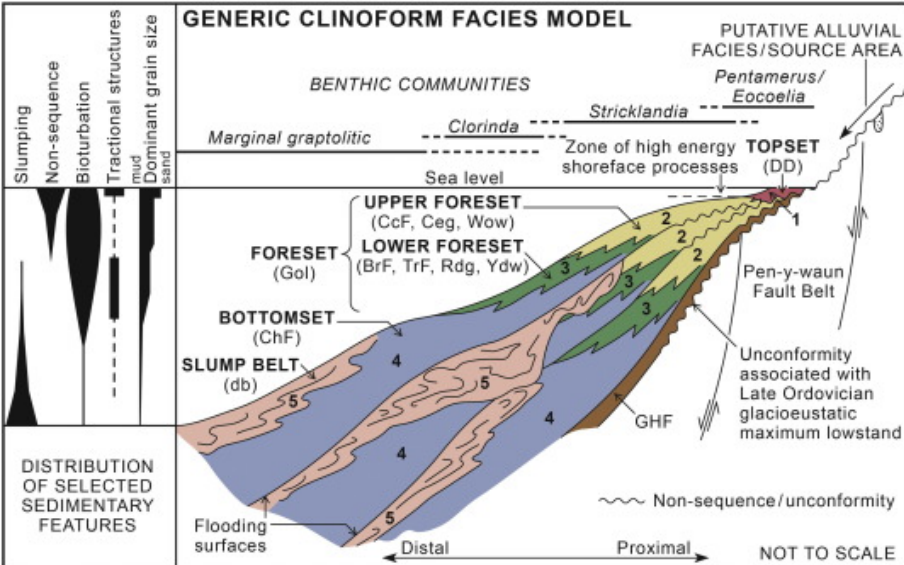
1578 **Table caption**

1579 **Table 1.** Range of palaeogeographical (see Fig. 1) and proxy datasets used in the calculation
1580 of the Eustasy Index for Type Llandovery base level movements as shown on Fig. 15 (see
1581 text and Supplementary data).

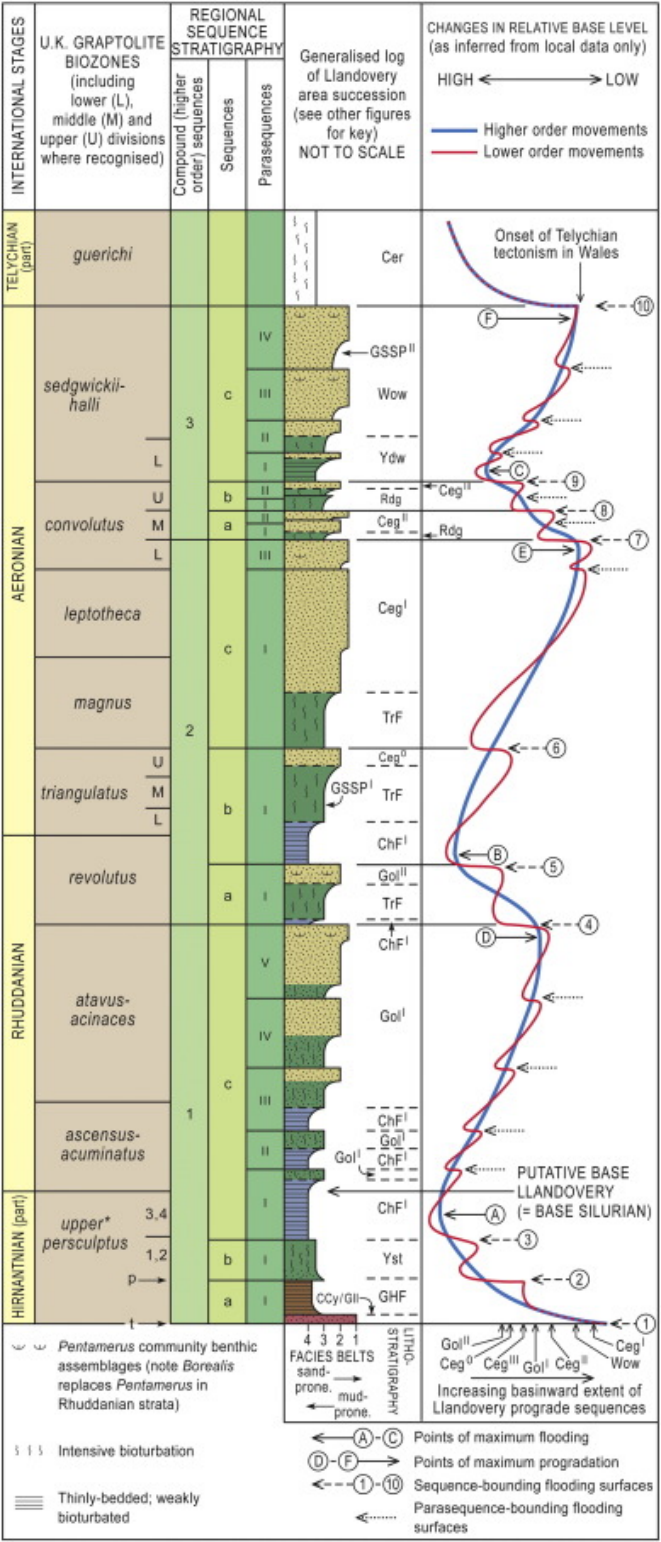


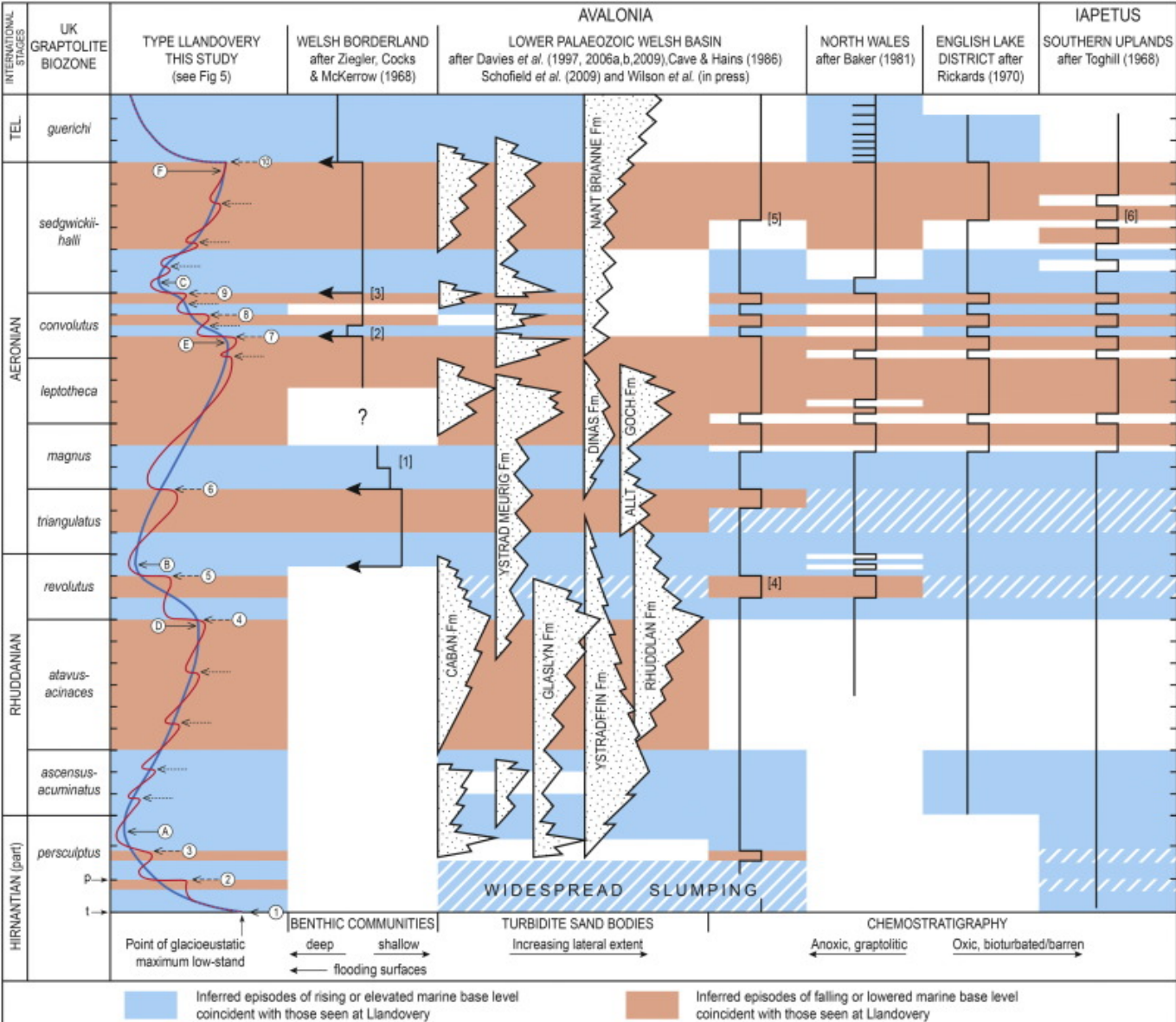


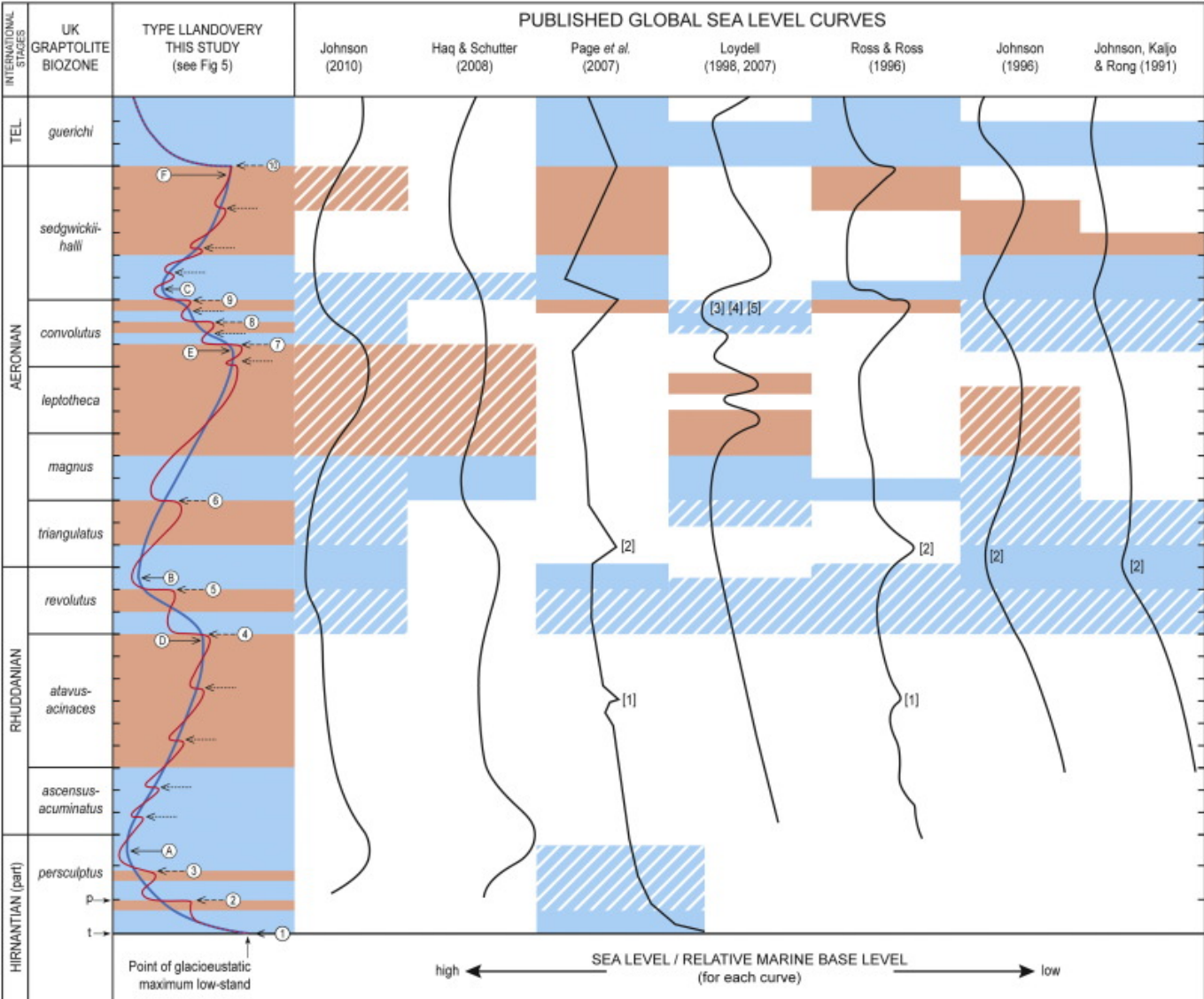
GENERIC CLINOFORM FACIES MODEL

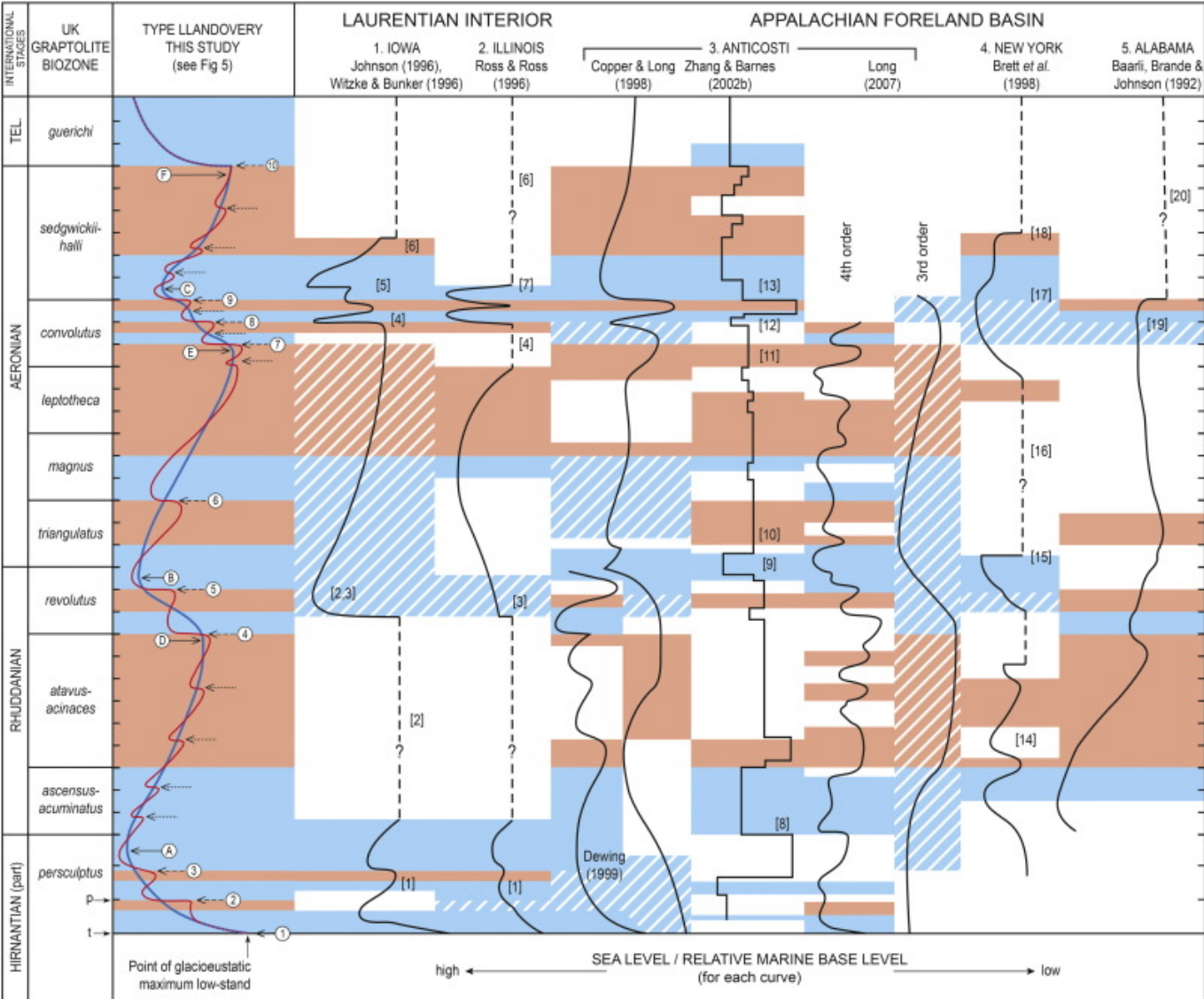


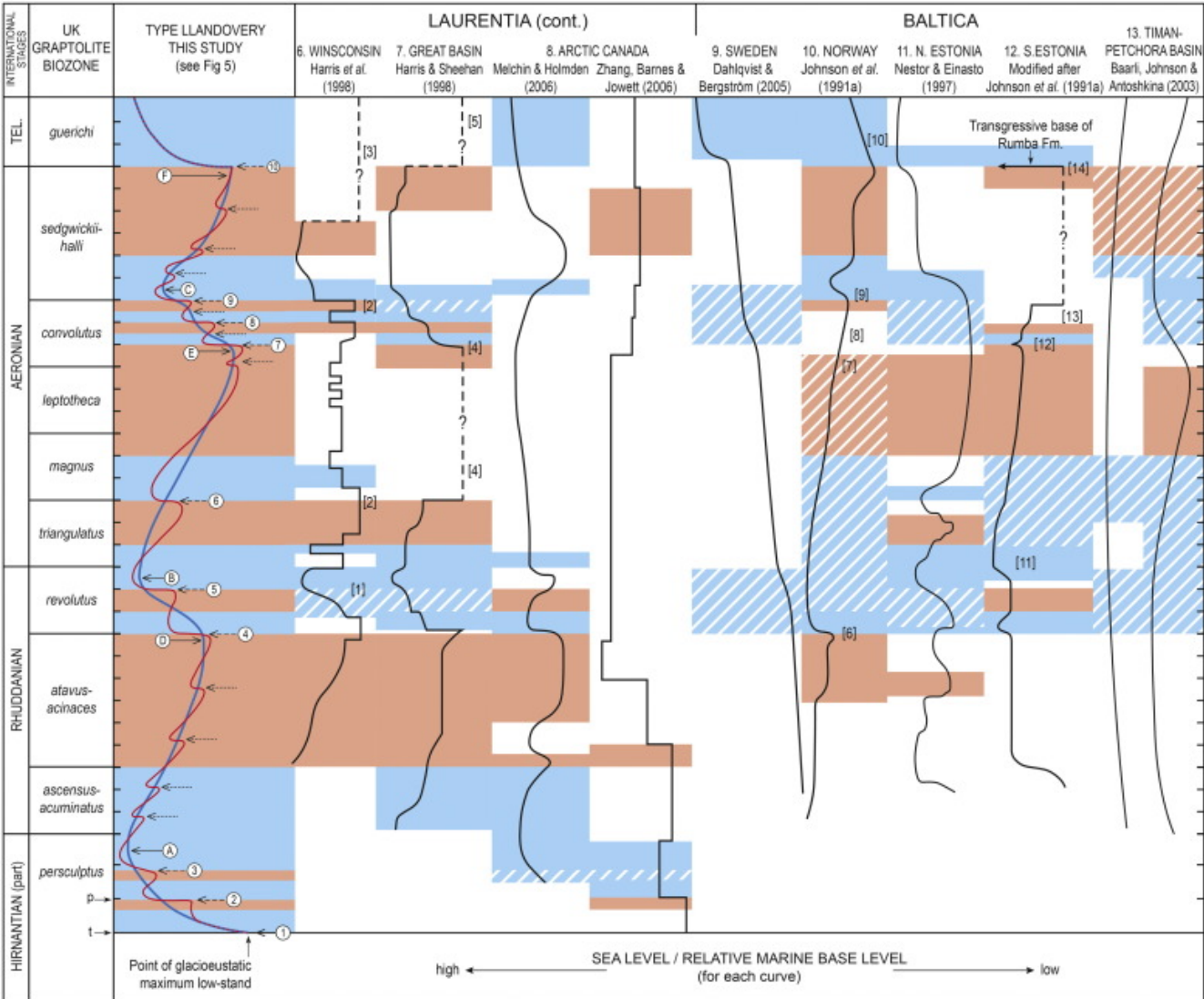
Clinoform facies belts	Principal component lithologies (inc. typical relative percentages)	Formation/member	Principal sedimentary structures	BA	BI	Selected trace fossils
1 TOPSET	Sandstone, medium-bedded, medium- to coarse-grained (95) Pebble and granule conglomerate (2-5)	DD, Wow	Cross-stratification; pentamerid brachiopod coquinas; common burrow-mottling	2/3	2-4	<i>Skolithos</i> , <i>Diplocraterion</i>
2 UPPER FORESET	Sandstone, intensely bioturbated, thick-bedded, fine- to medium-grained, with dispersed granules and pebbles (20) Muddy sandstone, intensely bioturbated, thick-bedded, fine- to medium-grained, with dispersed granules and pebbles (70) Sandstone as thin, sharp-based beds and laminae with bioturbated tops (2-10)	CcF, Ceg, Wow, Gol	Pervasive burrow-mottling; parallel- and cross-lamination only common in thin sandstone beds; pebble and granule lags	3/4	4-5	<i>Teichichnus</i> , <i>Palaeophycus</i> , <i>Planolites</i> , <i>Zoophycus</i> , <i>Chondrites</i>
3 LOWER FORESET	Sandy mudstone, strongly bioturbated, medium bedded, with dispersed coarse sand grains and granules (85) Sandstone as thin, sharp-based beds and laminae with bioturbated tops (2-10) Silty mudstone with thin, weakly bioturbated sandstone and siltstone beds and laminae (5)	BrF, TrF, Rdg, Gol, Yst, Ydw Ydw	Pervasive burrow-mottling (sparse in Ydw); parallel- and cross-lamination only common in thin sandstone and siltstone beds	5	3-4 2-3	<i>Thalassinoides</i> , <i>Planolites</i> , <i>Zoophycus</i> , <i>Chondrites</i> <i>Zoophycus</i> , <i>Chondrites</i>
4 BOTTOMSET	Mudstone, silty, thin-bedded with diffuse colour banding (90) Thin, unbioturbated beds and laminae of sandstone and siltstone (2-10)	ChF	Poorly preserved hemipelagic lamination; sparse burrow-mottling; minor slump-related convolutions	6	1-2	<i>Chondrites</i> (small diameter)
5 SLUMP BELT	Disturbed bottomset mudstone (75-95) Mélange/debrite – mudstone with ill-sorted angular and rounded clasts (5-20) Large displaced rafts of other facies belt lithologies (dominant in some slump complexes)	db (locally affects most formations)	Slump folds and convolute bedding; listric surfaces; basal and internal slide planes			Not applicable

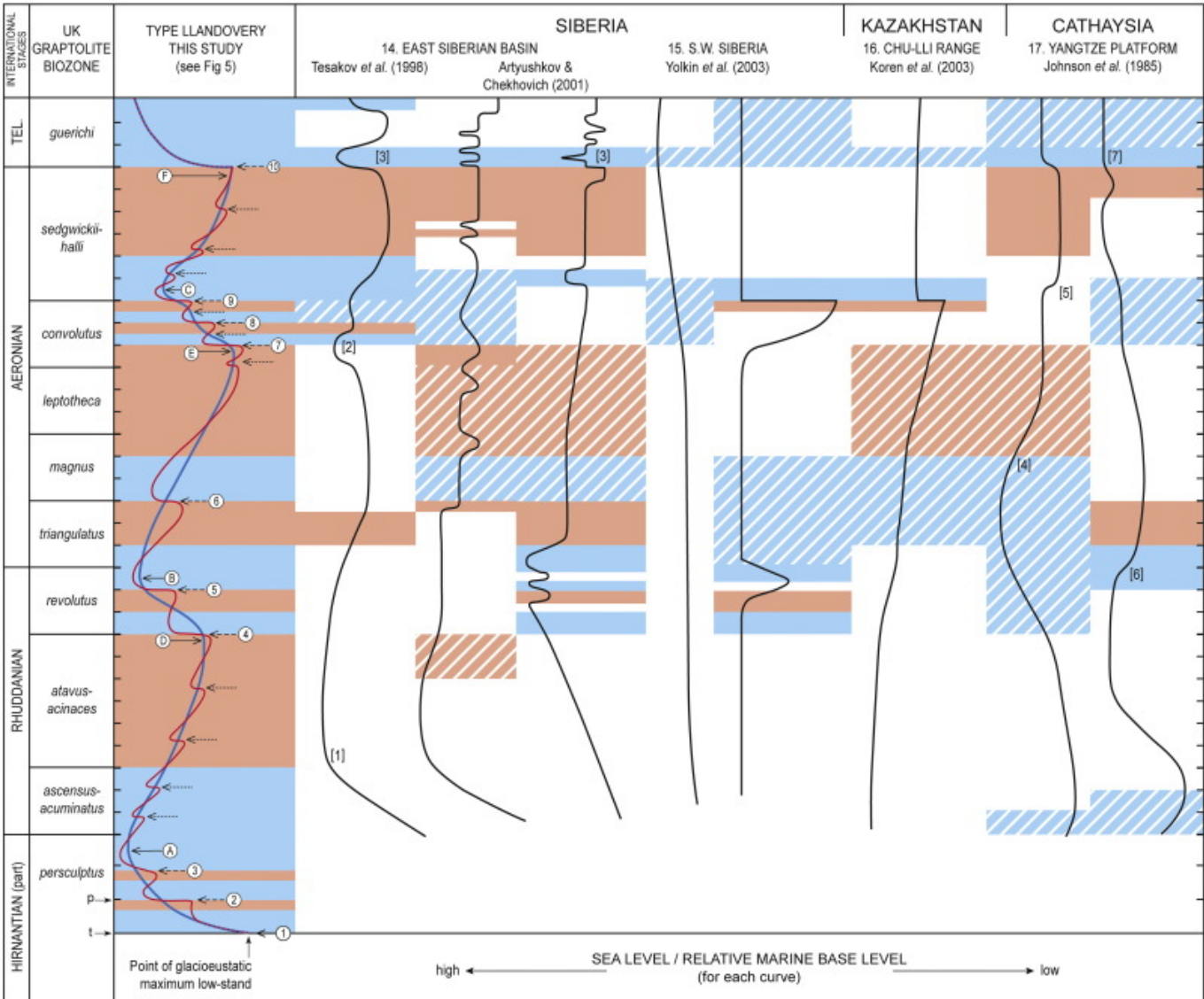


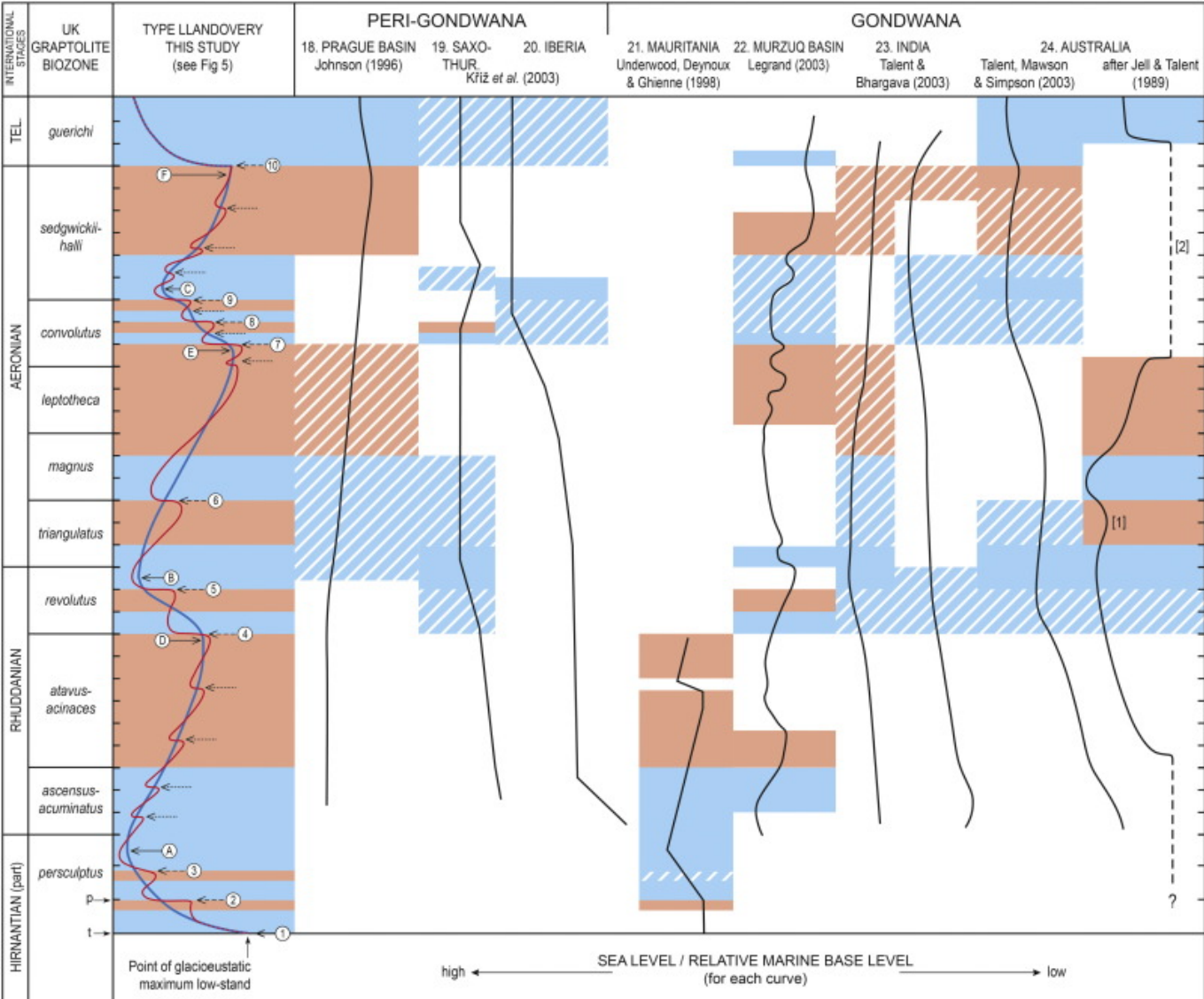


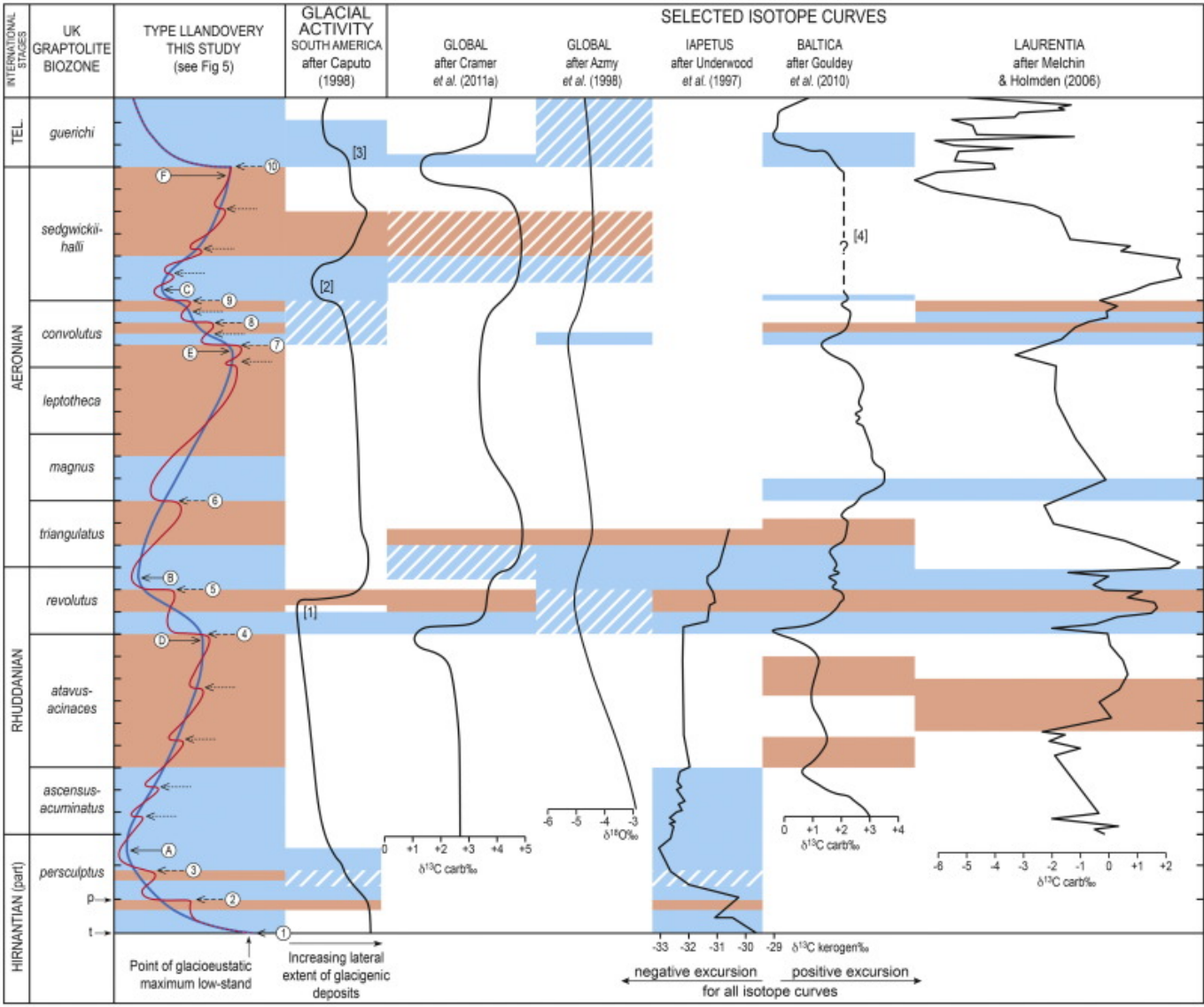


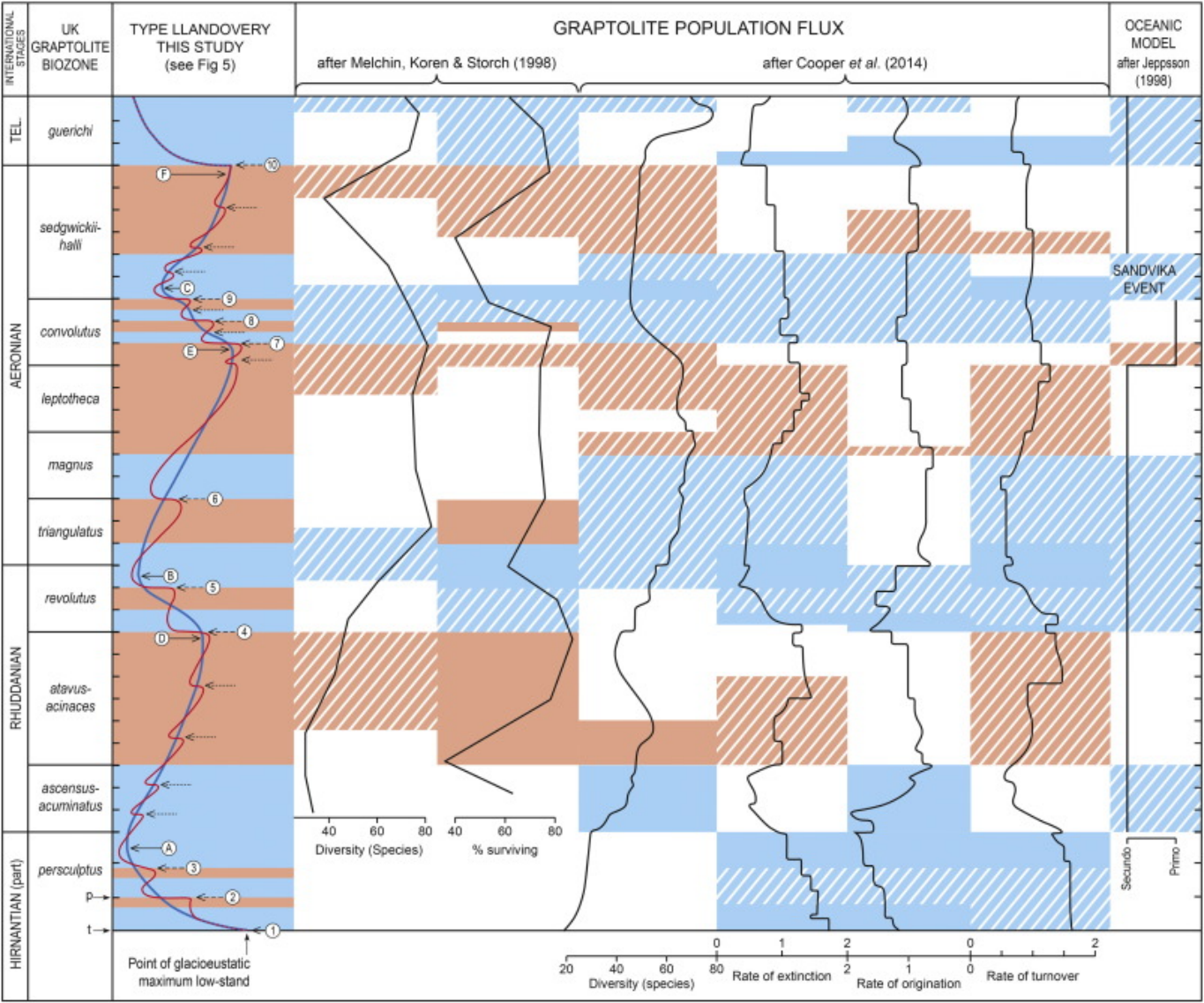


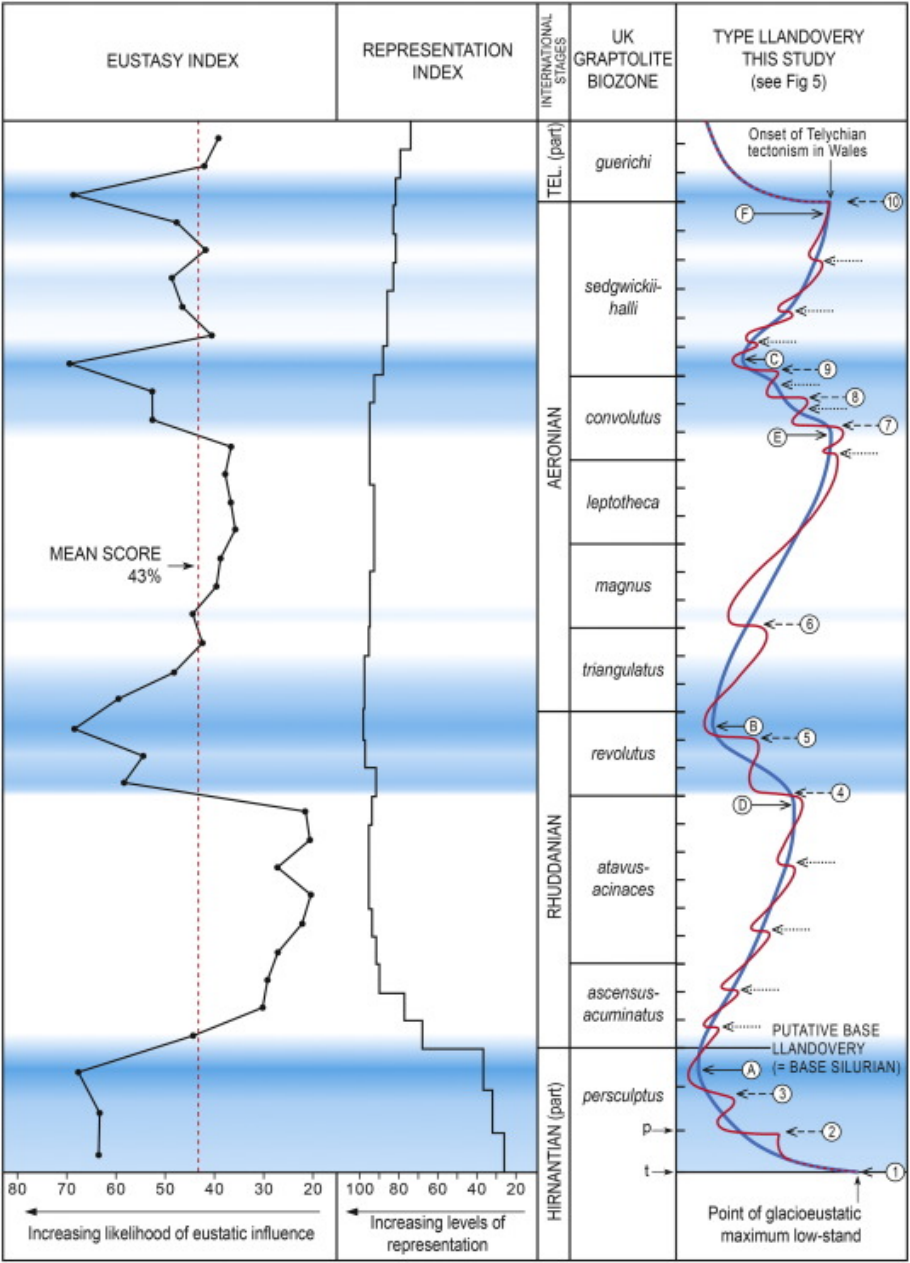


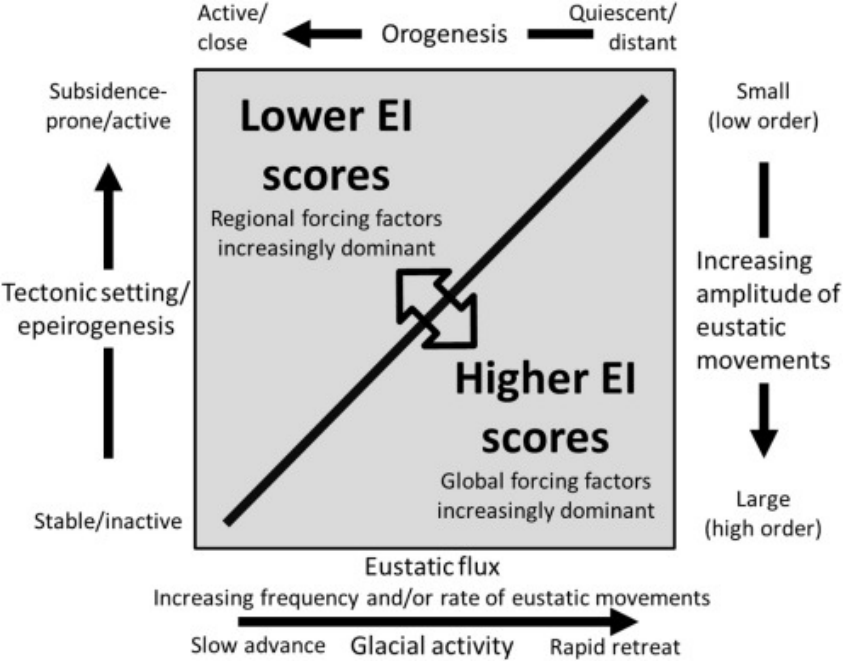












Palaeogeographical and proxy datasets		Relevant text figure	Number of datasets
UK (Avalonian & Iapetus)*		7	6
Laurentia		9,10	13
Baltica		10	6
Siberia		11	5
Kazakhstan		11	1
Cathaysia (South China)		11	2
Peri-Gondwana		12	3
Gondwana		12	6
Global		8	7
Proxy datasets	Glacial deposits	13	1
	Isotopes	13	5
	Graptolite flux	14	6
	Oceanic model	14	1
Total number of datasets			62



5 cm

Supplementary data

Biostratigraphical notes and background to correlations used to recalibrate base level and proxy curves; numbers refer to those shown [in square brackets] on Figures 5, 7-13

In Wales, chitinozoans identified as, or comparable to, *Spinachitina taugourdeau* are present in non-graptolitic strata that underlie the lowest occurrence of *persculptus* Biozone graptolites (Vandenbroucke, 2008; Vandenbroucke *et al.* 2008; Davies *et al.*, 2009, 2013; Challands *et al.* 2014). However, published data suggest that the *S. taugourdeau* Biozone equates with part of the *persculptus* Biozone (Melchin, Holmden & Williams, 2003; Ghienne *et al.*, 2014) and that both biozones embrace the upper part of the Late Ordovician glacial maximum and linked HICE event. Taken at face value, this implies that strata (Garth House Formation and its correlatives) deposited during the initial post-glacial maximum transgression (Davies *et al.* 2009) must now be considered to be of *persculptus* Biozone age even though they pre-date the regional first appearance of *persculptus* Biozone graptolites. In post-dating the glacial maximum, the occurrences of *S. taugourdeau* and *S. cf. taugourdeau* chitinozoans in Wales are higher/younger than elsewhere and in need of further investigation (Challands *et al.* 2014). Late first appearances of *persculptus* Biozone graptolites are a feature of many late Hirnantian successions (e.g. Melchin *et al.*, 2013) and it seems that strata assigned to the *persculptus* Biozone in Wales must now be interpreted as spanning only its upper part. Strata that intervene between the glacial maximum low-stand event and the base of the *ascensus-acuminatus* Biozone in Wales are here assigned to an upper *persculptus* biozonal interval equivalent to the Hi2 time slice of Bergström *et al.* (2009) (See Fig. 5, note [20] below). However, for eustasy index assessments (see Section 8), this period has continued to be treated as the equivalent of a single biozone.

Subspecies of the *Stricklandia* brachiopod lineage, *S. lens lens* and *S. lens prima*, previously thought to range into the *revolutus (cyphus)* graptolite Biozone, are now known to be restricted to earlier strata. It is their successor, *S. lens intermedia*, that has its FAD at about the base of the *revolutus* Biozone. Critically, key elements of the *Stricklandia* and *Eocoelia* brachiopod lineages co-existed. The ranges of *S. lens progressa* and *E. hemispherica* and their successor species, *S. laevis* and *E. intermedia*, all overlap in the lower *sedgwickii* Biozone. *Stricklandia lens progressa* and *E. hemispherica* range into this interval from the underlying *convolutus* Biozone, whereas *S. laevis* ranges from the *sedgwickii* Biozone into rocks of Telychian age (Fig 5). These findings endorse those of Baarli & Johnson (1988), who established that species and subspecies of *Stricklandia* co-existed within evolving Norwegian populations. This emphasises the importance of last appearances (LADs) of key taxa for Silurian correlation (e.g. Cocks *et al.*, 1984) in addition to first appearances (FADs). Noteworthy amongst other brachiopods used for Llandovery correlation are species of the pentamerids *Virgiana*, *Borealis*, *Pentamerus* and *Pentameroides* (e.g. Bassett, 1989; Jin & Copper, 2008) (Fig 5).

The new work shows that the *fisherii* acritarch Biozone is confined to the pre-*revolutus* graptolite Biozone interval and, in contrast to previous reports (Hill & Dorning in Cocks *et al.*, 1984), that the *microcladum* Biozone completely, and *estillis* Biozone partly, pre-date the *sedgwickii* Biozone. *Gracilisphaeridium encantador*, the eponymous species of the *G. encantador* acritarch Biozone, has its FAD in the Type Llandovery area in the *guerichi* Biozone, lower than envisaged by Davies *et al.* (1997). An initial study of Type Llandovery chitinozoans by De Permentier & Verniers (2002), and a more detailed assessment of the *electa*, *maennili* and *dolioliformis* biozones by Davies *et al.* (2013), showed in particular that *Eisenackitina dolioliformis* occurred in the upper *convolutus* Biozone at Llandovery and therefore stratigraphically lower than reported in Baltica (e.g. Nestor, 2010).

There is a paucity of information on conodont assemblages from the Type Llandovery area due to facies constraints. The single record of an *I. discreta*–*I. deflecta* Biozone (= *D. kentuckyensis* Biozone, Aldridge, 1985) assemblage from the Bronydd Formation is consistent with the formation's Rhuddanian age (Cocks *et al.*, 1984). For many Llandovery successions around the world, notably

those dominated by shallow water carbonates, conodonts provide the principal means of dating and correlation. Hence, to meet the objectives of this paper, it is important briefly to discuss the evolving conodont biozonal scheme for the Llandovery Series, and its shortcomings. Dahlqvist & Bergstrom (2005) and Mannik (2007) provided reviews of conodont biostratigraphical research that reflect extensive recent work, particularly in the Baltic region (see also Rubel *et al.*, 2007; Loydell, Nestor & Mannik, 2010), but also in North America (e.g. Zhang & Barnes, 2002a; Kleffner, 2004; Kleffner, Barrick & Drachen, 2004). The level of subdivision now achieved in the Telychian is beginning to rival that provided by graptolites, but establishing a detailed conodont biozonation for the Rhuddanian and Aeronian has proved elusive. Until quite recently just two biozones were recognised within this interval, the *D. kentuckyensis* Biozone and the succeeding *D. staurognathoides* Biozone (e.g. Aldridge, 1985). Zhang & Barnes (2002a) put forward a more detailed subdivision based on the succession on Anticosti Island, Québec, but the wider applicability of their scheme has been questioned (e.g. Dahlqvist & Bergstrom, 2005). Their *O. hassi* Biozone, spanning the Hirnantian–Llandovery boundary, is applicable in North America (e.g. Mikulic *et al.*, 1985), but has not been recognised elsewhere (e.g. Mannik, 2007).

Most relevant to this study has been the erection and widespread acceptance of the *Pranognathus tenuis* Biozone in place of the upper part of the *D. kentuckyensis* Biozone (see Dahlqvist & Bergstrom, 2005). The presence of the index taxon distinguishes lower–middle Aeronian rocks. However, the relationship between this conodont biozone and the graptolite biozonal scheme is ambiguous. Melchin, Cooper & Sadler (2004), Cramer *et al.* (2011b) and Melchin, Sadler & Cramer (2012) all located its base within the *triangulatus* Biozone and its top in the *leptothea* Biozone. However, in an intervening paper, Cramer *et al.* (2011a) placed its base in the *convolutus* Biozone and its top within the *sedgwickii* Biozone, albeit with boundaries that indicated uncertainty with respect to the graptolite biozonation (Cramer *et al.*, 2011a, fig. 3). Discoveries by Loydell, Nestor & Manick (2010) in Latvia confirm that the FAD of *P. tenuis* lies within the *triangulatus* Biozone there. In Norway, Aldridge & Mohamed (1982) recovered the taxon from the same levels that Johnson *et al.* (1991) report *S. lens progressa* (see Fig 10, note [9]) and, in the UK, it is known at different localities to co-occur with *E. hemispherica* and *convolutus* Biozone graptolites, but not with *E. intermedia* or *sedgwickii* Biozone graptolites (Aldridge, 1972, 1975). In the light of the revised brachiopod ranges established in the Llandovery area, these findings suggest that the *P. tenuis* conodont Biozone ranges from the *triangulatus* Biozone into, but not above the *convolutus* Biozone. Below the *P. tenuis* Biozone, the short lived *Aspeludia? expansa* conodont Biozone (Armstrong, 1990) spans the *cyphus (revolutus)*–*triangulatus* biozonal boundary (e.g. Loydell, Nestor & Mannik, 2010) (Fig 5).

Following Davies *et al.*'s (2013) re-appraisal of the current GSSPs for the Aeronian and Telychian stages, both erected in the Llandovery area, the base Aeronian GSSP is now known to be in the middle of the *triangulatus* Biozone rather than at its base. Moreover, the FAD of *S. laevis* is now known to be below the Telychian GSSP and significantly below the first appearance of *guerichi* Biozone graptolites. Consequently, it should not now be used as a proxy for the base of the Telychian Stage. In addition, Cocks *et al.*'s (1984) use of the brachiopod *Eocoelia curtisi* and the acritarch *Deunffia monospinosa* in the Type Llandovery succession have been called into question by Davies *et al.*'s (2010, 2011, 2013) discovery that key specimens recorded by Cocks *et al.* (1984) came from a synsedimentary melange. In particular, the presence of *E. curtisi* by itself can no longer be taken as evidence of a post-*sedgwickii* Biozone age, following the work of Doyle, Hoey & Harper (1991), who showed that its FAD at Girvan, southern Scotland, was below beds yielding upper *sedgwickii* Biozone graptolites.

Figure 5. Compilation of selected biostratigraphical ranges and biozonal schemes in use for the late Hirnantian and Llandovery series.

1. The *ascensus-acuminatus* Biozone is recognised as a single biozone in the UK, but is increasingly shown as two separate biozones in other areas and on international charts (e.g. Melchin, Sadler & Cramer, 2012).
2. The *atavus* and *acinaces* biozones are commonly indistinguishable in many regional accounts both in the UK and elsewhere (e.g. Davies *et al.*, 1997).
3. The base of the *revolutus* Biozone is commonly shown as slightly younger than the *cyphus* Biozone it replaces (see Zalasiewicz *et al.*, 2009).
4. The *halli* Biozone is now well established in the UK, but continues to be conflated with the *sedgwickii* Biozone in many schemes (e.g. Melchin, Sadler & Cramer, 2012).
5. Following the widespread adoption of the *guerichi* Biozone, the terms *sensu lato* (s.l.) and *sensu stricto* (s.s.) are used to distinguish the former and modern usages, respectively, of the *turriculatus* Biozone (see Davies *et al.*, 2013).
6. See Cocks & Rickards (1969), Baarli (1986) and Davies *et al.* (2013).
7. *Eocoelia hemispherica* is unknown in the Type Llandovery area below the upper *convolutus* Biozone (Davies *et al.*, 2013), and Baarli & Johnson (1988) suggested that this is the case worldwide. However, Cocks *et al.* (1984; also Cocks, 1989; Bassett, 1989) placed its FAD in the *leptothea* Biozone. The earliest record of the genus is from Rhuddanian rocks in South America (Zeigler, 1966).
8. Baarli & Johnson (1988) recognised *Borealis osloensis* as extending into the range of *S. lens progressa*.
9. e.g. Loydell, Nestor & Mannik (2010)
10. See Biostratigraphical notes above.
11. Former base of the *Pterospathodus celloni* Biozone (see Mannik, 2007).
12. Known ranges of *Spinachitina taugourdeau* and *S. cf. taugourdeau* in Wales, but not internationally; see above and Challands *et al.* (2014) for discussion.
13. Former base of the *Eisenackitina dolioliformis* Biozone (e.g. Loydell, Nestor & Mannik, 2009).
14. See Kiipli *et al.* (2010).
15. Former base of the *Gracilisphaeridium encantador* Biozone (Davies *et al.*, 1997).
16. See Davies *et al.* (2011, 2013).
17. See Burgess (1991).
18. Brett *et al.* (1998) recorded *Zygobolba excavata* Biozone ostracodes from the same beds as *Eocoelia intermedia*, the Wallington Limestone Member (Reynales Limestone Formation) and the overlying lower Sodus Shale Formation in the lower part of the Clinton Group, western and central New York State.
19. Brett *et al.* (1998) correlate the interval from the *Zygobolba decoris* Biozone to the *Mastigobolbina lata* Biozone to the *P. celloni* s.l. conodont Biozone, i.e. from the former base of the *P. celloni* Biozone (see [11] above) to the top of the restricted *celloni* Biozone as depicted on Fig. 5.
20. In the absence of published isotope data, the marked facies changes that mark the onset of the late Hirnantian, post glacial maximum transgression at Llandovery and throughout Wales (see Davies *et al.*, 2009) are taken to mark the intra-*persculptus* Biozone boundary between the Hi1 and Hi2 times slices of Bergström *et al.* (2009) and, by inference, the end of the HICE excursion.

Figure 7. Other UK datasets

1. The absence of *Eocoelia* indicates a pre-*leptothea* Biozone age for shelly assemblages from the ‘Pentamerus Beds’ (= Venusbank Fm. of Cocks *et al.*, 1992) in the Hamperley Borehole, Shropshire. Otherwise, Cocks & Rickards (1968) regarded the assemblages from the Hamperley Borehole as being identical to those of the mid-late Aeronian *Eocoelia* Benthic Community. This supports a *magnus* Biozone age (see Fig 5, note [7]) for the underlying flooding event that

- introduced marine faunas. The onset of Silurian sedimentation in this region was within the range of *S. lens intermedia* and therefore no older than the *revolutus* Biozone.
2. In the Shelve and Church Stretton areas of Shropshire, Cocks & Rickards (1968) and Zeigler, Cocks & McKerrow (1968) widely recognised forms of *S. lens* that are transitional between *S. lens intermedia* and *S. lens progressa*. The presence of such forms in the Hamperley Borehole, associated with *convolutus* Biozone graptolites but 15 m below a *sedgwickii* Biozone graptolite assemblage (Cock & Rickards, 1968), is consistent with the mid *convolutus* Biozone age now established for that transition, and serves to date the flooding episode recorded by the *Stricklandia* Benthic Community assemblage, to which they belong (Johnson, Rong & Kershaw, 1998).
 3. Zeigler, Cocks & McKerrow (1968) recognised *E. intermedia* in the basal beds of the Venusbank Formation along the southern flank of the Shelve Inlier at Norbury, Shropshire, which dates the marine inundation at this locality as *sedgwickii* Biozone in age.
 4. Within an otherwise anoxic Rhuddanian succession, Cullum & Loydell (2011; see also Cave & Hains, 1986) reported an oxic interval within the ‘*cyphus* Biozone’ in the Rheidol Gorge, mid Wales.
 5. Davies *et al.* (1997, p. 87) reported *halli* Biozone graptolites in the upper part of the ‘*M. sedgwickii* shales’ in mid Wales.
 6. Loydell (1991) recognised graptolite assemblages from strata at Dob’s Linn, Southern Uplands, previously assigned to the now defunct early Telychian *maximus* Subzone, as being diagnostic of the late Aeronian *halli* Biozone.

Figure 8. Published global sea level curves

1. See note [1] for Fig. 9.
2. See notes [2] and [3] for Fig. 9.
3. Late Aeronian deepening. Long acknowledged as a period of falling sea levels, debate has centred on whether this peaked during the *convolutus* (e.g. Loydell, 1998) or *sedgwickii* biozones (see [4] and [5] below). Based on data presented by Wills & Smith (1922), Loydell (1998) emphasised the anoxic nature of *convolutus* Biozone rocks in North Wales as justification for locating the highstand in this biozone. However, extensive recent work on rocks of this age in mid Wales show this to have been a period during which oxic and anoxic bottom conditions alternated within the Lower Palaeozoic Welsh Basin.
4. Basal *sedgwickii* Biozone highstand. This was first recognised as a ‘global’ feature by McKerrow (1979) and is now well entrenched in the literature. Graptolite dating was based on the Type Llandovery collections of Jones (1925), which underpinned his original definition of the basal Upper Llandovery C1 interval and which were used in turn to calibrate ranges for the *Stricklandia* (Williams, 1951) and *Eocoelia* (Ziegler, 1966; also Ziegler, Cocks & McKerrow, 1968) brachiopod lineages. Modifications by Cocks *et al.* (1984) did not impact on this early work. Thus, in many areas, the dating of a basal *sedgwickii* Biozone highstand has been based on the calibrated brachiopod biostratigraphy, specifically the presence of *Stricklandia lens progressa*. New work in the type area has since shown, however, that the FAD of *S. lens progressa* and the localities where it is most abundant are stratigraphically below lower *sedgwickii* Biozone graptolites. Hence, the presence of this brachiopod subspecies on its own cannot be used as evidence of a *sedgwickii* Biozone age. Moreover, the ranges of *S. lens progressa* and its successor species, *S. laevis*, overlap in rocks of *sedgwickii* Biozone age, so *S. laevis* cannot be used in isolation as a proxy for the *guerichi* graptolite Biozone (= lower *turriculatus* Biozone of earlier usage). It is also now reasonable to infer the presence of *Eocoelia hemispherica*, *E. intermedia* and *E. curtisi* in rocks of *sedgwickii* Biozone age. It follows that the *sedgwickii* Biozone (or mid Aeronian) deepening phase depicted in many of the key sections used to construct regional and global sea level curves, including those of Johnson (e.g. 1996, 2006; Johnson, Rong & Yang, 1985 and Johnson *et al.*, 1991) and Ross & Ross (1996), must be regarded with circumspection as these were commonly dated by brachiopod lineages and lack

independent graptolitic evidence of age. Nevertheless, there is clear evidence at Llandovery that the incoming of *sedgwickii* Biozone graptolites was linked to a marked regional transgression within the overlapping ranges of *S. lens progressa* and *S. laevis*.

5. Late Aeronian lowstand. Based on his analysis of graptolitic facies, Loydell (1998) rejected the evidence for a deepening event of early *sedgwickii* Biozone age. He suggested that the presence of oxic facies in many areas, bracketed by dark graptolite-bearing units of *convolutus* Biozone age below and *guerichi* Biozone age above, showed that the *sedgwickii-halli* biozonal interval was a period of sustained regression. In other areas, he cited the absence of *sedgwickii* Biozone aged rocks as evidence of contemporary emergence and erosion. The overstepping nature of *sedgwickii* Biozone rocks at Llandovery and in the Welsh Borderland counters this assessment. At Llandovery, lower *sedgwickii* Biozone transgressive facies (Ydw Member; Davies *et al.*, 2013) are preserved beneath a thick, shoaling upwards sequence. In other areas, above their transgressive base, rocks of the *sedgwickii-halli* biozonal interval record deposition only under shoal conditions, but the evidence overall suggests that these form part a single T-R cycle. On Baltica, in Danish and Swedish sections where *sedgwickii* Biozone graptolites are unrecorded, bioturbated mudstones succeed graptolitic facies that yield the upper *convolutus* Biozone marker *Cephalograptus cometa extrema*, and underlie beds with 'lower' *turriculatus* (= *guerichi*) Biozone graptolites (Johnson, Kaljo & Rong, 1991). Loydell (1998) cited this as evidence against a basal *sedgwickii* Biozone highstand. Oxic facies also succeed *C. c. extrema*-bearing graptolitic facies in the Welsh Basin (e.g. Cave & Hains, 1986; Davies *et al.*, 1997), but there they underlie the FAD of lower *sedgwickii* Biozone assemblages within the basin-wide *M. sedgwickii* Shales Member. Loydell (1994, 1998) invoked basin isolation to explain the presence of organic-rich graptolitic mudstones at this level in Wales, despite evidence on the adjacent platform for a coeval marine transgression (see Fig. 7, note [3]). It is arguably the Danish and Swedish sections that are aberrant. There, within condensed successions, the absence of *sedgwickii* Biozone graptolites could indicate either omission, or bioturbation or erosion of an attenuated graptolite-bearing transgressive unit as sea level fell during the later part of the interval (i.e. regressive submarine erosion), or enhanced tectonic activity in basins adjacent to an advancing Scandian orogenic front (see Section 8).

Figure 9. Published circum-Iapetus sea level curves: Laurentian interior and Appalachian Foreland Basin

1. Ross & Ross (1996) recognised a lowstand event linked to the Mosalem Formation of Iowa and the equivalent Schweizer Member (Wilhelmi Fm.) of Illinois that they considered to be mid Rhuddanian ('*vesiculosus*' Biozone), but reassessments of age discussed below now suggest that it is of *persculptus* Biozone age. Graptolites from these units were assigned by Ross (1962, 1964) to the late *acuminatus* or early *vesiculosus* (= *atavus-acinaces*, see Fig. 5) biozones (= mid Rhuddanian). Berry & Boucot (1970) reassigned the fauna to the mid Rhuddanian-lower Aeronian interval. Ross & Ross (1996) implied that the graptolite bearing beds marked a deepening event, but accounts of sections in Illinois by Willman (1973; Willman & Atherton, 1975) and in Iowa by Johnson, Rong & Yang (1985; Johnson, 1987) and Witzke (1992) provided no evidence of a subsequent shallowing. The contact with the succeeding Tete des Morts Formation (= Birds Member, Wilhelmi Fm) was described as gradational and the Mosalem and Tete des Morts formations were reported by Witzke (1992) to form part of an uninterrupted period of deepening. Witzke & Bunker (1996) gave an alternative view, suggesting that the Mosalem Formation might form a 'discrete T-R cycle'. The top of the shoaling phase shown by Ross & Ross (1996) was subsequently adopted and widely correlated by subsequent workers in the US as an intra-Rhuddanian sequence (or sub-sequence) boundary (e.g. Harris *et al.*, 1998), despite a lack of firm biostratigraphical evidence to support the correlation. Loydell *et al.* (2002) recognised the graptolite fauna as being *persculptus* Biozone or, at the youngest, early *ascensus-acuminatus* Biozone in age. The implications of this revised dating were apparently not fully digested by Page *et al.* (2007), who seem to have followed Ross & Ross (1996) closely in the

- construction of their global curve. The event must be significantly older than first thought and is perhaps more likely to compare with one of the intra-*persculptus* Biozone events seen at Llandovery (Davies *et al.*, 2009).
2. Johnson, Rong & Yang (1985) associated the earliest of their Llandovery deepening episodes with the Blanding Formation of Illinois and Iowa, considered by them to be basal Aeronian in age. Johnson (1996) subsequently matched this highstand with the older Tete des Morts Formation (see above), a unit previously included in the Rhuddanian but shown by Johnson (1996) as spanning the Rhuddanian-Aeronian boundary in accord with Berry & Boucot (1970; see above). The pitting and erosion displayed by the top of the Tete des Morts Formation (Willman, 1973) justified its recognition by Ross & Ross (1996) as indicating a stage boundary lowstand event. Loydell *et al.*'s (2002) graptolite revisions (see above) called both of these interpretations into question. Llandovery rocks in both Iowa and Illinois comprise condensed dolomitic carbonate successions. Erosional diastems and hardgrounds have been recognised and cryptic omission surfaces are likely to be present. However, the Tete des Morts Formation and its equivalents are widely shown to succeed the Mosalem Formation conformably (e.g. Ross & Ross, 1996) and the revised dating suggests that it is unlikely to extend above the lower Rhuddanian. The pitted top of the Tete des Morts Formation might record the effects of an intra-Rhuddanian lowstand widely recognised in other North American successions rather than a stage boundary lowstand as argued by Ross & Ross (1996). This implies a significant non-sequence beneath the transgressive base of the Blanding Formation (= Elwood Fm), and suggests that the latter unit was deposited during a late Rhuddanian highstand (Witzke, 1992; also Metzger, 2005). In Illinois, Mikulic *et al.* (1985) recorded the conodont *Ozarkodina hassi* in both the Bird Member (see [1] above) and overlying Elwood Formation. Zhang & Barnes (2002b) recognised an *O. hassi* Biozone as spanning the Hirnantian–Rhuddanian boundary, but *O. hassi* itself is known to range into the early Aeronian (e.g. Loydell, Nestor & Mannik, 2010).
 3. FAD of *S. lens intermedia*. Johnson's (1987) and Johnson, Kaljo & Rong's (1991) designation of a global highstand at or just above the Rhuddanian–Aeronian boundary owed much to its recognition and dating in the Iowa area at a time when the FAD of *S. lens intermedia* was linked to the base of the *triangulatus* Biozone. Following work in Norway by Baarli (1986), who placed the FAD of *Stricklandia lens intermedia* in the *cyphus* (= *revolutus*) graptolite Biozone, Johnson *et al.* (1991) favoured an older placement (i.e. pre-*triangulatus* Biozone) for this deepening episode in Iowa (Laurentia) and globally. However, in all subsequent reviews, Johnson (1996, 2006) continued to refer to a highstand peak 'at or near' to the stage boundary. Davies *et al.* (2013) confirmed the biostratigraphical recalibration of the FAD of *S. lens intermedia* in the Llandovery area. In Iowa, *Stricklandia lens intermedia* is first recorded in the Blanding Formation (Witzke, 1992), possibly deposited during a late Rhuddanian highstand (see [2]).
 4. FAD of *S. lens progressa*. Following on from [3], the stratigraphy spanning the Rhuddanian–Aeronian stage boundary subsequently became linked to a shallowing episode associated with a period of glacial re-advance in South America (Johnson, 1996, 2006; see Section 7.a). However, the position of the Rhuddanian–Aeronian contact is poorly constrained in many areas, including the critical successions in Iowa and Illinois. Above the deepening event recorded by the Blanding Formation, the presence of *Stricklandia lens progressa* mid-way through the overlying Sweeny Member (Hopkinton Fm.) has been taken as evidence of a *sedgwickii* graptolite Biozone age (e.g. Johnson, Rong & Yang, 1985; Johnson, 1987). However, the revised range of this subspecies at Llandovery now suggests that the earliest Iowan assemblages likely equate with the *convolutus* Biozone (see also Baarli, 1986). The base of the Sweeny Member (= base Drummond Mbr, Kankakee Fm) is recorded as a marked unconformity in the Illinois Basin and in Wisconsin by Ross & Ross (1996). The erosive lowstand event recorded by the unconformity appears to have been widely recognised as a sequence boundary (e.g. Brett *et al.*, 1998) and could account for the removal of late Rhuddanian to early Aeronian strata in Iowa, Illinois and more widely in North America. However, Ross (1962), Willman (1973), Mikulic *et al.* (1985) and Witzke (1992) recognised the contact between the Blanding Formation and the Sweeny Member, and their equivalents, as gradational. If this is the case, the Blanding Formation together with the lower levels of the Sweeny Member must span the whole of the *revolutus*–*leptotheca* biozonal interval.

It follows that the lower to mid Aeronian would have been a protracted period of condensed shoal facies deposition bracketed by well-constrained highstand events. Therefore, and contrary to Ross & Ross (1996), Page *et al.* (2007) and Haq & Schutter (2008), evidence for a discrete early Aeronian shallowing phase is considered to be lacking in these key sections.

5. FAD of *S. laevis*. Johnson, Rong & Yang (1985; Johnson, 1987) considered the appearance of *S. laevis* in the Iowan Farmers Creek Member to establish an early Telychian *guerichi* (= lower *turriculatus* s.l.) Biozone highstand. However, the FAD of this species at Llandovery is now established as occurring within the *sedgwickii* Biozone. In the absence of other dating constraints, the assumption must be that this is also true in Iowa and throughout the circum-Iapetus realm (e.g. Johnson, Cocks & Copper, 1981; Johnson *et al.*, 1991; Brett *et al.*, 1998).
6. Following Kluessendorf & Mikulic (1996), Witzke & Bunker (1996) recognised the top of the Picture Rock Member as a regional unconformity (disconformity). The Farmers Creek Member (below the Picture Rock Member) bears *Stricklandia laevis* whereas the overlying Johns Creek Quarry Member (basal Scotch Grove Formation) contains the late Llandovery genera *Costistricklandia* and *Pentameroides*. The unconformity could therefore account for the removal or non-deposition of early to mid Telychian strata in Iowa. However, Kluessendorf & Mikulic (1996) contended that erosion pre-dated the first appearance of *celloni* Biozone conodonts in the Brandon Bridge Member (Joliet Formation) of Illinois and Wisconsin, and since Witzke (1992) recorded conodonts of the *celloni* Biozone in the upper Picture Rock Member, it seems more likely that the level of the erosive event/lowstand? in Iowa is within or at the base of the Picture Rock Member rather than at the top. In either case, unambiguous evidence for an early Telychian highstand is lacking throughout these states.
7. It follows that the rocks immediately below this regional disconformity in Illinois (Plaines Member, Kankakee Formation), placed by Ross & Ross (1996) in the *griestoniensis* Biozone, are also much older. Traditionally the *Pentamerus*-rich Plains Member has been correlated with the upper part of the Iowan Sweeny Member, distinguished locally as the Marcus Formation, implying that it lies within the range (*convolutus*–*sedgwickii* biozones) of *S. lens progressa* (Witzke, 1992).
8. The *Ozarkodina hassi* conodont Biozone of Zhang & Barnes (2002a) spans the Hirnantian–Rhuddanian stage boundary.
9. *S. lens* is first recorded in the Merrimack Formation on Anticosti Island (Jin & Copper, 2010).
10. Graptolites no younger than the *triangulatus* Biozone have been reported from the lower part of the Gun River Formation (Johnson, Cocks & Copper, 1981; Jin & Copper, 1999; Zhang & Barnes, 2002).
11. Upper levels of the Gun River Formation were reported to contain *D. staurognathoides* Biozone conodonts by Zhang & Barnes (2002a). This implies an age no older than the *sedgwickii* Biozone, but see discussion by Dahlqvist & Bergstrom (2005) and Biostratigraphical Notes above.
12. Graptolites in the succeeding Jupiter Formation, from below the distinctive *Panderodus* conodont-bearing interval of the Goeland Member (= Member 3 of Zhang & Barnes, 2002b), are consistent with the *convolutus* Biozone (Johnson, Cocks & Copper, 1981; Jin & Copper, 1999).
13. The FAD of *sedgwickii* Biozone graptolites coincides with the transgressive base of the East Point Member (Johnson, Cocks & Copper, 1981; Jin & Copper, 1999; Zhang & Barnes, 2002b). Johnson, Cocks & Copper (1981) also reported *E. curtisi* and *turriculatus* s.l. Biozone graptolites close to the top of the Jupiter Fm.
14. Age of the Medina Group. The upper Whirlpool, Power Glen and lower Cabot Head formations are said to contain diverse Silurian shelly assemblages suggestive of an ‘early–middle Rhuddanian’ age (Brett *et al.*, 1998).
15. Age of lower Clinton Group. Kleffner (2004; quoted in Dahlqvist & Bergstrom, 2005 and Cramer *et al.*, 2011a) reported *tenuis* Biozone conodonts from the upper Neahga Shale Formation and the overlying Reynales Limestone Formation (Hickory Corner Member). Current understanding suggests that this conodont biozone spans the ‘mid’ *triangulatus*-*convolutus* biozonal interval (see Section 2 for background and discussion).
16. Following on from [11], the overstepping base of the Reynales Limestone (Furnaceville Hematite Member and its lateral equivalents) is recognised as a significant non-sequence (Brett *et al.*,

- 1998). This can now be seen to separate the level of the first appearance of *tenuis* Biozone conodonts (upper Neahga Shale) from the overlying *tenuis*-bearing levels of the Reynales Limestone. If the occurrence of *tenuis* Biozone conodonts within the lower Clinton Group is taken to encompass the total range of the biozone, the basal Reynales Limestone non-sequence likely spans much or all of the late *triangulatus*-early *convolutus* biozonal interval.
17. The uppermost beds of the Reynales Limestone (Wallington Member), in common with the succeeding lower Sodus Shale Formation, contain *E. cf. intermedia* (Brett *et al.*, 1998), suggestive of a *sedgwickii* Biozone age.
 18. Brett *et al.* (1998) noted the presence of a 'shale-on-shale unconformity' at the contact between the lower and upper members of the Sodus Shale Formation. The presence above this contact of *E. curtisi*, *decora* Biozone ostracodes and *celloni* Biozone conodonts shows that the boundary marks a further significant non-sequence that accounts for the local absence of strata of upper *sedgwickii* to *turriculatus* s.s. biozone age, comparable to that recognised in Illinois by Kluessendorf & Mikulic (1996) (see [8] above).
 19. The FAD *S. lens progressa*, reported by Baarli, Brande & Johnson (1992) to occur above the Big Seam.
 20. The presence of forms transitional between *Pentamerus oblongus* and *Pentameroides suberectus* in the *S. laevis*-bearing Ida Seam suggests that a significant non-sequence, accounting for the local absence of much of the late Aeronian and early Telychian, is present at the base of this unit.

Figure 10. Published circum-Iapetus sea level curves: Laurentian (continued) and Baltica

1. Harris *et al.* (1998) cited the presence of *Virgiana mayvillensis* in the uppermost Mayville Formation to infer a late Rhuddanian age for the associated high-stand event. This is based on the restricted occurrence of the species in Canada, notably in the Merrimack Formation on Anticosti Island as confirmed by Jin & Copper (2010).
2. LAD of *D. kentuckyensis* Biozone conodonts. Harris *et al.* (1998) reported conodont assemblages ranging from the upper part of the Byron Dolostone and throughout the overlying Hendricks Formation of the Door Peninsula, Wisconsin, as being indicative of the upper part of the *I. discreta*-*I. deflecta* Biozone (= *D. kentuckyensis* Biozone, Aldridge, 1985). Though this was prior to the erection of the *tenuis* conodont Biozone, it can now be inferred that these too pre-date the *sedgwickii* graptolite Biozone (see Fig. 5 and Biostratigraphical notes above).
3. Harris *et al.* (1998) recognised the regional unconformity identified in Illinois by Kluessendorf & Mikulic (1996) [see note 6 for Fig. 9? above] as forming the boundary between the Wisconsin Manistique and Waukesha formations. However, their report of both *Pentamerus* and *Pentameroides* in the Manistique Formation suggests that this unit contains strata of mid Telychian (*griestoniensis* Biozone) age that postdate the regional unconformity. Consequently, the regional hiatus is more likely to be either within or at the base of the Manistique Formation.
4. FAD of *Pentamerus* (Sheehan, 1980). *Virgiana*-bearing assemblages present in the lower part of the High Lake Member (Laketown Dolomite Fm) can now be regarded as no younger than the *magnus* Biozone (e.g. Johnson, 1987). Their replacement in the upper part of the member by assemblages containing *Pentamerus*, above a non-sequence that Harris & Sheehan (1996, 1998) associated with their S2/3 sequence boundary, implies a flooding episode within the *convolutus* Biozone.
5. Hurst, Sheehan & Pandolfi (1985) recognised major facies changes at the base of the Gettel Member and its correlatives within the Laketown Dolomite Formation, associated with the FAD of the mid-late Telychian genus *Pentameroides* (Sheehan, 1980). This implies that a significant hiatus separates these units from the underlying *Pentamerus*-bearing High Lake Member, regarded by Harris & Sheehan (1996, 1998) as being exclusively Aeronian in age.
6. FAD *S. lens intermedia* according to Baarli (1986).
7. LAD *Borealis borealis* according to Johnson *et al.* (1991).
8. FADs *S. lens progressa* and *tenuis* Biozone conodonts according to Aldridge & Mohamed (1982), Baarli (1986) and Johnson *et al.* (1991). Though previously taken to indicate a *sedgwickii*

- Biozone age, Davies *et al.* (2013) placed the FAD of *S. lens progressa* in the *convolutus* Biozone.
9. Norwegian Oslo succession. In the Asker area, on which the Norwegian curve is based, Aldridge & Mohamed (1982) recorded a primitive form of *D. staurognathoides* just below the top of the Solvik Formation. In the light of these findings, Dahlquist & Bergstrom (2005) placed the base of the *D. staurognathoides* conodont Biozone at the same level as the boundary between the Solvik Formation and the overlying Rytteråker Formation, within the local range of *S. lens progressa* (Baarli & Johnson, 1988; Johnson *et al.* 1991). Following Davies *et al.* (2013), this suggests that the base of the *S. laevis*-bearing Rytteråker Formation, and the deepening event associated with it in the Asker area (e.g. Johnson *et al.* 1991), though not marking the local FAD of *S. laevis*, lies at or very close to the *convolutus*–*sedgwickii* biozonal boundary (in agreement with Worsley *et al.*, 1983). Baarli & Johnson (1988) recognised the range of *E. hemispherica*, found in the Skien district, as overlapping the lower part of the range of *S. lens progressa*.
 10. The earliest examples of definite *S. laevis* occur in the top of the Rytteråker Formation and basal Vik Formation, in transgressive strata that Baarli & Johnson (1988) correlated with the base of the *turriculatus* s.l. (*guerichi*) Biozone. However, Johnson *et al.* (1991) suggested that the transition from *S. lens progressa* occurred at a lower level in the Rytteråker Formation of the Asker and Syling areas, suggesting that the top Rytteråker–basal Vik occurrences there lay within and not at the base of the range of *S. laevis*.
 11. FAD *triangulatus* Biozone graptolites in the lower part of the Saarde Formation in the Ikla borehole (Rubel, 1977; Johnson *et al.*, 1991).
 12. FAD *S. lens progressa* in the Saarde Formation, at a depth of 355 m in the Ikla borehole (Rubel, 1977). This was taken by Johnson *et al.* (1991; also Nestor & Nestor, 2002) to indicate a *sedgwickii* Biozone age, but the taxon is now known to have its FAD in the *convolutus* Biozone (Davies *et al.*, 2013).
 13. FADs of *S. laevis* and *E. dolioliformis* and the age and relationships of the Rumba Formation. Nestor (1976) recognised that the base of the Rumba Formation overlay a regional unconformity in Estonia, but that the magnitude of the unconformity was reduced in the distal succession proved in the Ikla borehole. Gouldey *et al.* (2010) suggested that this non-sequence was formed in a submarine setting. Most authors appear to recognise the base of the Rumba Formation as marking the abrupt onset of a deepening episode, which has been interpreted as a *sedgwickii* Biozone event (e.g. Nestor, 1997; Kaljo & Martma, 2000). In contrast, Johnson *et al.* (1991), Nestor & Nestor (2002; also Nestor, *et al.*, 2003) and Loydell, Nestor & Mannik (2010; and references therein) regarded the base of the Rumba Formation as a basal Telychian flooding episode. This appears to have been based, in part, on the understanding, no longer valid, that the FAD of *S. laevis*, 1.2 m above the base of the Rumba Formation (Rubel, 1977), equated with the FADs of *guerichi* Biozone graptolites and *dolioliformis* Biozone chitinozoans. At the top of the Rumba Formation, Mannik (2007) recorded the base of the *P. eopennatus* conodont Superbiozone (base of the *P. eopennatus* ssp. n. 1 Biozone) in the top metre of the formation in the Estonian Viki core. This biozone was unproven in the Latvian Kolka-54 core, where graptolite assemblages suggest a non-sequence and the possible removal or non-deposition of strata equivalent to the uppermost Rumba Fm (Loydell, Nestor & Mannik, 2010). Rubel *et al.* (2007) also noted that the *P. eopennatus* ssp. n. 1 Biozone had not been identified in the Estonian Viirelaid core, and suggested a possible gap or condensed interval in the upper part of the Rumba Formation there. The top of the formation in the Ikla core, Estonia, was identified as an unconformity that Gouldey *et al.* (2010) again considered to be submarine in origin. Geochemical fingerprinting by Kiipli, Kiipli & Kallaste (2006) of the ‘O’ Bentonite in the upper part of the Rumba Formation showed its equivalence to the widespread Osmundsberg Bentonite, which is known elsewhere in the Baltic region to overlie *turriculatus* s.s. Biozone graptolites. In her review of east Baltic chitinozoan assemblages, Nestor (2012) showed the Rumba Formation as spanning the *turriculatus*–*crispus* biozonal boundary, and the current consensus places the base of the formation at the local base of the *turriculatus* s.l. (*guerichi*) Biozone (e.g. Kaljo & Martma, 2000; Gouldey *et al.*, 2010). These correlations are reflected in Figure 10. However, from the revised Llandoverly area data, the reported occurrences of *dolioliformis* Biozone

chitinozoans and *S. laevis* in the Rumba Formation are compatible with an age as early as the *sedgwickii* Biozone. Hence, it is possible that the formation represents a highly condensed succession, bounded by and possibly containing non-sequences, that spans much or all of the *sedgwickii* - *guerichi* - *turriculatus* biozonal interval.

14. Following on from [12] and [13], many authors have associated the widespread non-sequence seen below the Rumba Formation throughout much of Estonia with a late Aeronian (*sedgwickii* Biozone) shoaling episode and also with glacioeustatic forcing (e.g. Nestor & Nestor, 2002). However, if the current consensus placing the base of the Rumba Formation at the base of the *turriculatus* s.l. Biozone is accepted, and given that *S. lens progressa* can no longer be regarded as indicative of the *sedgwickii* Biozone (see [12] above), the possibility emerges that the whole of the *sedgwickii* Biozone is unrepresented in the Ikla section. The likely presence of a stratigraphical break at the base of the Rumba Formation in the Ikla drill core is additionally significant as the C¹³ isotope curve obtained for this borehole is widely used in texts assessing Llandovery isotope trends, yet an equivalent gap in the isotope record is commonly not shown (e.g. Munnecke & Mannik, 2009; Gouldey *et al.*, 2010) (see Fig. 13).

Figure 11. Published curves for Siberia, Kazakhstan and Cathaysia (South China)

1. Tesakov *et al.* (1998) located the post-glacial deepening maximum in Siberia above the base of the *acuminatus* Biozone and below the FAD of *cyphus* Biozone graptolites. However, they provided inconsistent and in places contradictory data for the dating of younger flooding events, which undermines the reliability of their sea level curve.
2. Tesakov *et al.* (1998) recognised a high-stand event associated with the *convolutus* Biozone, but which they also recognised as basal Aeronian.
3. Tesakov *et al.* (1998) recognised a high-stand event that significantly precedes the FAD of *turriculatus* Biozone graptolites. They associated it with the FAD of *celloni* Biozone conodonts, but Artyushkov & Chekhovich (2001) placed this event within the *staurognathoides* conodont Biozone.
4. In the Hanjiadian district of the Yangtze Platform, south China, Johnson, Rong & Yang (1985) recognised a graptolite diversity maximum spanning the *cyphus* and *gregarius* biozones as an evidence of a deepening episode.
5. Mu, Chen & Rong (1989) recognised the Shihniulan Formation of the Hanjiadian district as spanning the *sedgwickii* Biozone.
6. The northwards younging base of the Xiangshuyuan Formation, of *cyphus* Biozone age in the Leijatun district, must be significantly younger in the more northern Longjingopo district (Johnson, Rong & Yang, 1985; Mu, Chen & Rong, 1989).
7. Johnson, Rong & Yang (1985) associated the FAD of *Stricklandia traversa*, a species endemic to China, with the base of the *turriculatus* s.l. Biozone. Consequently, this does not correlate with the FAD of *S. laevis* in the UK and more widely, as they contended.

Figure 12. Published curves for Peri-Gondwana and Gondwana

1. Jell & Tallent (1989) presented graptolite dates and facies descriptions for the Cadia Group. These imply the presence of a high-stand event linked to the Bridge Creek Limestone, which spans the *cyphus* (*revolutus*)–*triangulatus* biozonal boundary, and of a subsequent shallowing linked to the ‘Upper Clastic Member’. The post glacial deepening maximum appears to have been reached during the *magnus* Biozone, marked by the maximum extent of the Cadia Shale Formation.
2. Jell & Tallent (1989) recognised a significant hiatus separating levels of the Cadia Shale of *leptotheca* and possible early *convolutus* biozone age from the transgressive, early Telychian Cobbler’s Creek Limestone Formation.

Figure 13. Proxy datasets

1. DiazMartinez & Grahn (2007) report the Rhuddanian chitinozoan *Belonechitina cf. postrobusta* from marine sediments underlying Llandovery glacigenic deposits in Peru and Bolivia.
2. Caputo (1998) reported early Aeronian 'Monograptus gregarius' Biozone graptolites from marine sediments immediately overlying glacigenic deposits in the Amazon Basin.
3. Caputo (1998) viewed the presence of early Telychian chitinozoans in marine rocks 'lateral to tillites' as evidence for a glacial advance that peaked during the late Aeronian (see also Johnson, 2006).
4. Marked negative C isotope excursions coincide with the Rumba Formation (e.g. Munnecke & Mannik, 2009), and Kaljo & Martma (2000) recognised a non-sequence beneath the lowest of these excursions, which coincides with the base of the Rumba Formation. They associated the onset of this excursion and the base of the Rumba Formation with the base of the *sedgwickii* Biozone, but the consensus view now places the base of the Rumba Formation and therefore the negative $\delta^{13}\text{C}$ excursion at the base of the Telychian Stage. See notes [13] and [14] for Figure 10.

References (Supplementary data only)

- ALDRIDGE, R. J. 1972. Llandovery conodonts from the Welsh Borderland. *Bulletin of the British Museum (Natural History): Geology Series* **22**, 127-231.
- ALDRIDGE, R. J. 1975. The stratigraphic distribution of conodonts in the British Silurian. *Journal of the Geological Society, London* **131**, 607-18.
- ALDRIDGE, R. J. 1985. Conodonts of the Silurian System from the British Isles. In *A stratigraphical index of conodonts* (eds A. C. Higgins & R. L. Austin), pp. 68-92. Ellis Horward, Chichester.
- ALDRIDGE, R. J. & MOHAMED, I. 1982. Conodont biostratigraphy of the early Silurian of the Oslo region. In *Field Meeting Oslo region 1982. IUGS, Subcommission on Silurian stratigraphy* (ed D. Worsley), pp. 109-20. Palaeontological contributions, University of Oslo, 278.
- ARMSTRONG, H. A. 1990. Conodonts from the Upper Ordovician-Lower Silurian carbonate platform of North Greenland. *Grønlands Geologiske Undersøgelse Bulletin* **159**, 1-151.
- ARTYUSHKOV, E.V. & CHEKHOVICH, P. A. 2001. The East Siberian basin in the Silurian: evidence for no large-scale sea-level changes. *Earth and Planetary Science Letters* **193**, 183-96.
- BAARLI, B. G. 1986. A biometric re-evaluation of the Silurian brachiopod lineage *Stricklandia lens/S. laevis*. *Palaeontology* **29**, 187-205.
- BAARLI, B. G. & JOHNSON, M. E. 1988. Biostratigraphy of selected brachiopods from the Llandovery Series (Lower Silurian) of the Oslo region. *Norsk Geologisk Tidsskrift* **68**, 259-74.
- BAARLI, B. G., BRANDE, S. & JOHNSON, M. E. 1992. Proximality-trends in the Red Mountain Formation (Lower Silurian) of Birmingham, Alabama. *Oklahoma Geological Survey Bulletin* **145**, 1-17.
- BASSETT, M. G. 1989. Brachiopods. In *A Global standard for the Silurian System* (eds C. H. Holland & M. G. Bassett), pp. 232-42. National Museum of Wales, Geological Series no. 10.
- BERGSTRÖM, S.M., CHEN, X., GUTIÉRREZ-MARCO, J.C. & DRONOV, A. 2009. The new chronostratigraphic classification of the Ordovician System and its relations to major regional series and stages and to $\delta^{13}\text{C}$ chemostratigraphy. *Lethaia*, **42**, 97-107.

- BERRY, W.B.N. & BOUCOT, A.J. 1970: Correlation of the North American Silurian rocks. *Geological Society of America Special Publication* **102**, 1–289.
- BLACKETT, E., PAGE, A., ZALASIEWICZ, J. A., WILLIAMS, M., RICKARDS, R. B., & DAVIES, J. R. 2009. A refined graptolite biostratigraphy for the late Ordovician–early Silurian of central Wales. *Lethaia* **43**, 83–96.
- BRETT, C.E., BAARLI, B.G., CHOWNS, T., COTTER, E., DRIESE, S., GOODMAN, W. & JOHNSON, M.E. 1998. Early Silurian condensed intervals, ironstones, and sequence stratigraphy in the Appalachian Foreland Basin. In *Silurian Cycles: Linkages of Dynamic Stratigraphy with Atmospheric, Oceanic, and Tectonic Changes* (eds E. Landing & M. E. Johnson), pp.89–143. New York State Museum Bulletin, 491.
- BURGESS, N.D. 1991. Silurian cryptospores and miospores from the type Llandovery area, south-west Wales. *Palaeontology* **34**, 575–599.
- CAPUTO, M. V. 1998. Ordovician–Silurian glaciations and global sea-level changes. In *Silurian Cycles: Linkages of Dynamic Stratigraphy with Atmospheric, Oceanic and Tectonic Changes* (eds E. Landing & M. E. Johnson), pp. 15–25. New York State Museum Bulletin no. 491.
- CAVE, R & HAINS, B A. 1986. Geology of the country between Aberystwyth and Machynlleth. *Memoir of the British Geological Survey*, Sheet 163 (England and Wales).
- CHALLANDS, T. J., VANDENBROUKE, T. R. A., ARMSTRONG, H. A. & DAVIES, J.R. 2014. Chitinozoan biozonation in the upper Katian and Hirnantian of the Welsh Basin, UK. *Review of Palaeobotany and Palynology* **210**, 1–21.
- COCKS, L. R. M. 1989. The Llandovery Series in the Llandovery area. In *A global standard for the Silurian System* (eds C. H. Holland & M. G. Bassett), pp.36–50. National Museum of Wales, Geological Series no. 9, Cardiff.
- COCKS, L. R. M. & RICKARDS, R. B. 1969. Five boreholes in Shropshire and the relationships of shelly and graptolitic facies in the Lower Silurian. *Quarterly Journal of the Geological Society of London* **124**, 213–38.
- COCKS, L. R. M, WOODCOCK, N. H., RICKARDS, R. B., TEMPLE, J. T. & LANE, P. D. 1984. The Llandovery Series of the type area. *Bulletin of the British Museum (Natural History)*, *Geology Series* **38**, 131–82.
- COCKS, L. R. M., HOLLAND, C. H. & RICKARDS, R. B. 1992. *A revised correlation of Silurian Rocks in the British Isles*. Geological Society, London, Special Report **21**, 32pp.
- CRAMER, B.D., BRETT, C.E., MELCHIN, M.A., MÄNNIK, P., KLEFFNER, M.A., MCCLAUGHLIN, P.I., LOYDELL, D.K., MUNNECKE, A., JEPSSON, L., CORRADINI, C., BRUNTON, F.R., & SALTZMAN, M.R. 2011a . Revised chronostratigraphic correlation of the Silurian System of North America with global and regional chronostratigraphic units and $\delta^{13}\text{C}_{\text{carb}}$ chemostratigraphy. *Lethaia* **44**, 185–202.
- CRAMER B. D., DAVIES, J. R., RAY, D. C., THOMAS A. T. & CHERNS, L. 2011b. Siluria Revisited: An Introduction. In *Siluria Revisited: A Field Guide. International Subcommission on Silurian Stratigraphy, Field Meeting 2011* (ed D.C. Ray), pp. 7 – 28.
- CULLUM, A. & LOYDELL, D. 2011 The Rhuddanian/Aeronian transition in the Rheidol Gorge, mid Wales. *Proceedings of the Yorkshire Geological Society* **58**, 261–6.

- DAHLQVIST, P. & BERGSTROM, S. M. 2005. The lowermost Silurian of Jämtland, central Sweden: conodont biostratigraphy, correlation and biofacies. *Transactions of the Royal Society of Edinburgh: Earth Sciences* **96**, 1-19.
- DAVIES, J. R., FLETCHER, C. J. N., WATERS, R. A., WILSON, D., WOODHALL, D. G. & ZALASIEWICZ, J. A. 1997 Geology of the country around Llanilar and Rhayader. *Memoir of the British Geological Survey*, Sheets 178 and 179 (England and Wales).
- DAVIES, J. R., WATERS, R. A., WILLIAMS, M., WILSON, D., SCHOFIELD, D. I. & ZALASIEWICZ, J. A. 2009. Sedimentary and faunal events revealed by a revised correlation of post-glacial Hirnantian (late Ordovician) strata in the Welsh basin, U.K. *Geological Journal* **44**, 322- 40.
- DAVIES, J. R., MOLYNEUX, S. G., VANDENBROUCKE, T. R. A., VERNIERS, J., WATERS, R. A., WILLIAMS, M. & ZALASIEWICZ, J. A. 2011. Pre-conference field trip to the Type Llandovery area. In *Siluria Revisited: A Field Guide* (ed. D. C. Ray), pp. 29-72. International Subcommittee on Silurian Stratigraphy, Field Meeting, 2011.
- DAVIES, J. R., WATERS, R. A., MOLYNEUX, S. G., WILLIAMS, M., ZALASIEWICZ, J. A., VANDENBROUCKE, T. R. A. & VERNIERS, J. 2013. A revised sedimentary and biostratigraphical architecture for the Type Llandovery area, central Wales, UK. *Geological Magazine* **150**, 300-32.
- DE PERMENTIER, J. & VERNIERS, J. 2002. Chitinozoans from the global stratigraphical sections and points (GSSP) of the bases of the Aeronian and the Telychian (Llandovery) in Wales, UK. In *Palaeozoic Palynology in the Third Millennium: New Directions in Acritarch, Chitinozoan and Miospore Research*, International Meeting and Workshops of the Commission Internationale de Microflore du Paleozoique, 5–7 September 2002, Lille, France. Abstracts Volume, p. 8.
- DIAS-MARTINEZ, E. & GRAHN, Y. 2007. Early Silurian glaciation along the western margin of Gondwana (Peru, Bolivia and northern Argentina): Palaeogeography and geodynamic setting. *Palaeogeography, Palaeoclimatology, Palaeoecology* **252**, 62-81.
- DOYLE, E. N., HOEY, A. N. & HARPER, D. A. T. 1991. The rhynchonellide brachiopod *Eocoelia* from the upper Llandovery of Ireland and Scotland. *Palaeontology* **34**, 439-454.
- GHIENNE, J. F., DESROCHERS, A., VANDENBROUKE, T. R. A., ACHAB, A., ASSELIN, E., DABARD M-P., FARLEY, C., LOI, A., PARIS, F., WICKSON, S. & VEIZIER, J. 2014. A Cenozoic-style scenario for the end-Ordovician glaciation. *Nature Communications* 5:4485, doi: 10.1038/ncomms5485.
- GOULDEY, J. C., SALTZMAN, M. R., YOUNG, S. A. & KALJO, D. 2010. Strontium and carbon isotope stratigraphy of the Llandovery (Early Silurian): Implications for tectonics and weathering. *Palaeogeography, Palaeoclimatology, Palaeoecology* **296**, 264-75.
- HARRIS, M. T. & SHEEHAN, P. M. 1996, Upper Ordovician - Lower Silurian Sequences determined from inner shelf sections, Barn Hills and Lakeside Mountains, Eastern Great Basin. In *Paleozoic Sequence Stratigraphy: North American Perspectives - Views from the North American Craton* (eds B. J. Witzke, G. A. Ludvigson & J. E. Day), pp. 161-76. Geological Society of America Special Publication 306.
- HARRIS, M. T. & SHEEHAN, P. M. 1998. Early Silurian stratigraphic sequences of the eastern Great Basin (Utah and Nevada). In *Silurian Cycles: Linkages of Dynamic Stratigraphy with Atmospheric, Oceanic, and Tectonic Changes* (eds E. Landing & M. E. Johnson), pp.51-61. New York State Museum, Bulletin, 491.

- HARRIS, M. T., KUGLITSCH, J. J., WATKINS, R., HEGRENES, D. P., & WALDHUETTER, K. R. 1998. Early Silurian stratigraphic sequences of eastern Wisconsin. In *Silurian Cycles: Linkages of Dynamic Stratigraphy with Atmospheric, Oceanic and Tectonic Changes* (eds E. Landing & M. E. Johnson), pp. 15–25. New York State Museum Bulletin no. 491.
- HAQ, B. U. & SCHUTTER, S. R. 2008. A chronology of Paleozoic sea-level change. *Science* **322**, 64–8.
- HURST, J. M., SHEEHAN, P. M. & PANDGOLFI, J. M. 1984. Silurian carbonate shelf and slope evolution in Nevada – a history of faulting, drowning and progradation. *Geology* **13**, 185–8.
- JELL, J. S. & TALENT, J. A. 1989. Australia: The most the most instructive sections. In *A Global standard for the Silurian System* (eds C. H. Hollland & M. G. Bassett), pp. 232–42. National Museum of Wales, Geological Series no. 10.
- JIN, J. & COPPER, P. 1999. The deep water brachiopod *Dicoelosia* King, 1850 from the Early Silurian tropical carbonate shelf of Anticosti Island, eastern Canada. *Journal of Palaeontology* **73**, 1042–55.
- JIN, J. & COPPER, P. 2008. Response of brachiopod communities to environmental change during the Late Ordovician mass extinction interval, Anticosti Island, eastern Canada. *Fossils and Strata* **54**, 41–51.
- JIN, J. & COPPER, P. 2010. Origin and evolution of the Early Silurian (Rhuddanian) virgianid pentameride brachiopods — the extinction recovery fauna from Anticosti Island, eastern Canada. *Bolletino della Società Paleontologica Italiana* **49**, 1–11.
- JOHNSON, M.E., 1987. Extent and bathymetry of North American platform seas in the Early Silurian. *Paleoceanography* **2**, 185–211.
- JOHNSON, M.E., 1996. Stable cratonic sequences and a standard for Silurian eustasy. In *Palaeozoic Sequence Stratigraphy: Views from the North American Craton* (eds B. J. Witzke, & G. A. Ludvigson,), pp. 203–11. Geological Society of America, Special Paper 306.
- JOHNSON, M. E. 2006. Relationship of Silurian sea-level fluctuations to oceanic episodes and events. *GFF* **128**, 115–21.
- JOHNSON, M.E., COCKS, L. R.M. & COPPER, P. 1981. Late Ordovician-Early Silurian fluctuations in sea level from eastern Anticosti Island, Quebec. *Lethaia* **14**, 73–82.
- JOHNSON, M.E., BAARLI, B.G., NESTOR, H., RUBEL, M. & WORSLEY, D. 1991. Eustatic sea-level patterns from the Lower Silurian (Llandovery Series) of southern Norway and Estonia. *Geological Society of America Bulletin* **103**, 315–35.
- JOHNSON, M. E., KALJO, D. K. & RONG, J.-Y. 1991. Silurian eustasy. In *The Murchison Symposium: Proceedings of an international conference on the Silurian System* (eds M. G. Bassett, P. D. Lane & D. Edwards), pp. 145–63. Special Papers in Palaeontology no. 44, The Palaeontological Association.
- JOHNSON, M. E., RONG, J. & KERSHAW, S., 1998. Calibrating Silurian eustasy against the erosion and burial of coastal paleotopography. In *Silurian Cycles: Linkages of Dynamic Stratigraphy with Atmospheric, Oceanic, and Tectonic Changes* (eds E.Landing, & M. E. Johnson), pp. 3–13, New York State Museum Bulletin, 491.
- JOHNSON, M. E., RONG, J. U. & YANG, X, C. 1985. Intercontinental correlation by sea-level events in the early Silurian of North America and China (Yangtze platform). *Bulletin of the Geological Society of America* **96**, 1384–97.

- JONES, O. T. 1925. The geology of the Llandovery district. Part I: The southern area. *Quarterly Journal of the Geological Society of London* **81**, 344-88.
- KALJO, D. & MARTMA, T. 2000. Carbon isotopic composition of Llandovery rocks (East Baltic Silurian) with environmental interpretation. *Proceedings of the Estonian Academy of Sciences, Geology* **49**, 267-83.
- KALJO, D., MARTMA, T., MANNIK, P. & VIIRA, V. 2003. Implications of Gondwana glaciations in the Baltic Late Ordovician and Silurian and a carbon isotopic test of environmental cyclicity. *Bulletin de la Socié'te' Ge'ologique de France* **174**, 59-66.
- KIIPLI, E., KIIPLI, T. & KALLASTE, T. 2006. Identification of O-bentonite in deep shelf sections with implication on stratigraphy and lithofacies, East Baltic Silurian. *GFF* **128**, 255-260.
- KIIPLI, T., KALLASTE, T., NESTOR, V & LOYDELL, D.K. 2010. Integrated Telychian (Silurian) K-bentonite chemostratigraphy and biostratigraphy in Estonia and Latvia. *Lethaia* **43**, 32-44.
- KLEFFNER, M. A. 2004. Lower Silurian Medina and Clinton Groups of the Niagara region. *Geological Society of Canada – Mineralogical Association of Canada meeting 2004, Brock University, St Catherines Ontario – Pander Society Field Trip*, 1-5.
- KLEFFNER, M.A., BARRICK, J.E. & DRACHEN, A. 2004. Conodont-, graptolite-, and chitonozoa-based Silurian composite developed using graphic correlation aids new calibration of current Silurian chronostratigraphy. *Association of Canada 2004 joint Annual Meeting Abstracts volume. Geological Association of Canada, Cordilleran Section*, pp. 96.
- KLUESSENDORF, J. & MIKULIC, D. G. 1996. An early sequence boundary in Illinois and Wisconsin. In *Palaeozoic Sequence Stratigraphy: Views from the North American Craton* (eds B. J. Witzke, G. A. Ludwigson & J. Day), pp. 177-85. Geological Society of America, Special paper 306.
- LOYDELL, D. K. 1998. Early Silurian sea-level changes. *Geological Magazine* **135** 447-71.
- LOYDELL D.K. 1991. The biostratigraphy and formational relationships of the upper Aeronian and lower Telychian (Llandovery, Silurian) formations of western mid-Wales. *Geological Journal* **26**, 209-44.
- LOYDELL D.K. 1994. Early Telychian changes in graptoloid diversity and sea level. *Geological Journal* **29** 355-68.
- LOYDELL, D. K., NESTOR, V. & MANNIK, P. 2010. Integrated biostratigraphy of the lower-Silurian of the Kolka-54 core, Latvia. *Geological Magazine* **147**, 253-80
- LOYDELL, D. K., MALLETT, A., MIKULIC, D. G., KLUESSENDORF, J. & NORBY, R.D. 2002. Graptolites from near the Ordovician-Silurian boundary in Illinois and Iowa. *Journal of Palaeontology* **76**, 134-7.
- MCKERROW, W. S. 1979. Ordovician and Silurian changes in sea level. *Journal of the Geological Society of London* **136**, 137-45.
- MANNIK, P. 2007: An updated Telychian (Late Llandovery, Silurian) conodont zonation based on Baltic faunas. *Lethaia* **40**, 45-60.
- MELCHIN, M., J., HOLMDEN, C. & WILLIAMS, S.H. 2003. Correlation of graptolite biozones, chitinozoa biozones and carbon isotope curves through the Hirnantian. In *Ordovician from the Andes*,

Volume 17 (eds G. L. Albanesi, M. S. Beresi & S. H. Peralta), pp 101-4. Tucumam, Argentina, Comunicart Editorial.

MELCHIN, M. J., SADLER, P. M. & CRAMER, B.D. 2012. The Silurian Period. In *A Geologic Time Scale 2012* (eds F. M. Gradstein, J. G. Ogg & A. G. Smith), pp. 525-58. Elsevier.

METZGER, R. A. 2005. Conodont biostratigraphy of the Scotch Grove and Laporte City formations (Late Llandovery-Early Wenlock; Silurian) in eastern Iowa. In *A standing ovation: Papers in honor of Gilbert Klapper* (eds J. E. Barrick & H. R. Lane). *Bulletins of American Paleontology* **369**, 93-104.

MIKULIC, D. G., SARGENT, M. I., NORBY, R. D. & KOLATA, D. R.. 1985. Silurian geology of the Des Plaines River valley, northeastern Illinois. *Illinois Geological Survey Guidebook* 17.

MU, E-Z., CHEN, X. & RONG, J-Y. 1989. The Llandovery Series in China. In *A global standard for the Silurian System* (eds C. H. Holland & M. G. Bassett), pp.201–5. National Museum of Wales, Geological Series no. 9, Cardiff.

MUNNECKE, A. & MANNIK, P. 2009. New biostratigraphic and chemostratigraphic data from the Chicotte Formation (Llandovery, Anticosti Island, Laurentia) compared with the Viki core (Estonia, Baltica). *Estonian Journal of Earth Science* **58**, 159-69.

NESTOR, V. 1976. A microplankton correlation of boring sections of the Raikküla Stage, Estonia. *Eesti NSV Teaduste Akadeemia Toimetised, Keemia Geoloogia* **25**, 319-324.

NESTOR, H. 1997. Silurian. In *Geology and Mineral Resources of Estonia* (eds A. Raukas & A. Teedumae), pp. 89–106. Estonian Academy Publishers, Tallinn.

NESTOR, V. 2012. A summary and revision of the East Baltic Silurian chitinozoan biozonation. *Estonian Journal of Earth Sciences* **61**, 242–60.

NESTOR, H. & NESTOR, V. 2002. Upper Llandovery to middle Wenlock (Silurian) lithostratigraphy and chitinozoan biostratigraphy in southwestern Estonia and northernmost Latvia. *Proceedings Estonian Academy of Sciences, Geology* **51**, 67-87.

NESTOR, H., EINASTO, R., MÄNNIK, P., & NESTOR, V. 2003. Correlation of lower–middle Llandovery sections in central and southern Estonia and sedimentation cycles of lime muds. In *Proceedings of the Estonian Academy of Sciences, Geology* **52**, 3-27.

PAGE, A. A., ZALASIEWICZ, J. A., WILLIAMS, M. & POPOV, L. E. 2007. Were transgressive black shales a negative feedback modulating glacioeustasy during the Early Palaeozoic Icehouse? In *Deep time perspectives on climate change: marrying the signal from computer models and biological proxies* (eds M. Williams, A. M. Haywood, F. J. Gregory & D. N. Schmidt), pp. 123-56. The Micropalaeontological Society Special Publications, The Geological Society, London.

ROSS, C. A. 1962. Early Llandoveryan (Silurian) graptolites from the Edgwood Formation, northeastern Illinois. *Journal of Paleontology* **36**, 1383-6.

ROSS, C. A. 1964. Early Silurian graptolites from the Edgwood Formation of Iowa. *Journal of Paleontology* **38**, 1107-8.

ROSS, C. A. & ROSS, R. P. 1996. Silurian sea level fluctuations. In *Paleozoic sequence stratigraphy: Views from the North American craton* (eds B. J. Witzke, G. A. Ludvigson & J. Day), pp. 187-192. Geological Society of America Special Paper no. 306.

- RUBEL, M. 1977. Evolution of the genus *Stricklandia* (Pentamerida, Brach). In *Facies and fauna of the Baltic Silurian* (ed D. Kaljo), pp. 193-212. Academy of Sciences of Estonian Soviet Socialist Republic, Institute of Geology.
- RUBEL, M., HINTS, O, MANNIK, P., MEIDLA, T., NESTOR, V. SARV, L. & SIBUL, I. 2007. Lower Silurian biostratigraphy of the Viireland core, western Estonia. *Estonian Journal of Earth Science* **56**, 193-204.
- SHEEHAN, P.M. 1980. Paleogeography and marine communities of the Silurian carbonate shelf in Utah and Nevada. In *Paleozoic Paleogeography of West-Central United States, West-Central United States Paleogeography Symposium*. (eds T.D. Fouch, and E.R. Magathan), pp. 19–37. Society of Economic Paleontologists and Mineralogists, Rocky Mountain Section, Vol. 1.
- TESAKOV, Y. I., JOHNSON, M. E., PREDTETCHENSKY, N. N., KHROMYCH, V. G. & BERGER, A. Y. A. 1998. Eustatic fluctuations in the East Siberian Basin (Siberian Platform and Taymyr Peninsula). In *Silurian Cycles: Linkages of Dynamic Stratigraphy with Atmospheric, Oceanic, and Tectonic Changes* (eds E. Landing & M. E. Johnson), pp.63-73. New York State Museum Bulletin 491.
- VANDENBROUCKE T.R.A. 2008. An Upper Ordovician chitinozoan biozonation in British Avalonia (England and Wales). *Lethaia* **41**, 275–294.
- VANDENBROUCKE, T.R.A. HENNISSSEN, J. ZALASIEWICZ, J.A. & VERNIERS J.. 2008. New chitinozoans from the historical type area of the Hirnantian and additional key sections in the Wye Valley, Wales, UK. *Geological Journal* **43**, 397–414.
- WORSLEY, D., ALDRIDGE, R. J. , BAARLI, B. G. , HOWE, M. P. A. & JOHNSON, M. E. 1983. The Llandovery Series of the Oslo Region - A submission to the Subcommittee on Silurian Stratigraphy. *Paleontologica/ Contributions from the University of Oslo*, No. 287, 38 p.
- WILLIAMS, A. 1951. Llandovery brachiopods from Wales with special reference to the Llandovery district. *Quarterly Journal of the Geological Society of London* **107**, 85-136.
- WILLMAN, H. B. 1973. Rock stratigraphy of the Silurian system in northeastern and northwestern Illinois. *Illinois State Geological Survey*, Circular 479.
- WILLMAN, H B. & ATHERTON, E. 1975. Silurian System. In *Handbook of Illinois Stratigraphy* (eds H. B. Willman, E. Atherton, T. C. Buschbach, C. Collinson, J. C. Frye, M. E. Hopkins, J. A. Lineback, & J. A. Simon), pp 87-103. Illinois State Geological Survey Bulletin 95.
- WILLS, L. J. & SMITH, B. 1922. The Lower Palaeozoic rocks of the Llangollen area with special reference to the tectonics. *Quarterly Journal of the Geological Society of London* **78**, 176-226.
- WITZKE, B. J. 1992. Silurian stratigraphy and carbonate mound facies of eastern Iowa. *Iowa Department of Natural Resources, Geological Survey Bureau, Guidebook Series* no 11, 111pp.
- WITZKE, B. J. & BUNKER, B. J. 1996. Relative sea-level changes during Middle Ordovician through Mississippian deposition in the Iowa area, North American craton. In *Paleozoic Sequence Stratigraphy: Views from the North American Craton* (eds B. J. Witzke, G. A. Ludwigson & J. Day), pp. 307-30. Geological Society of America Special Paper 306.
- ZALASIEWICZ, J. A., TAYLOR, L., RUSHTON, A. W. A., LOYDELL, D. K., RICKARDS, R. B. & WILLIAMS, M. 2009. Graptolites in British stratigraphy. *Geological Magazine* **146**, 785-850.

ZHANG, S. & BARNES, C. R. 2002a A new Llandovery (Early Silurian) conodont biozonation and conodonts from the Becscie, Merrimack, and Gun River formations, Anticosti Island, Quebec. *Paleontological Society Memoir* **57**, 1–46.

ZHANG, S. & BARNES, C. R. 2002b. Late Ordovician-Early Silurian (Ashgillian-Llandovery) sea level curve derived from conodont community analysis, Anticosti Island, Quebec. *Palaeogeography, Palaeoclimatology, Palaeoecology* **180**, 5-32.

ZHANG, S., BARNES, C. R. & JOWETT, D. M. S. 2006. The paradox of the global standard Late Ordovician –Early Silurian sea level curve: evidence from conodont community analysis from both Canadian Arctic and Appalachian margins. *Palaeogeography, Palaeoclimatology, Palaeoecology* **236**, 246-71.

ZIEGLER, A. M. 1966. The Silurian brachiopod *Eocelia hemisphaerica* (J. de C. Sowerby) and related species. *Palaeontology* **9**, 523-43.

ZIEGLER, A. M., COCKS, L. R. M., & MCKERROW, W. S. 1968. The Llandovery transgression of the Welsh Borderland. *Palaeontology* **11**, 736-82.

UK Graptolite Biotone	Fig 7		Fig 8		Fig 9		Fig 10		Fig 11		Fig 12		Fig 13		Fig 14		Representation index (R/Max)%	Eustasy Index raw score per subdivision (IR)	EUSTASY INDEX (EI)	UK Graptolite Biotone
	R (6 max) order	R (6 High order)	R (7 Low order)	R (7 High order)	R (10 Low order)	R (10 High order)	R (6 Low order)	R (6 High order)	R (9 Low order)	R (9 High order)	R (6 Low order)	R (6 High order)	R (7 Low order)	R (7 High order)	R (7 Low order)	R (7 High order)				
35	4	3	0	3	0	0	0	0	0	0	0	0	0	0	0	0	73	17.5	39	guerichi
36	6	4	0	4	0	0	0	0	0	0	0	0	0	0	0	0	49	20	41	guerichi
33	6	6	0	6	0	0	0	0	0	0	0	0	0	0	0	0	81	33	68	guerichi
34	6	6	0	6	0	0	0	0	0	0	0	0	0	0	0	0	50	24	47	guerichi
32	6	6	0	6	0	0	0	0	0	0	0	0	0	0	0	0	62	24	47	guerichi
31	6	6	0	6	0	0	0	0	0	0	0	0	0	0	0	0	81	20.5	41	seodwicki-halli
30	6	4	0	4	0	0	0	0	0	0	0	0	0	0	0	0	81	20.5	41	seodwicki-halli
29	6	4	0	4	0	0	0	0	0	0	0	0	0	0	0	0	85	24.5	46	seodwicki-halli
28	6	6	0	6	0	0	0	0	0	0	0	0	0	0	0	0	85	21	40	seodwicki-halli
27	6	4	0	4	0	0	0	0	0	0	0	0	0	0	0	0	87	37.5	69	convolutus
26	6	6	0	6	0	0	0	0	0	0	0	0	0	0	0	0	92	29.5	52	convolutus
25	6	6	0	6	0	0	0	0	0	0	0	0	0	0	0	0	94	30	52	convolutus
24	6	6	0	6	0	0	0	0	0	0	0	0	0	0	0	0	94	21.5	37	convolutus
23	5	0	5	7	0	3	1.5	8	0	4	2	3	5	0	0	0	92	20.5	36	leporthea
22	5	0	4	7	1	3	2.5	8	0	4	2	3	5	0	0	0	92	20	35	leporthea
21	3	5	0	3	2.5	8	0	4	0	4	2	3	5	0	0	0	92	21.5	38	magnus
20	6	6	0	6	0	0	0	0	0	0	0	0	0	0	0	0	84	22.5	39	magnus
19	6	6	0	6	0	0	0	0	0	0	0	0	0	0	0	0	84	22.5	39	magnus
18	6	6	0	6	0	0	0	0	0	0	0	0	0	0	0	0	85	24.2	41	magnus
17	6	3	4.5	7	0	3	1.5	8	0	4	2	3	5	0	0	0	85	24.2	41	triangulatus
16	6	2	4	6	0	3	1.5	8	0	4	2	3	5	0	0	0	87	38.5	68	triangulatus
15	6	6	0	6	0	0	0	0	0	0	0	0	0	0	0	0	88	38.5	68	triangulatus
14	5	2	3	3.5	7	1	6	3	9	4	2	5	6	5	1	5	87	32.5	54	revolutus
13	5	0	5	7	1	6	3	9	4	2	5	6	5	1	5	5	92	33.5	59	revolutus
12	5	0	5	7	1	6	3	9	4	2	5	6	5	1	5	5	92	33.5	59	revolutus
11	5	1	0	1	7	0	0	0	0	0	0	0	0	0	0	0	58	21	21	axvis-acinaces
10	5	1	0	1	7	0	0	0	0	0	0	0	0	0	0	0	59	15	25	axvis-acinaces
9	5	1	0	1	7	0	0	0	0	0	0	0	0	0	0	0	59	15	25	axvis-acinaces
8	4	1	0	1	7	0	0	0	0	0	0	0	0	0	0	0	64	12	20	axvis-acinaces
7	4	1	0	1	7	0	0	0	0	0	0	0	0	0	0	0	64	12	20	axvis-acinaces
6	4	1	0	1	7	0	0	0	0	0	0	0	0	0	0	0	64	12	20	axvis-acinaces
5	4	3	0	3	5	0	0	0	0	0	0	0	0	0	0	0	92	15.5	27	acensius-acuminatus
4	4	4	0	4	0	0	0	0	0	0	0	0	0	0	0	0	90	16	29	acensius-acuminatus
3	3	2	0	3	3	0	0	0	0	0	0	0	0	0	0	0	77	14.5	30	acensius-acuminatus
2	3	2	2	3	3	0	0	0	0	0	0	0	0	0	0	0	63	17	44	acensius-acuminatus
1	3	1	2	2	1	1	0	1	0	0	0	1	0	0	0	0	37	15.5	67	upper*
																	2232	13.5	64	perscipuus
																	1886	11	61	perscipuus
																	84.5	Mean EI score	43	

Eustasy Index scores for the Type Landovery succession (see text for explanation and interpretation)